

# From Source to Sink: Responses of a Coastal Catchment to Large-scale Changes (Golden Strand Catchment, Achill Island, County Mayo)

Authors: Eugene Farrell, Mary Bourke, Tiernan Henry, Gesche Kindermann, Kevin Lynch, Terry Morley, Barry O'Dwyer, John O'Sullivan and Jonathan Turner



## ENVIRONMENTAL PROTECTION AGENCY

The Environmental Protection Agency (EPA) is responsible for protecting and improving the environment as a valuable asset for the people of Ireland. We are committed to protecting people and the environment from the harmful effects of radiation and pollution.

### The work of the EPA can be divided into three main areas:

**Regulation:** *We implement effective regulation and environmental compliance systems to deliver good environmental outcomes and target those who don't comply.*

**Knowledge:** *We provide high quality, targeted and timely environmental data, information and assessment to inform decision making at all levels.*

**Advocacy:** *We work with others to advocate for a clean, productive and well protected environment and for sustainable environmental behaviour.*

## Our Responsibilities

### Licensing

We regulate the following activities so that they do not endanger human health or harm the environment:

- waste facilities (*e.g. landfills, incinerators, waste transfer stations*);
- large scale industrial activities (*e.g. pharmaceutical, cement manufacturing, power plants*);
- intensive agriculture (*e.g. pigs, poultry*);
- the contained use and controlled release of Genetically Modified Organisms (*GMOs*);
- sources of ionising radiation (*e.g. x-ray and radiotherapy equipment, industrial sources*);
- large petrol storage facilities;
- waste water discharges;
- dumping at sea activities.

### National Environmental Enforcement

- Conducting an annual programme of audits and inspections of EPA licensed facilities.
- Overseeing local authorities' environmental protection responsibilities.
- Supervising the supply of drinking water by public water suppliers.
- Working with local authorities and other agencies to tackle environmental crime by co-ordinating a national enforcement network, targeting offenders and overseeing remediation.
- Enforcing Regulations such as Waste Electrical and Electronic Equipment (WEEE), Restriction of Hazardous Substances (RoHS) and substances that deplete the ozone layer.
- Prosecuting those who flout environmental law and damage the environment.

### Water Management

- Monitoring and reporting on the quality of rivers, lakes, transitional and coastal waters of Ireland and groundwaters; measuring water levels and river flows.
- National coordination and oversight of the Water Framework Directive.
- Monitoring and reporting on Bathing Water Quality.

## Monitoring, Analysing and Reporting on the Environment

- Monitoring air quality and implementing the EU Clean Air for Europe (CAFÉ) Directive.
- Independent reporting to inform decision making by national and local government (*e.g. periodic reporting on the State of Ireland's Environment and Indicator Reports*).

## Regulating Ireland's Greenhouse Gas Emissions

- Preparing Ireland's greenhouse gas inventories and projections.
- Implementing the Emissions Trading Directive, for over 100 of the largest producers of carbon dioxide in Ireland.

## Environmental Research and Development

- Funding environmental research to identify pressures, inform policy and provide solutions in the areas of climate, water and sustainability.

## Strategic Environmental Assessment

- Assessing the impact of proposed plans and programmes on the Irish environment (*e.g. major development plans*).

## Radiological Protection

- Monitoring radiation levels, assessing exposure of people in Ireland to ionising radiation.
- Assisting in developing national plans for emergencies arising from nuclear accidents.
- Monitoring developments abroad relating to nuclear installations and radiological safety.
- Providing, or overseeing the provision of, specialist radiation protection services.

## Guidance, Accessible Information and Education

- Providing advice and guidance to industry and the public on environmental and radiological protection topics.
- Providing timely and easily accessible environmental information to encourage public participation in environmental decision-making (*e.g. My Local Environment, Radon Maps*).
- Advising Government on matters relating to radiological safety and emergency response.
- Developing a National Hazardous Waste Management Plan to prevent and manage hazardous waste.

## Awareness Raising and Behavioural Change

- Generating greater environmental awareness and influencing positive behavioural change by supporting businesses, communities and householders to become more resource efficient.
- Promoting radon testing in homes and workplaces and encouraging remediation where necessary.

## Management and structure of the EPA

The EPA is managed by a full time Board, consisting of a Director General and five Directors. The work is carried out across five Offices:

- Office of Environmental Sustainability
- Office of Environmental Enforcement
- Office of Evidence and Assessment
- Office of Radiation Protection and Environmental Monitoring
- Office of Communications and Corporate Services

The EPA is assisted by an Advisory Committee of twelve members who meet regularly to discuss issues of concern and provide advice to the Board.

**EPA RESEARCH PROGRAMME 2021–2030**

**From Source to Sink: Responses of a  
Coastal Catchment to Large-scale Changes  
(Golden Strand Catchment, Achill Island,  
County Mayo)**

**(2014-CCRP-MS.22)**

**EPA Research Report**

Prepared for the Environmental Protection Agency

by

National University Ireland Galway

**Authors:**

**Eugene Farrell, Mary Bourke, Tiernan Henry, Gesche Kindermann, Kevin Lynch,  
Terry Morley, Barry O'Dwyer, John O'Sullivan and Jonathan Turner**

**ENVIRONMENTAL PROTECTION AGENCY**

An Ghníomhaireacht um Chaomhnú Comhshaoil  
PO Box 3000, Johnstown Castle, Co. Wexford, Ireland

Telephone: +353 53 916 0600 Fax: +353 53 916 0699

Email: [info@epa.ie](mailto:info@epa.ie) Website: [www.epa.ie](http://www.epa.ie)

## **ACKNOWLEDGEMENTS**

This report is published as part of the EPA Research Programme 2021–2030. The EPA Research Programme is a Government of Ireland initiative funded by the Department of the Environment, Climate and Communications. It is administered by the Environmental Protection Agency, which has the statutory function of co-ordinating and promoting environmental research.

The authors would like to acknowledge the members of the project steering committee, namely Phillip O’Brien (EPA), Marc Kierans (ex-EPA), Margaret Desmond (EPA), Robert Devoy (University College Cork – UCC), Conor Murphy (Maynooth University – MU), Caroline Cusack (Marine Institute), and also Oonagh Monahan (Research Manager on behalf of the EPA). Donal Ó hÉanacháin (Geography, National University Ireland Galway – NUIG) and Sinead Horgan (Applied Ecology Unit, NUIG) were contributing authors to Chapter 5.

The authors would like to acknowledge the landowners and community in Achill Island who supported the research. The authors would like to acknowledge Patrick Belmont (Utah State University, USA), Guillermo Castro Camba (NUIG), Cecile Collot (NUIG), Thomas Gorman (NUIG), Linda Heerey (University College Dublin – UCD), Sinead Horgan (NUIG), Ciaran Nash (Trinity College Dublin – TCD), Anna Rymaszewicz (UCD), David Serrano Giné (Universitat Rovira i Virgili, Spain) and Sinead Wilkes Orozco (NUIG) for their field support.

## **DISCLAIMER**

Although every effort has been made to ensure the accuracy of the material contained in this publication, complete accuracy cannot be guaranteed. The Environmental Protection Agency, the authors and the steering committee members do not accept any responsibility whatsoever for loss or damage occasioned, or claimed to have been occasioned, in part or in full, as a consequence of any person acting, or refraining from acting, as a result of a matter contained in this publication. All or part of this publication may be reproduced without further permission, provided the source is acknowledged.

This report is based on research carried out/data from December 2015 to October 2017. More recent data may have become available since the research was completed.

The EPA Research Programme addresses the need for research in Ireland to inform policymakers and other stakeholders on a range of questions in relation to environmental protection. These reports are intended as contributions to the necessary debate on the protection of the environment.

## **EPA RESEARCH PROGRAMME 2021–2030**

Published by the Environmental Protection Agency, Ireland

ISBN: 978-1-84095-997-0

June 2021

Price: Free

Online version

## Project Partners

### **Dr Mary Bourke**

Department of Geography  
Trinity College Dublin  
College Green  
Dublin 2  
Ireland  
Tel.: + 353 1 896 1888  
Email: bourkem4@tcd.ie

### **Dr Eugene Farrell**

Discipline of Geography  
School of Geography, Archaeology and Irish  
Studies  
National University Ireland Galway  
Galway  
Ireland  
Tel.: + 353 91 494336  
Email: eugene.farrell@nuigalway.ie

### **Dr Tiernan Henry**

Discipline of Earth & Ocean Sciences  
College of Science and Engineering  
National University Ireland Galway  
Galway  
Ireland  
Tel.: + 353 91 495096  
Email: tiernan.henry@nuigalway.ie

### **Dr Gesche Kindermann**

Applied Ecology Unit  
School of Natural Sciences  
National University Ireland Galway  
Galway  
Ireland  
Tel.: + 353 91 493862  
Email: gesche.kindermann@nuigalway.ie

### **Dr Kevin Lynch**

Discipline of Geography  
School of Geography, Archaeology and Irish  
Studies  
National University Ireland Galway  
Galway  
Ireland  
Tel.: + 353 91 495779  
Email: kevin.lynch@nuigalway.ie

### **Dr Terry Morley**

Discipline of Geography  
School of Geography, Archaeology and Irish  
Studies  
National University Ireland Galway  
Galway  
Ireland  
Tel.: + 353 91 493897  
Email: terry.morley@nuigalway.ie

### **Dr Barry O'Dwyer**

Centre for Marine and Renewable Energy  
(MaREI)  
Environmental Research Institute  
University College Cork  
Cork  
Ireland  
Tel.: +353 21 486 4326  
Email: b.odwyer@ucc.ie

### **Dr John O'Sullivan**

School of Civil Engineering  
University College Dublin  
Dublin  
Ireland  
Tel.: + 353 1 716 3213  
Email: jj.osullivan@ucd.ie

### **Dr Jonathan Turner**

School of Geography  
University College Dublin  
Dublin 4  
Ireland  
Tel.: + 353 1 716 8175  
Email: jonathan.turner@ucd.ie



# Contents

<b>Acknowledgements</b>	<b>ii</b>
<b>Disclaimer</b>	<b>ii</b>
<b>Project Partners</b>	<b>iii</b>
<b>List of Figures</b>	<b>vii</b>
<b>List of Tables</b>	<b>x</b>
<b>Executive Summary</b>	<b>xiii</b>
<b>1 Introduction</b>	<b>1</b>
1.1 Work Packages	1
1.2 Study Site: Golden Strand, Achill Island, County Mayo	3
<b>2 WP2 – Response of Beach–Dune Systems to Atlantic Storms</b>	<b>12</b>
2.1 Introduction	12
2.2 Beach–Dune Response to Storms	13
2.3 Methods	15
2.4 Results	17
2.5 Discussion	23
<b>3 WP3 – Tracing Internal Moisture and Salinity Changes in Dunes</b>	<b>26</b>
3.1 Introduction	26
3.2 Methods	26
3.3 Results	26
3.4 Conclusions	28
<b>4 WP4 – Groundwater Dynamics in a Coastal Sand Dune</b>	<b>30</b>
4.1 Introduction	30
4.2 Geological Setting and Links to Subsurface Flow Dynamics	30
4.3 Methods	30
4.4 Results	32
4.5 Discussion	32
4.6 Conclusion and Recommendations	34

<b>5</b>	<b>WP5 – Plant Functional Diversity and Habitat Change in a Machair System</b>	<b>36</b>
5.1	Introduction	36
5.2	Site Description and Methodology	37
5.3	Results	39
5.4	Discussion	41
5.5	Conclusions	45
<b>6</b>	<b>WP6 – Hydrology, Water Quality and Catchment Exports</b>	<b>46</b>
6.1	Introduction	46
6.2	Water Quality Parameters	46
6.3	Description of the Study Area	50
6.4	Materials and Methods	50
6.5	Results	56
6.6	Discussion	64
6.7	Concluding Remarks	65
<b>7</b>	<b>WP7 – Recommendations</b>	<b>66</b>
	<b>References</b>	<b>70</b>
	<b>Abbreviations</b>	<b>81</b>
	<b>Appendix 1 Exploration of the Statistical Relationships Between the Water Parameters</b>	<b>82</b>



# List of Figures

Figure 1.1.	Location of Golden Strand, Achill Island, County Mayo	4
Figure 1.2.	Overview of WP monitoring locations in the study catchment	4
Figure 1.3.	Aerial photographs showing locations of beach, dune, machair and stream systems of Golden Strand	5
Figure 1.4.	Aerial photograph of Golden Strand catchment, Achill Island, County Mayo	5
Figure 1.5.	Boundaries of the protected areas in the study catchment. Doogort Machair/Lough Doo SAC (SAC 001497), Doogort East Bog Natural Heritage Areas (NHA 002381) and Doogort Machair Special Protection Area (SPA 004235)	6
Figure 1.6.	Distribution map of sand dune habitats, including machair, within Doogort Machair/Lough Doo SAC	7
Figure 1.7.	(a) Local bedrock geology: RP, Ridge Point Psammitic Formation; DA, Dooega Head Formation. (b) Study catchment area	8
Figure 1.8.	(a) Surface drainage of the Golden Strand catchment. (b) Elevation changes within the Golden Strand catchment	10
Figure 1.9.	(a) Soil map of the Golden Strand catchment. (b) CORINE landcover map of the Golden Strand catchment	10
Figure 2.1.	Location of the five cross-shore profiles at Golden Strand repeatedly surveyed from December 2015 to October 2017	15
Figure 2.2.	View of time lapse camera (inset) deployed on headland overlooking Golden Strand	17
Figure 2.3.	Profiles 1–5 obtained from repeat surveying using a GNSS	18
Figure 2.4.	(a) Location of the PlotWatcher camera (red filled circle) and football field. (b) Close-up aerial view of man-made dune ridges running oblique to foredune. Note the embryo dune development. (c) View of profile 5 at distal end of beach adjacent to the headland. (d) View of profile 1 with gravel storm berm	19
Figure 2.5.	Changes in elevation across each profile for each survey	21
Figure 2.6.	The maximum (accretion), minimum (erosion) and average elevations changes across each profile during the monitoring programme	22
Figure 2.7.	(a) $H_s$ data from the Marine Institute East Atlantic SWAN Wave Model for local conditions (54.047370°, –10.024985°). (b) Tide data from Ballyglass Harbour, Co. Mayo, with storm durations overlain	23
Figure 2.8.	Captured images from the low-resolution PlotWatcher camera for Storms 7–14. Dates and times of the maximum observed wave run-up are: (a) 17 November 2016, 09:32; (b) 23 December 2016, 14:36;	

	(c) 25 December 2016, 15:51; (d) 12 January 2017, 17:21; (e) 12 January 2017, 17:21; (f) 7 February 2017, 06:25; (g) 15 March 2017, 08:28	24
Figure 3.1.	(a) Installing EasyAG capacitance probes equipped with Sentek TriSCAN moisture and salinity sensors. (b) Approximate location of sensors along profile 3 (WP2). (c) Close up of inset box in (b)	27
Figure 3.2.	(a) Distribution of moisture values per site and depth. (b) Rainfall intensity (mm/h) plotted against range of moisture per depth for each of the 10 subset rainfall events	28
Figure 3.3.	(a) Distribution of salinity values per site and depth. (b) Rainfall intensity (mm/h) plotted against range of salinity per depth for each of the 10 subset rainfall events	29
Figure 4.1.	Falling head test locations	31
Figure 4.2.	Monitoring well and data loggers	31
Figure 4.3.	Data logger installation at borehole 1 (BH1)	32
Figure 4.4.	Distribution of $K$ values (m/s)	33
Figure 4.5.	BH water levels (m) and rainfall (mm)	33
Figure 4.6.	(a) Monthly rainfall totals (mm). (b) Site rainfall (mm) versus site ER (mm)	34
Figure 5.1.	Habitat map showing the identified sand dune habitats using Fossitt (2000) codes for (a) 1995, (b) 2000, (c) 2005, (d) 2010 and (e) 2016	41
Figure 6.1.	YSI EXO2 Multiparameter Sonde	50
Figure 6.2.	(a) Location of Teledyne ISCO autosampler in custom-built box beside bridge. (b) Close-up view of ISCO sampler containing sampling bottles. (c) The PVC pipe housing the EXO2 sonde	51
Figure 6.3.	Location of monitoring site at the road bridge on the unnamed stream, south of Doogort beach and dune area	52
Figure 6.4.	Monitoring site set-up showing (1) the PVC pipe housing the EXO2 sonde, (2) the custom-made box housing the Storm 3 data logger and (3) the box housing the ISCO autosampler	53
Figure 6.5.	SSC–turbidity relationship for field samples ( $n = 30$ )	54
Figure 6.6.	Laboratory set-up for the preparation of the in-house standards. Inset shows close-up of the two sediment types with Fe-rich sediment on the left	54
Figure 6.7.	Linear calibration models for in-house standards for sediments collected from the river bed in the unnamed stream	55
Figure 6.8.	Comparison of the field samples and in-house standards	55
Figure 6.9.	Map showing relative positions of cross-sections and long-profile surveys for flow reconstruction	56

Figure 6.10.	High-resolution (15 min) temperature time series (black) plotted with EXO2 water level (blue) and tidal data from Ballyglass tidal gauge (grey). The hourly rainfall data above each plot (also in blue) are from the Dooagh water treatment plant, south-west Achill Island	58
Figure 6.11.	High-resolution (15 min) SC time series (black) plotted with EXO2 water level (blue) and tidal data from Ballyglass tidal gauge (grey). The hourly rainfall data above each plot (also in blue) are from the Dooagh water treatment plant, south-west Achill Island	58
Figure 6.12.	High-resolution (15 min) SC (black) plotted with EXO2 water level (blue) and tidal data from Ballyglass tidal gauge (grey) for two specific periods. (a) The asymmetrical SC pattern that is inversely related to water level. (b) The timing of SC spikes and high tides. The hourly rainfall data shown above each plot (also in blue) are from the Dooagh water treatment plant, south-west Achill Island	59
Figure 6.13.	High-resolution (15 min) pH time series (black) plotted with EXO2 water level (blue) and tidal data from Ballyglass tidal gauge (grey). The hourly rainfall data above each plot (also in blue) are from the Dooagh water treatment plant, south-west Achill Island	60
Figure 6.14.	High-resolution (15 min) DO time series (black) plotted with EXO2 water level (blue) and tidal data from Ballyglass tidal gauge (grey). The hourly rainfall data above each plot (also in blue) are from the Dooagh water treatment plant, south-west Achill Island	60
Figure 6.15.	High-resolution (15 min) turbidity time series (black) plotted with EXO2 water level (blue) and tidal data from Ballyglass tidal gauge (grey). The hourly rainfall data above each plot (also in blue) are from the Dooagh water treatment plant, south-west Achill Island	61
Figure 6.16.	High-resolution (15 min) tryptophan fluorescence time series (black) plotted with EXO2 water level (blue) and tidal data from Ballyglass tidal gauge (grey). The hourly rainfall data above each plot (also in blue) are from the Dooagh water treatment plant, south-west Achill Island	61

## List of Tables

Table 1.1.	Conservation status of Annex I sand dune habitats at study site	7
Table 2.1.	WP2 objectives	13
Table 2.2.	Observed changes in elevation across each profile	21
Table 2.3.	Details of storm events observed during study	22
Table 3.1.	WP3 objectives	26
Table 4.1.	WP4 objectives	30
Table 5.1.	WP5 objectives	37
Table 5.2.	Transformation of Domin scale values in the Biomar study to percentage cover values	38
Table 5.3.	Plant functional traits used to assess machair sites	38
Table 5.4.	Plant species composition cover in Doogort machair, County Galway, as recorded from the Biomar 1995 surveys and our 2016 resurveys	39
Table 5.5.	Habitat cover change (%) at Doogort from 1995 to 2016	40
Table 5.6.	CWM trait values for SLA, CH, LDMC, SM, TV, Ellenberg L and Ellenberg N across all six sites	42
Table 5.7.	Mason index of functional diversity for SLA, CH, LDMC, SM, TV, Ellenberg L and Ellenberg N across all six sites	42
Table 5.8.	Mean values for the Simpson index, SLA, CH, LDMC, SM, TV, Ellenberg L, Ellenberg N and functional diversity across all six sites	42
Table 6.1.	Typical values for EC	48
Table 6.2.	WP6 objectives	50
Table 6.3.	EXO sensors specifications	51
Table 6.4.	ISCO programmes run during the monitoring period	52
Table 6.5.	Dates of sensor calibration	53
Table 6.6.	Descriptive statistics and summary of data collected for each water parameter	57
Table A1.1.	Spearman's rank correlation matrix for all data (WP6)	82
Table A1.2.	Spearman's rank correlation matrix for summer 2016 (June to August)	82
Table A1.3.	Spearman's rank correlation matrix for autumn 2016 (September to November)	82
Table A1.4.	Spearman's rank correlation matrix for winter 2016/2017 (December to February)	83
Table A1.5.	Spearman's rank correlation matrix for spring 2017 (March to May)	83

Table A1.6.	Spearman's rank correlation matrix for summer 2017 (June to August)	83
Table A1.7.	Spearman's rank correlation matrix for autumn 2017 (September to November)	84
Table A1.8.	Spearman's rank correlation matrix for winter 2017/2018 (December to February)	84
Table A1.9.	Spearman's rank correlation matrix for spring 2018 (March to May)	84



# Executive Summary

Climate action to “build capacity” and “increase climate resilience” is now implemented in Irish policy via the Climate Action Plan 2019 and the National Adaptation Framework (NAF). It is a fundamental scientific requisite that any insights into building landscape resilience in Ireland need to be facilitated by extensive regional monitoring programmes, in terms of both the forcing processes and system response (via states, triggers, thresholds and feedback mechanisms). This is to address the major challenge of developing predictive tools to extrapolate the impacts from projected climate changes, such as extreme storminess, rising sea levels and changing temperatures and precipitation patterns (Devoy, 2015a; EPA, 2017). This report provides a summary of results from a series of integrated, multidisciplinary field experiments (called work packages, WPs) that monitored the behaviour of a coastal catchment during fairweather and storm conditions over a 2-year period at Golden Strand, Achill Island, County Mayo.

The results from beach morphology monitoring illustrated that Golden Strand is attuned to high-energy wave conditions and seems to be largely insensitive to storms observed during the monitoring programme. This supports previous findings in western Ireland that beaches and dunes exposed to high-energy wave regimes require extreme storms to cause significant morphological change (Cooper *et al.*, 2004; Williams *et al.*, 2015). This closed beach system is geologically controlled and is compartmentalised by two prominent headlands, with sediment being supplied from offshore and/or adjacent cliffs that have visual evidence that they are chronically eroding. It is uncertain how much time is needed or what combination of conditions (or “drivers”) needs to occur (wind direction, coastline orientation, tidal stage, water level, antecedent state of the beach) for a substantial volume of sediment to be removed and push the system landwards via rollover processes. What we can infer is that the likelihood of these conditions coinciding increases if the number of storms and their intensity increases (EPA, 2017). The extent to which Golden Strand will undergo significant process and domain changes over time to break the existing “cyclical” operation (cross-shore sediment

exchanges) is difficult to assess on account of the uncertainty about the nature of storms required to generate change (Devoy, 2015a; Williams *et al.*, 2015). The results of this WP need to be supplemented with more field monitoring programmes. For example, the Irish coastline varies significantly in terms of static (geology, orientation, sediment size and abundance) and dynamic (wave, tide) conditions (Scott *et al.*, 2011; Masselink *et al.*, 2016a), resulting in very diverse coastal environments (beaches, dunes, cliffs, barriers, lagoons, estuaries, embayments, mudflats, saltmarshes). One model does not fit all.

The coastal dune system is an inherently dynamic geomorphological landform that has high sensitivity to water fluxes (groundwater and near-surface flow) through the system and climate shifts. The near-surface water (vadose zone) of dunes influences species diversity. However, it is unknown how this vadose zone or vegetation cover (type and distribution) will respond to significant changes in climate (e.g. hotter, drier summers and warmer, wetter winters). The results from this project indicate that an analysis of vegetation effects on dune stability and salinity would be beneficial in order to model dune evolution. The monitoring of the machair system in the study catchment suggests that it is already showing evidence of transitioning to a new state that is more representative of a fixed dune or wet machair system. The recommendations from this project suggest reducing and/or changing the existing grazing regime (from sheep to cattle) and reducing soil-compacting practices to enhance machair stability and longevity.

The groundwater study recommends that future work should take a four-dimensional approach and consider the physical make-up of the study site in terms of location and depth (seating it in a geological context). The results from hydrological monitoring illustrate why any period of future monitoring should be longer (at least 10 years) to more effectively capture inherent environmental variability. Building an empirically based understanding of process–response to extreme climate events will require investment in multidecadal-scale monitoring programmes. Although suspended

sediment concentrations reported in this study carry high uncertainty, potentially short-lived, elevated fluxes of carbon-rich sediment from peatland catchments

warrant further investigation and this should be carried out alongside quantification of dissolved organic matter loads.



# 1 Introduction

One of the key challenges facing Ireland in the coming decades is to increase our resilience to extreme weather events that are affecting, in many cases in devastating ways, our natural and built environments. The case for building resilience in Ireland is urgent given that the causes of vulnerability are embedded in the chronic degradation of our ecosystems and pervasive threats of a changing climate. The capacity for our ecosystems to regenerate after extreme events and maintain the delivery of critical ecosystem goods and services essential to human livelihoods can no longer be taken for granted (Adger *et al.*, 2005). The Climate Action Plan 2019 (DCCAE, 2019), released by the Irish government to tackle climate breakdown between now and 2030, and also leading up to 2050, is arguably very ambitious. A key element of the plan is the National Adaptation Framework (published in January 2018), which focuses on climate adaptation to reduce our vulnerability to climate change impacts that are already locked and which will continue to evolve for the foreseeable future (DCCAE, 2019).

It is a fundamental scientific requisite that any insights into building landscape resilience in Ireland need to be facilitated by extensive regional monitoring programmes, in terms of both the forcing processes and system response (via states, triggers, thresholds and feedback mechanisms). This is to address the major challenge of developing predictive tools to extrapolate the impacts from projected climate changes, such as extreme storminess, rising sea levels and changing temperatures and precipitation patterns (Masselink *et al.*, 2016b; EPA, 2017).

We may have implemented new climate policy and climate adaptation plans, but it is imperative to also resource the scientists so that adaptation strategies can be designed with known degrees of certainty (low–medium–high). Currently, we would argue that there is a paucity of long-term observational data in Ireland of how our geomorphic and hydrological systems respond and/or recover in the aftermath of low-frequency, high-magnitude climate events. It is critical to acknowledge that to fully grasp the implications of a changing climate in Ireland for our natural landscape systems, we need to understand the complexity

that drives the variability within these systems (climate, hydrological, geomorphological, biological, biogeochemical, geological, ecological) where one small change, or tipping point, in one system can lead to numerous significant, and sometimes irreversible, changes in one or more connected systems (Devoy, 2015b).

Furthermore, ecosystems influence, and are influenced by, the dynamics of the surfaces they inhabit and have been equally neglected in long-term monitoring programmes. Without scientific understanding, linking cause and effect with any degree of confidence becomes imprudent, at best, and any long-term management strategies for our geomorphic and ecological systems (uplands, rivers, peatlands, soils, coasts) may be ineffective, especially in practice.

This research project addresses these challenges by implementing a 2-year monitoring programme using state-of-the-art technology deployed in a series of seven integrated work packages (WPs) to observe geomorphic (beach–dune), hydrological (stream; groundwater) and ecological (dune; machair) systems in a small coastal catchment in Achill Island, County Mayo.

## 1.1 Work Packages

Each WP in the project was designed to be an independent, stand-alone project that provides, at the very least, (1) baseline field data measuring components of a coastal catchment on the west coast of Ireland and (2) the geomorphic, hydrological and/or ecological response of part of the catchment system to fairweather and storm conditions.

### 1.1.1 WP1: preliminary work

The work from WP1 comprised developing working partnerships with Mayo County Council (MCC), the Environmental Protection Agency (EPA), the National Parks and Wildlife Service (NPWS) and the Western River Basin District in Ireland to obtain permission to conduct the field experiments and to engage with them

as important stakeholders. Each WP leader completed a desktop study to review the relevant scientific, planning and policy literature in Ireland pertaining to their WP.

### ***1.1.2 WP2: response of beach–dune systems to Atlantic storms***

WP2 measured the geomorphological response of beach–dune systems to storms using repeat cross-shore profile surveys to observe the sediment exchange between the beaches and dunes. Documenting sediment exchange between the beach and dune systems through periodic resurveying is critical to assess the resilience of coastal dune ecosystems – especially as they are a valuable defence against flooding and function naturally as a control on coastal erosion. Since, and including, winter 2013–2014, research on the impacts of storm on coastlines dominated by extensive beach–dune systems has been extensively documented throughout north-west Europe, in particular in the UK (Loureiro *et al.*, 2014, 2016; Dissanayake *et al.*, 2014, 2015a,b; Spencer *et al.*, 2015; Masselink *et al.*, 2016b; Scott *et al.*, 2016; Burvingt *et al.*, 2017; Guisado-Pintado and Jackson, 2018; Loureiro and Cooper, 2018), France (Coco *et al.*, 2014; Castelle *et al.*, 2015), the Netherlands (Keijser *et al.*, 2015; de Winter and Ruessink, 2017) and Ireland (Loureiro *et al.*, 2014, 2016; Kandrot *et al.*, 2016; Masselink *et al.*, 2016b; Guisado-Pintado and Jackson, 2018; Loureiro and Cooper, 2018). These experiments mostly report the morphological response of spaced cross-shore beach profiles (generally represented as the beach area extending from the low-water mark to the dune crest). These monitoring programmes provide critical information on the beach elevation changes and shoreline position for different storm-type events (dune breakdown) and/or fairweather conditions (dune building). The generic controls that influence all coasts occur in different combinations over varying time and spatial scales. These controls include, but are not limited to, wave–wind action, storm surge, tides, relative sea level, geological configuration, nearshore and offshore bathymetry, accommodation space and sediment budgets (Devoy, 2015b). The magnitude of their respective roles cannot be assessed without relevant long-term monitoring data on the drivers and responses (O'Connor *et al.*, 2011); however, even then, conventional experimental approaches

consider only single (mostly) or coupled (rarely) parts of the nearshore–beach–dune (NBD) continuum. This WP provides similar information related to changes in beach morphology as reported in the north-west Europe and UK case studies referenced previously for the west coast of Ireland.

### ***1.1.3 WP3: tracing internal moisture and salinity changes in dunes***

Moisture and salinity are two key factors that affect dune stability, but there is a paucity of research on internal dune hydrology and salinity in Ireland. WP3 reports baseline environmental data that traced internal moisture and salinity dynamics within the near-surface water (vadose) zone of the coastal dune system in the west of Ireland.

### ***1.1.4 WP4: groundwater dynamics in a coastal sand dune***

The coastal dune system is an inherently dynamic geomorphological landform. It is highly sensitive to water fluxes (groundwater and near-surface flow) and climate shifts. In coastal zones, the natural equilibrium between seawater and freshwater is still poorly understood, largely because of the complex mixing processes found in such heterogeneous environments. For example, the winter storms of 2013/2014 perturbed the western coastal dune system, causing erosion, destabilisation and a fresh supply of sediment. The vadose zone of dunes influences species diversity but it is unknown how this vadose zone responds to significant erosion and depositional events. This poor understanding has limited our knowledge of the fundamental drivers of change in coastal dune field dynamics. WP4 (and WP6) observed surface and subsurface flows to get a better understanding of the groundwater regime in a sand dune system.

### ***1.1.5 WP5: plant functional diversity and habitat change in a machair system***

Coastal sand dunes are considered extremely resource rich in terms of their ecological and economic functions. Plant species also play an important role in ecosystem functions, such as nitrification and nutrient cycling. Current threats to coastal systems, such as erosion, have been intensified by human interference via recreational and exploitive activities,

and in some cases have resulted in the stabilisation of dune habitat (Kindermann and Gormally, 2010) via soil compaction and increased erosion susceptibility via vegetation openings (blowouts) that exposed larger areas to erosion (Liddle and Grieg-Smith, 1975; Cooper *et al.*, 2005). The main effect of this is a loss of important vegetation structure and habitat that reduces the system's ability to absorb energy from storm events. We mapped plant communities to assess the response of these natural and managed ecosystems to extreme events that occurred during the time of the project (storms). Characteristic plant communities reflect both past and current environmental pressures and conditions. Plant community assessment and management have historically focused on species diversity and richness components. However, more recently, research in plant functional traits to determine functional diversity has gained significant attention (Diaz and Cabido, 2001). The assessment of habitat changes over time, together with an assessment of habitat quality and investigation of current land use and threats, can be used to determine appropriate site management. Based on the overall understanding of dune processes, the main aim of WP5 was to assess the changes in a coastal system containing machair habitat over a 20-year period and investigate possible causes, both anthropogenic and natural, of plant community and functional change.

#### ***1.1.6 WP6: hydrology, water quality and catchment exports***

Patterns in the sediment routing system (transport of sediment and solutes from the net erosional – the “source” – to the net depositional – the “sink” – parts of the system) were observed in WP6. This WP focused on hydrology, water quality and the export of waterborne sediment and pathogens from the catchment draining into the Golden Strand area. The principal aim of WP6 was to investigate how catchment exports influenced the coastal zone under a range of flow conditions, including extreme events. The water quality parameters that were selected for monitoring were temperature, pH, electrical conductivity (EC), dissolved oxygen (DO), turbidity (as a proxy for suspended sediment concentration – SSC) and tryptophan fluorescence (as a proxy for faecal-based coliforms). A subsidiary aim of WP6 was to explore process interactions through the

high-resolution monitoring of a range of water quality parameters and explore linkages to field observations from the coastal and dune surveys (WP2) and ecological investigations in the machair zone (WP5).

#### ***1.1.7 WP7: dissemination, final report and communication***

The EPA-funded project Ireland's Climate Information Platform (ICIP) has developed a one-stop, web-based resource of climatic and adaptation information for Ireland. More specifically, ICIP aims to facilitate decision-makers in Ireland in planning for climate change adaptation. Upon approval of the final report, WP7 will provide the results to ICIP and share a synopsis of the project results with two key stakeholders: MCC and the local community.

### **1.2 Study Site: Golden Strand, Achill Island, County Mayo**

This study explicitly links catchment and coastal processes in a small coastal catchment on Achill Island, County Mayo (Figures 1.1–1.4), dominated by Atlantic blanket bog, by detecting and characterising the geomorphic and ecological response to extreme events and perturbations. The Golden Strand site was chosen because it contains all the characteristics identified by the team required to complete each WP:

- The catchment is small (<10 km<sup>2</sup>).
- There is an extensive beach–dune system.
- The catchment includes a Special Area of Conservation (SAC) for a zone of machair located adjacent to the dunes.
- The surface hydrology of the area is dominated by an unnamed stream that drains a predominantly peatland catchment with no evidence of human engineering, apart from a minor road bridge located towards the mouth of the stream. The downstream side of this road bridge was a suitable monitoring site for WP5, as it provides a secure and stable location for the monitoring set-up.

#### ***1.2.1 Study site: beach, dune and machair systems***

The study site was chosen because a dune system extends along the entire beach and is very susceptible

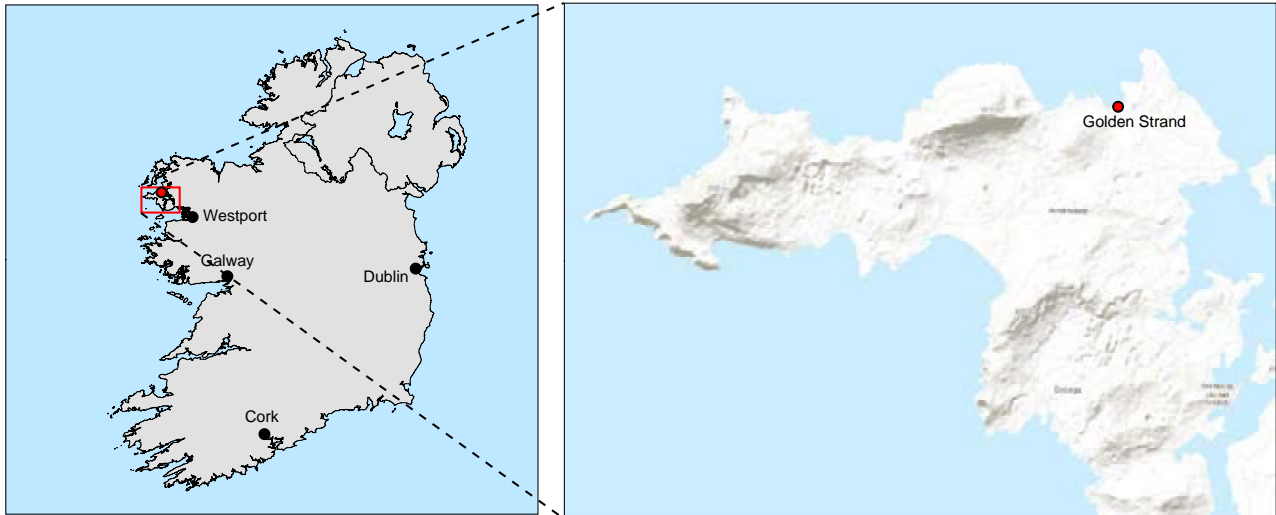


**Figure 1.1. Location of Golden Strand, Achill Island, County Mayo.**



**Figure 1.2. Overview of WP monitoring locations in the study catchment. Map data: Google, CNES, Airbus © 2020.**

to Atlantic storms all year round and especially so during the winter. The foredune system is pronounced with an easily discernible vegetation line (Figures 1.3 and 1.4). The dunes are densely vegetated with the common dune-building species *Ammophila arenaria* (marram). Visual observations showed that the vegetation structure changes dramatically

during the winter months, when sustained onshore winds move sand landwards from the beach across the dune, burying the vegetation. The dune system also comprises individual embryo dunes that form along the back beach above the high-tide mark and represent the initial stages of sand dune formation. These embryo dunes comprise unstable low hills or





**Figure 1.3. Aerial photographs showing locations of beach, dune, machair and stream systems of Golden Strand.**



**Figure 1.4. Aerial photograph of Golden Strand catchment, Achill Island, County Mayo.**

mounds of sand that rarely exceed 0.5m in height. They are sparsely vegetated but typically accumulate on Irish beaches in situations where salt-tolerant

plants, such as sand couch (*Elytrigia juncea*), lyme grass (*Leymus arenarius*), sea rocket (*Cakile maritima*), saltwort (*Salsola kali*) and sea sandwort

(*Honckenya peploides*), impede the movement of wind-blown sand. There are strong sediment exchange processes observed between the beach and dune systems. Further inland the stabilised fixed dunes are vegetated predominantly with marram and are mostly independent of the beach–dune sediment exchange process. In between these elevated dunes, the dune slacks comprise depressions that are wet for long periods during the winter after extended rainfall events. These depressions are close to the water table and are dominated by unidentified mosses and lichens. The beach mainly comprises medium- to coarse-sized sand grains (0.29–0.52 mm) and has a tidal range of 4.57 m using the UK Hydrographic Office (UKHO) VORF-08 model (UKHO, 2008).

The Golden Strand catchment forms part of the Doogort Machair/Lough Doo SAC (SAC 001497), Doogort East Bog Natural Heritage Area (NHA 002381) and Doogort Machair Special Protection Area (SPA 004235) (Figure 1.5). Two EU Annex I dune habitats were recorded in the Doogort Machair/Lough Doo SAC by Ryle *et al.* (2009), one of which, “machairs” (96.9 ha), is listed as a qualifying interest

for the SAC. The second mobile dunes habitat, “shifting dunes along the shoreline with *Ammophila arenaria*” (1.07 ha), was also recorded, but it is not a qualifying interest for the SAC (Figure 1.6). In the most recent report the condition of the mobile dune system at the study site was listed (Ryle *et al.*, 2009, p. 102) as “unfavourable – inadequate” and subject to natural erosion compounded by human activities. Machair is characterised by low-lying, fertile grassland that provides a habitat rich in biodiversity that is highly sensitive to changes in land use and climate (Gaynor, 2006). Machair habitat is rare both in Ireland and globally, and is protected under EU and Irish law. According to Crawford *et al.* (1998) there were only badly eroded relic foredunes present. Based on previous monitoring work, the future prospect of the mobile dunes is “unfavourable – inadequate”, with an overall EU designation rating of “unfavourable – bad” and an overall Irish assessment rating of “unfavourable–declining” (Table 1.1). The machair habitat, which is protected under the EU Habitats Directive (92/43/ECC), requires particular protection on account of its limited distribution and risk from habitat



**Figure 1.5. Boundaries of the protected areas in the study catchment. Doogort Machair/Lough Doo SAC (SAC 001497), Doogort East Bog Natural Heritage Areas (NHA 002381) and Doogort Machair Special Protection Area (SPA 004235). Map data: Google, CNES, Airbus © 2020.**





Figure 1.6. Distribution map of sand dune habitats, including machair, within Doogort Machair/Lough Doo SAC. Source: NPWS, 2017 (Appendix I, p. 17).

Table 1.1. Conservation status of Annex I sand dune habitats at study site

Habitat	EU conservation status assessment			Overall EU conservation status assessment	Proposed Irish conservation status system
	Favourable	Unfavourable – inadequate	Unfavourable – bad		
<b>Machair</b>		Extent, structure and functions; future prospects		Unfavourable – inadequate	Unfavourable – declining
<b>Mobile dunes</b>		Extent; future prospects	Structure and functions	Unfavourable – bad	Unfavourable – declining

Source: NPWS, 2017 (Table 114C, p. 18).

loss (O’Keeffe, 2008). In addition to the Annex I-listed habitats machair and grey dune, an Annex II species, petalwort (*Petalophyllum ralfsii*), has been recorded at this site; alongside machair it is one of the qualifying interests of the site (NPWS, 2013a).

### 1.2.2 Study site: geological setting and links to subsurface flow dynamics

The focus of WP4 was to better understand the behaviour of water in and on the ground. Therefore, to better understand how water interacts with the ground

it is important to characterise the make-up of the catchment. The key control on the shape and nature of the catchment is the bedrock geology.

The western portion of Mayo from Achill to Belmullet has a complex geology spanning more than 1 billion years. Some of the oldest rocks in Ireland are found in the Annagh area, several kilometres north of the study area, with the gneisses having ages of 1.6 billion years, whereas the youngest rocks – Devonian sandstones, which are approximately 390 million years old – are found around Mulranny on the north side of Clew Bay. The entire study area is underlain by rocks

that are approximately 700 million years old. Rocks of this age in this area are referred to as Neoproterozoic rocks of the Dalradian Supergroup (Long *et al.*, 1992). In the study area these are the Ridge Point Psammitic Formation and the Dooega Head Formation (Figure 1.7a). Both of these originated as sediments that were lithified to form sedimentary rocks, which were subsequently heated and pressurised to become the metamorphic rocks present in the study area. The parent material or sediment that formed the Ridge Point was probably a clay or very fine silt, and these sediments would have been laid down in deep, still water with little energy. They are now typically banded, grey to creamy white psammitic schists with thin semi-pelitic schist interbeds, with some calc-silicate bands. Heavy mineral bands are locally common, and cross-bedding is common throughout the formation. These bands would have formed after the initial rock was formed. The Dooega Head Formation is a bit more mixed in make-up, suggesting that the parent materials

were clay and silt, but with interbedded fine sands, suggesting a relatively quiet environment that had occasional inputs of coarser materials (sand). These are now predominantly composed of pale quartzites and psammitic schists with heavy mineral bands and cross-bedding. Both lithologies are more psammitic in the upper part and thin pelitic interbeds are common. These old rocks are resistant and very tough, and they are seen in outcrops at either end of the beach, at Gubaphorteen to the west and at Caraun Point to the east. The rocks dip steeply to the north-east ( $35\text{--}52^\circ$ ), mirroring the dip of cleavage and schistosity (crudely, these are the angles the beds are lying at – the rocks are sloping at relatively steep angles to the north-east). This observation is important in understanding the potential for controlling water movement in and on the rock.

In the study area there are effectively three separate catchments (Figure 1.7b):

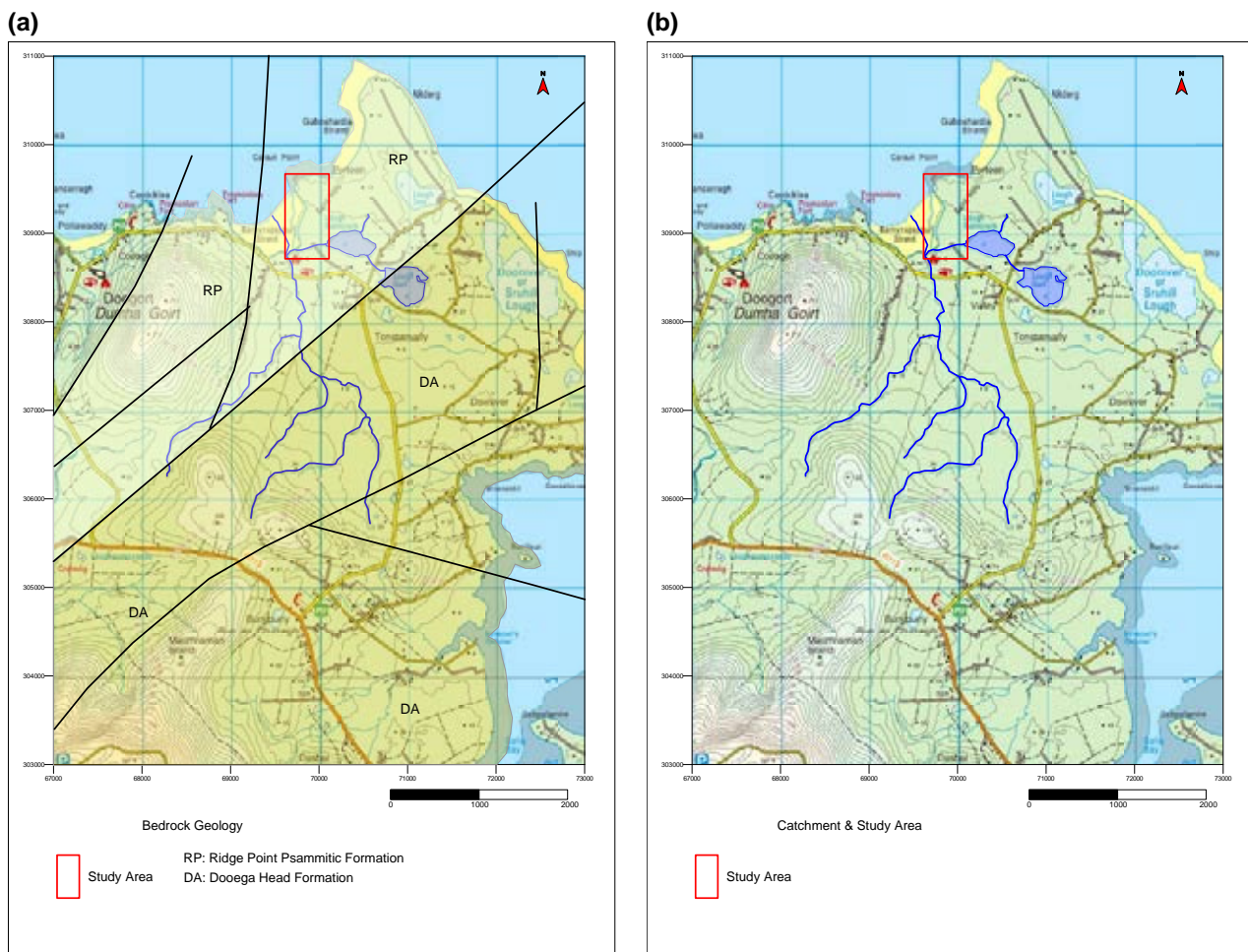


**Figure 1.7. (a) Local bedrock geology: RP, Ridge Point Psammitic Formation; DA, Dooega Head Formation. (b) Study catchment area (groundwater study site in red reference box).**



1. Barnynagappul stream. This drains an area of approximately 7.2 km<sup>2</sup> and the catchment is defined by high ground to the south and west and low-lying topography to the east. The river discharges directly to the bay, running across Barnynagappul Strand. The course of most of the river has not changed since it was first mapped in 1837–1841, except for its behaviour on Barnynagappul Strand. Where the river now discharges directly across the sand (to the north), it had previously flowed north-eastwards across the beach, discharging close to Caraun Point.
2. Lough Nambrack and Lough Gall. This drains an area of approximately 1 km<sup>2</sup>, immediately to the east of the Barnynagappul catchment. This area is low-lying, peaty and at an elevation of around 10–15 m above sea level. Lough Gall drains to Lough Nambrack, which discharges to the Barnynagappul stream on Barnynagappul Strand. The two systems are not otherwise connected.
3. Barnynagappul dune system. The dunes cover an area of approximately 0.1 km<sup>2</sup>. The functioning of the dune hydrology is the key focus of this WP. As previously stated, this system operates independently of the other two catchments.

The controls on these catchments are geological and topographical: the type and nature of the bedrock geology directly affects the ability of water to percolate to ground. Geological Survey Ireland (GSI) has classed the entire area (indeed all of Achill and most of north-west Mayo) as a “Poor Aquifer – Bedrock which is Generally Unproductive except for Local Zones” (GSI, 2020). This classification reflects the nature of the bedrock described previously. These thinly bedded schists and quartzites were squeezed and compacted through time and they have little connected space. From a groundwater perspective, these rocks are relatively impermeable (water will run off them or pool on them rather than get into them). Aquifers are rock or sediments that can store and transmit water but, in this case, these rocks exhibit very low transmissivity and storativity – they are poor aquifers. There is no evidence of fault controls on flows or any indication of faulting beneath the dune system. The bedrock exhibits extremely low values of hydraulic conductivity (expected to be within the range of  $3 \times 10^{-14}$ – $2 \times 10^{-10}$  m/s (Domenico and Schwartz, 1990). Consequently, disposition of the rainfall in the dune

system will be limited to losses to evapotranspiration, storage in the dune and discharge from the dunes to the sea. A geophysical investigation carried out by National University Ireland Galway (NUIG) researchers in 2018 suggests that the dune system is underlain by a low-permeability silt/clay deposit, probably related to deposition in standing water conditions. These fine sediments further isolate the dune (hydrologically) from the surrounding land. Rainfall across this entire area will be confined to the surface or shallow overburden within the dune.

The Achill Rovers football pitch and grounds are located between the dunes and Lough Nambrack, and anecdotal evidence collected by Dr Tiernan Henry in 2017 from members of the football club indicates that the portion of the pitch closest to the stream (running parallel to the stream draining Lough Gall and Lough Nambrack noted previously) is particularly poorly drained, whereas the others parts of the pitch drain freely. This suggests that the finer material identified in the geophysical survey is at or close to the surface adjacent to the stream.

### **1.2.3 Study site: hydrology**

The surface hydrology of the Golden Strand area of Achill Island is dominated by an unnamed stream that drains a predominantly peatland catchment and a number of small (<1 km<sup>2</sup>) lakes (some interconnected) in the coastal zone (Figure 1.8a). The second-order stream is approximately 3.7 km in length and has a catchment area of c. 11 km<sup>2</sup> (Figure 1.8a). This stream has been modified by a number of man-made ditches that have been cut to improve drainage for the harvesting of the peat. Most of the catchment is situated below the 50 m contour line (Figure 1.8b). Groundwater vulnerability ranges from low to extreme in this area, owing to the composition of peat and the shallow bedrock surface. In general, the regional aquifers have been described as poorly productive, with the exception of some localised areas. Soil types in the catchment are mainly blanket peat, with areas of loamy and sandy drift towards the coast producing mineral soils of variable permeability (Figure 1.9a). The corresponding Coordination of Information on the Environment (CORINE) land cover is categorised as peat bog, known as Doogort East Bog, with some localised areas of agricultural pasture (Figure 1.9b). Peat harvesting is widespread across the catchment, but locally cut drains and harvested areas did not

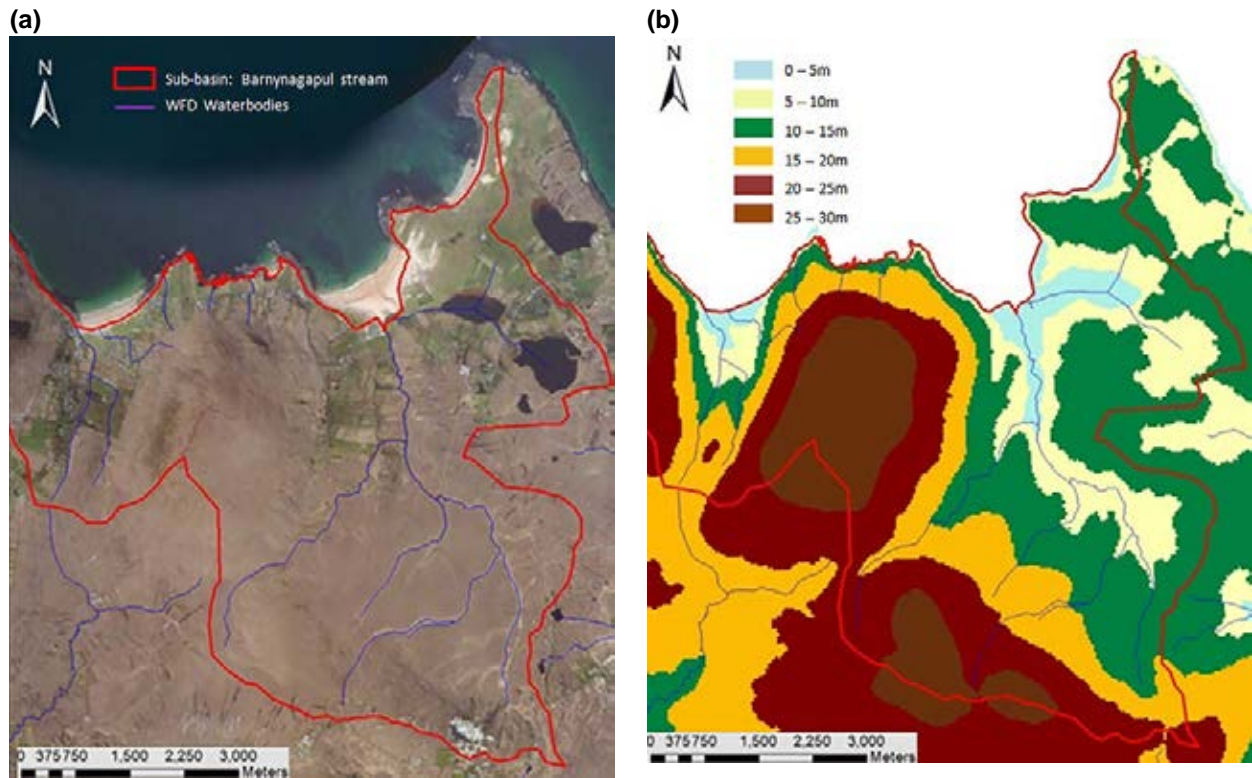


Figure 1.8. (a) Surface drainage of the Golden Strand catchment. (b) Elevation changes within the Golden Strand catchment. Map data: Google, CNES, Airbus © 2020.

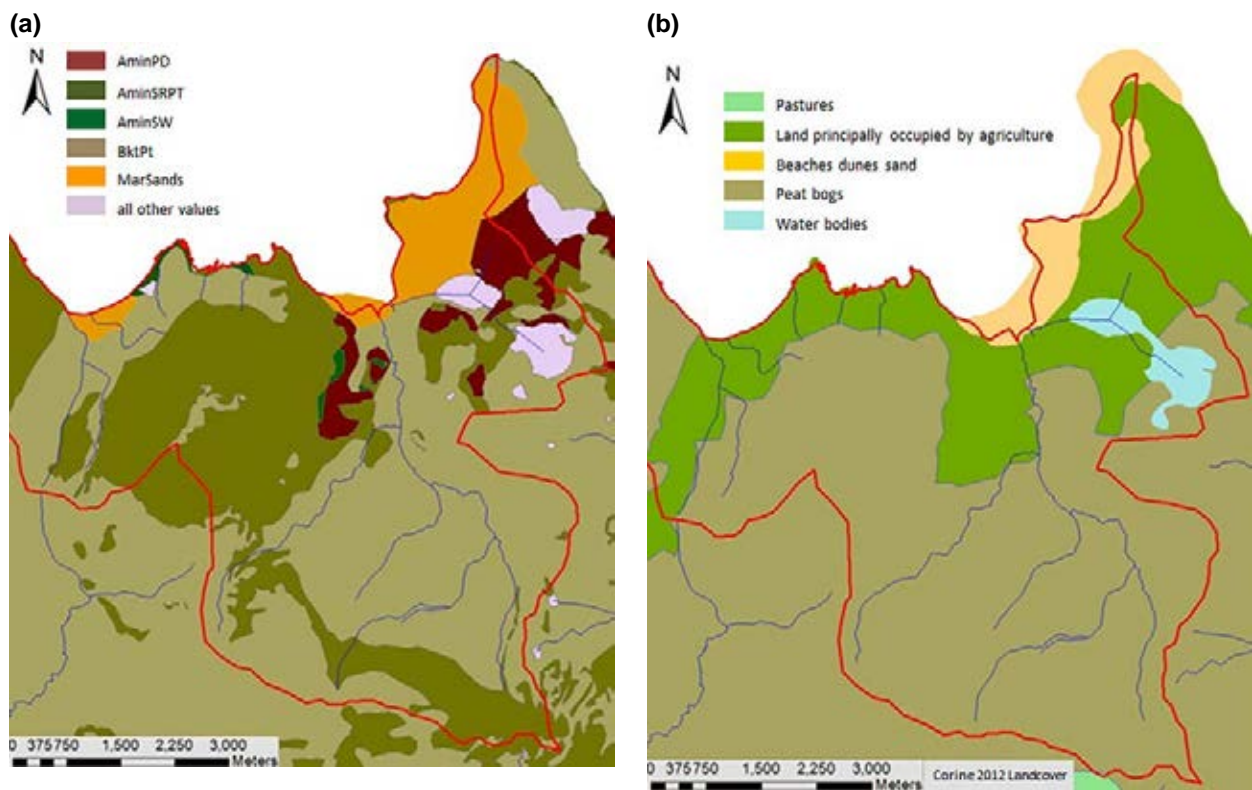


Figure 1.9. (a) Soil map of the Golden Strand catchment. (b) CORINE landcover map of the Golden Strand catchment. AminPD, mineral poorly drained (mainly acidic); AminSRPT, shallow, rocky, peaty/non-peaty mineral complexes; AminSW, shallow well drained mineral (mainly acidic); BktPt, blanket peat; MarSands, marine sand and gravel.

appear to expose underlying weathered bedrock or Quaternary sediments during field walks of the catchment.

Oceanic blanket bogs contain a high percentage of water (up to 90% in the most natural areas) (Malone and O'Connell, 2009) and are typically poorly drained (Coll *et al.*, 2014). These bogs include areas covered by grassy vegetation that can be extensively grazed, as is the case for parts of the Doogort East Bog. The formation and maintenance of this type of bog require precipitation levels to be roughly three times greater than the rate of evaporation, and there are typically no dry periods (Coll *et al.*, 2014). Similar conditions are found in Achill Island, which experiences the mild winters and cold summers necessary for this type of peat (Malone and O'Connell, 2009). Average annual rainfall in Achill ranges between 1000 and 1400 mm, which is consistent with blanket peat requirements (Sottocornola *et al.*, 2009). Doogort East Bog is protected as a Natural Heritage Area on the grounds of its biodiversity and has previously been damaged as a result of draining and mechanical cutting activities in the north-east section (Malone and O'Connell, 2009).

Initial field observations in June 2016 showed no evidence of in-stream aquatic fauna or in-channel vegetation. Given the low pH of bog water-draining peatlands, this is not uncommon (Hem, 1985) and this furthermore suggested that bio-fouling of instrumentation was unlikely. Apart from a minor road bridge located towards the mouth of the stream, there was no evidence of human engineering, including bank protection. The downstream side of this road bridge was selected as the monitoring site for WP5 (section 6.4), as it provided a secure and stable location for the monitoring set-up and was the only viable location in the catchment. At the time of monitoring, the mouth of the stream was characterised by a low-elevation sand barrier that appeared to be acting as a hydraulic control. These bar features are relatively common in small catchments along sandy coasts in the west of Ireland. However, they are typically mobile features and may therefore be subject to adjustments in morphology and position (Cooper, 2006).

## 2 WP2 – Response of Beach–Dune Systems to Atlantic Storms

### 2.1 Introduction

Ireland has a long history of research on coastal processes and landforms. The body of work spans a broad range of approaches (e.g. ecological, geomorphological, sedimentological) and scales (millennial to instantaneous). The initial formation of our dune systems occurred through the reworking of material deposited during the breakdown of the last major ice sheet between 20,000 and 15,000 years ago.

After the retreat of the last ice sheets – c.10,000 years before present (BP) – there were significant fluctuations in sea level, which in turn controlled the availability of sediments for periods of dune building (Guilcher, 1961; Carter *et al.*, 1987; Carter and Wilson, 1991; Delaney and Devoy, 1995; Devoy *et al.*, 1996; Wilson and McKenna, 1996; McGourty *et al.*, 2000; Cooper, 2006). The Irish coast has been subject to a range of sea level histories (Carter *et al.*, 1987, 1989; Carter and Wilson, 1991) with marked regional differences, most notably between the north and south of Ireland. However, the coastal landforms are all very similar, which is a reflection of wave climate, sediment type and sediment availability (McKenzie and Cooper, 2001).

For our soft sediment coastlines, erosion and deposition patterns are natural responses to storms with different signatures (size, duration, direction, clustering) and represent a coastal systems resilience (Houser *et al.*, 2015; Scarelli *et al.*, 2017). The most prolific sources of sediment tend to be of glacial origin, remnants of the Pleistocene inheritance (Devoy, 2008, 2015b). The term paraglacial refers to environments developed on or adjacent to formerly ice-covered terrain of which the glacial landforms or glacial sediments have a strong influence on the nature and evolution of the coast (Church and Ryder, 1972). These sediments have been extensively reworked onshore by wind and waves following the retreat of the ice. This ample supply of coarse material being reworked and being made available to littoral processes has supplied our beaches, dunes, estuary

and lagoon infills, and saltmarshes (Delaney and Devoy, 1995). The sources of sediment feeding our geomorphic systems do not just lie offshore or within the soft cliffs lining the coast. Knight and Harrison (2018) provide a comprehensive review of how episodic sediment releases can occur from glacial moraines, landslides and debris torrents.

Research that has sought to track more recent long-term changes in our dune systems includes that looking at climate drivers (Wintle *et al.*, 1998; Duffy and Devoy, 1999; Orford *et al.*, 1999, 2005; Cooper *et al.*, 2009a; O'Connor *et al.*, 2011), combining historical data and field surveys (Carter, 1975; O'Connor *et al.*, 2007), estuary dynamics (Burningham and Cooper, 2004; Devoy *et al.*, 2006; Cronin *et al.*, 2007; O'Shea *et al.*, 2011), human-induced change (Harris, 1974; Orford, 1988), stratigraphy (Maloney, 1985), sea level (Carter, 1982; Smith *et al.*, 2012) and the Little Ice Age (LIA) (Orford *et al.*, 2005; Jackson *et al.*, 2019). At the other end of the spectrum, research into short-term processes that contribute to dune development adds to the broader understanding of beach–dune dynamics and, as such, is less site specific than macro- and meso-scale work. Some examples include the role of fetch effects (Jackson and Cooper, 1999; Lynch *et al.*, 2008), topographic steering of airflow (Lynch *et al.*, 2009; Beyers *et al.*, 2010; Delgado-Fernandez *et al.*, 2013), surf zone hydrodynamics (Carter, 1980a; Malvarez and Cooper, 2000; Huang *et al.*, 2002; Guisado-Pintado *et al.*, 2014; Williams *et al.*, 2015), sediment supply and shoreface dynamics (Swift *et al.*, 2006; Backstrom *et al.*, 2015; Jackson *et al.*, 2007) and geological control (Duffy and Devoy, 1999; Jackson *et al.*, 2005; Loureiro *et al.*, 2012; Cooper *et al.*, 2018).

Other contributions to an understanding of Irish coastal dunes include ecological and vegetation studies (Wilcock and Carter, 1977; Carter, 1980b; Lamhna, 1982; Curtis, 1991a; Gardner *et al.*, 2019) and inventories (Bassett and Curtis, 1985; Curtis, 1991b; Quigley, 1991; Ryle *et al.*, 2009; Farrell and Connolly, 2019).

There is also a large body of literature on management practices and planning of the Irish coast (Power *et al.*, 2000; McKenna *et al.*, 2007, 2009; Cooper and McKenna, 2008; Gault *et al.*, 2011; Kindermann and Gormally, 2013; Devoy *et al.*, 2015a,b). More recent research has examined the degradation of dune ecosystem services by seasonal tourism activity (Farrell, 2018; Farrell *et al.*, 2020).

A changing ocean climate will have substantial impacts on large tracts of the Irish coastline. The frequency of intense cyclones (EPA, 2017), the height of waves (Dunne *et al.*, 2008) and sea levels (Church *et al.*, 2013) are all projected to increase over the next century (IPCC, 2018). In Ireland, this will increase coastal inundation and erosion rates from storm events (Devoy, 2008; Cooper and Pile, 2014). There is unequivocal evidence that the resilience of Irish beaches and dunes will decrease in many parts of the country and, in some cases, especially where mobility is not a valid response to anthropogenic pressures, these ecosystems will rapidly degrade (and/or be lost), with the loss of valuable ecosystems services (NPWS, 2013b; Martins *et al.*, 2018; Gardner *et al.*, 2019; Farrell and Connolly, 2019). However, the caveat is that beaches are highly variable in form and setting, and it is widely accepted that there is no single response to storms or sea level rise (Guisado-Pintado and Jackson, 2019; Cooper *et al.*, 2020). The site-specific nature of coastal response (local, regional and global factors) and the temporal variability means that we need to collect appropriate datasets to support coastal evolution models. These datasets should, preferably, span years to decades and include local environmental factors such as coastal morphology, sediment budgets, rates of sea level rise and nearshore dynamics (Cooper *et al.*, 2020).

WP2 focuses on event scales, and the broader international context is described in detail in section 2.2. This WP was designed to monitor a beach–dune system over a 2-year period to understand the climate drivers, processes, mechanisms, feedbacks and thresholds associated with its functioning in order to assess its resilience. Resolving how this site and others will respond to climate change projections (increased storm frequency and intensity) in the coming century cannot be done without first mapping their trajectories to current forcing using longitudinal monitoring programmes.

### 2.1.1 WP objectives

The list of WP2 objectives is provided in Table 2.1. Objectives 1 and 2 are addressed in this section. Objective 3 has been moved to WP6.

## 2.2 Beach–Dune Response to Storms

The ability of a storm event to cause significant change to a beach–dune system is related to the amount of energy it has. This is because energy is required to move sediment, and the more sediment that is moved, the greater the potential change. The power of a storm may be quantified using a power index using the units  $\text{m}^2/\text{h}$  (e.g. Dolan and Davis, 1992; Karunarathna *et al.*, 2014) or using specific physical characteristics directly related to erosion, such as wind speed or significant wave height (e.g. Roberts *et al.*, 2013; de Santiago *et al.*, 2017). Along with the storm size, water level is a critical factor in the effectiveness of a storm to do geomorphic work. This can occur as a result of a combination of storm surge, high tide and low atmospheric pressure. The duration of a storm is important, as the longer a storm lasts, the more time erosive forces are at work. In addition, in the later stages of a longer storm the beach–dune system may be in a weakened state as a result of erosion earlier in the storm. Longer storms also increase the likelihood of storm surge and high tide coinciding. The storm track, local geomorphology and coastal orientation can cause local to regional variations in the erosive power of any one storm (Guisado-Pintado and Jackson, 2018).

The response of beach–dune systems to storm events is controlled by three principal factors: (1) its inherent ability to resist erosive forces (dependent on dune size, morphology, vegetation cover), (2) its biophysical condition prior to and after the event (dependent on morphological/system state, synchronisation of

**Table 2.1. WP2 objectives**

Objective	Description
Objective 1	Measure the geomorphological response of beach–dune systems to storms
Objective 2	Determine the nearshore controls on sediment exchange between the beaches and dunes (what conditions are conducive to beach and dune construction?)
Objective 3	Measure the impact of floods on water quality in the nearshore and catchment

recovery mechanisms, accommodation space, human impacts) and (3) the characteristics of the storm event(s) (dependent on size, direction, duration) (Defeo *et al.*, 2009; Houser, 2009; Micallef and Williams, 2009; Masselink and van Heteren, 2014; Silva *et al.*, 2016; Guisado-Pintado and Jackson, 2018). In a general sense, relatively large (hundreds of metres in length) beach–dune systems on high-energy coasts are in tune with the prevailing conditions (Cooper *et al.*, 2004). They are able to reshape themselves over time depending on the level of energy inputs. High energy during storms may erode the beach and dunes, moving sediments offshore. Fairweather conditions between storms may move the sediment back onshore. In this way these systems are able to absorb the impacts of even very large storms (it is also one of the reasons why they are known as “barrier” systems, as they act as a barrier to storm effects further inland). It is this type of beach–dune system that is under consideration in this project. Although coastal systems may indeed have evolved to a type of equilibrium state, balancing their form and long-term weather patterns, the onset of climate change places new stresses on them to readjust and find new equilibria. The new climate stresses come at a time when existing challenges in Ireland of coastal management (Devoy, 2008; Cooper *et al.*, 2009b; McKenna *et al.*, 2009; Flannery *et al.*, 2015) and a sediment deficit (Carter *et al.*, 1987; Crapoulet *et al.*, 2015) are ongoing.

### **2.2.1 Conceptual models of beach–dune resilience**

Previous field experiments have investigated the effects of storms on coastal beach systems, establishing that storms exert a significant degree of control on short-term coastal evolution (e.g. Cooper *et al.*, 2004). This coastline adjustment can occur during a single storm or, as experienced during winter 2013–2014, during a series of closely spaced storm events within a storm season. Post-storm dune recovery processes were first documented by Carter *et al.* (1990), who observed that sequences of undercutting, slumping and reforming of dune slopes led to the recovery of the cross-shore topographic profile to its initial pre-storm position. However, this sequence of recovery is preconditioned by various dependencies such as sand availability, wind conditions and accommodation space (Suanez *et al.*,

2012). An alternative to the idea that large storms cause more change is that storms of equal size may have contrasting effects on coastal morphology, with antecedent conditions playing an important role. Beaches and other barrier systems in high-energy environments in north-west Europe may be considered to be in balance with the energy inputs. This equilibrium is dynamic, with erosion events followed by periods of recovery. If, however, a sufficient time does not pass before a new erosive storm arrives, this new storm will encounter a different coastline from the preceding storm, i.e. the antecedent conditions will be different. The second storm in the sequence, although similar in size, may cause greater change than the first storm (Woodroffe, 2002; Coco *et al.*, 2014; Loureiro *et al.*, 2014; Splinter *et al.*, 2014). Recent work has also demonstrated that the widespread coastal erosion and damage from storms may also not unfold as predicted (Backstrom *et al.*, 2015; Guisado-Pintado and Jackson, 2018). These field experiments have verified that the coastal sedimentary NBD system has quasi-unique, local (micro- to meso-scale) functioning characteristics. The generic controls that influence all coasts occur in different combinations over varying time and spatial scales. These controls include, but are not limited to, wave–wind action, storm surge, tides, relative sea level, geological configuration, nearshore and offshore bathymetry, accommodation space and sediment budgets (Devoy, 2015a,b). The magnitude of their respective roles cannot be assessed without the relevant long-term monitoring data on the drivers and responses (O'Connor *et al.*, 2011) but, even then, conventional experimental approaches consider only single (mostly) or coupled (rarely) parts of the NBD continuum.

The more notable conceptual models of beach–dune evolution over time, linking morphological variation to changes in energy inputs and sediment supply, are those of Cowell and Thom (1994), Wright and Short (1999) and Hesp (2002). The Cowell and Thom (1994) model illustrates how coastal morphodynamics operate within a hierarchy of temporal and spatial scales. Their model is relevant to this WP, as it places coastal resilience within a framework of event scale via response and recovery processes and morphological change. The Wright and Short (1999) model focuses primarily on beach form and processes, where a continuum of beach state ranges from dissipative at one end to reflective at the other. Foredunes tend to



be largest at the rear of dissipative beaches because of higher sand transport rates and supply. Hesp's (2002) model centres more on the dune component and incorporates a storm impact and response phase. Examples of specific storm-focused models include Morton (1994), Sallenger (2000), Masselink and van Heteren (2014) and Brenner (2018). Morton (1994) emphasised the need to tailor models to look specifically at longer timescales after a storm has passed, because recovery to a pre-storm state usually takes a number of years. He developed a four-stage conceptual model, moving from forebeach accretion, through backbeach aggradation, to dune restoration and revegetation. Masselink and van Heteren (2014) developed a "resilience trajectory" approach incorporating Morton's model into a state-space representation. They map out a beach-dune system's resilience and destruction as a function of barrier width and elevation. Their model pays particular attention to thresholds within the system and can thus factor in how change over time, such as diminishing sediment supply or a rising sea level, can shift the threshold horizon and reduce the resilience of the system. Sallenger (2000) proposed the "Storm Impact

Scale" model, which utilises four critical cross-shore topographic points to characterise different storm regimes. These regimes can potentially be used to forecast a storm's morphological impacts as it approaches the coast. The critical points delimit the swash zone and backbeach/dune elevation, with ratios of these parameters defining the storm regimes. In the *swash regime* the beach erodes, but returns quickly post storm with little net change; wave run-up collides and erodes the foredune in the *collision regime*, with sand not readily returning post storm; the *overwash and inundation regimes* result in barrier breakdown, with sand being transported and lost landward.

### 2.3 Methods

Ten different surveys of the cross-shore profile were carried out in all seasons for a period of 22 months from December 2015 to October 2017 (Figure 2.1). Morphological changes in the study site were quantified using a geographic information system (GIS) and global navigation satellite system (GNSS)-derived beach topography (Trimble R8 post-processed



**Figure 2.1.** Location of the five cross-shore profiles at Golden Strand repeatedly surveyed from December 2015 to October 2017. Map data: Google, CNES, Airbus © 2020.

kinematic – PPK) for five cross-shore profiles (Figure 2.1).

### **2.3.1 Morphological analysis**

Topographic data were integrated in the ArcGIS 10.3 GIS to quantify changes in the shoreline position and beach elevation and width. The following steps were conducted to complete the morphological analysis and plot the profiles, and to quantify the change in profile shape and elevation over the monitoring periods:

1. From each full survey shapefile (Achill  $n=10$ ), the points from each profile were isolated and exported into their own individual profile shapefile based on location and point identification (ID)/label using “export selected features”.
2. Using “points to path” in QGIS, a line was automatically generated using the points for each profile for each survey (ordered by easting). Lines were then examined for inconsistencies and corrected as necessary.
3. Each generated path was then buffered by a minimum of 10 m (with square ends) to get a polygon to constrain the digital elevation model (DEM). We chose 10 m so that all profile lines would overlap; however, if the profiles of the same number from each survey were spaced more than 10 m apart, then a larger buffer size was selected to ensure an overlap.
4. The “Spline with Barriers” tool was used in ArcGIS with the profile points and the buffer polygon to generate a DEM for each profile, for each survey, that was constrained to the shape of each buffer.
5. All the buffers were merged together for the same profile number to get a polygon that would cover the range of all surveys at that profile to select an appropriate transect. A polyline shapefile was created and a transect line that ensured overlap between all surveys was drawn.
6. Points were generated every 5 m along the transect line using “construct points” in ArcGIS, and each point was labelled with its cross-shore distance in metres.
7. The “Add Values to Points” tool was used in ArcGIS to extract the elevation values from each

Raster DEM layer for every 5 m along each transect.

8. The results were exported to a comma-separated values (CSV) file and the elevation change was calculated in Microsoft Excel. A plot was created for each profile (see Figure 2.2).
9. The software programmes R and ggplot2 were used to create “heatmap” plots of elevation change for each profile (see Figure 2.4).

### **2.3.2 Storm detection**

Wave data were not monitored locally so the Marine Institute East Atlantic SWAN Wave Model dataset was used to derive wave parameters approximately 4 km offshore of the site at 54.047370°, -10.024985°. Thresholds for storm detection are site specific. Consequently, the method reported in Guisado-Pintado and Jackson (2019) was used to identify storm events where  $H_s$  (significant wave height) exceeds the 5% exceedance wave height and lasts for a minimum threshold of 12 hours to guarantee that a storm event extends over at least one high tide. We calculated the exceedance threshold based on 4 years (1 December 2015 to 31 December 2019) of modelled data from the East Atlantic SWAN Wave Model.

### **2.3.3 Water levels**

Water level records were obtained from the Marine Institute Irish National Tide Gauge Network at Ballyglass Harbour, Co. Mayo, located approximately 27 km north of the study site (54.2536°, -9.8928°). Data from a closer tide gauge station were not available for the time period of interest. The sampling frequency is 6 minutes and water levels are referenced to both the Malin Head datum and the Lowest Astronomical Tide (LAT).

### **2.3.4 Wave run-up**

Wave run-up observations were recorded using a low-cost (€200), low-resolution (.jpg with 1280 × 720 pixel dimensions and 96 dpi) time lapse camera (Day 6 Outdoors PlotWatcher Pro Trail Camera) that captured oblique photographs of the beach–dune system spanning profiles 3, 4 and 5. The camera was deployed on 20 June 2016 in a weatherproof case and mounted on a stake on the elevated headland



just north of profile 5 (Figure 2.2). The camera was powered by eight AA batteries and pictures were stored on a micro SDHC card every 10 minutes during daylight hours as there was no infrared capability. Pictures were viewed using the customized Game Finder software programme that allowed the picture files to be saved one at a time, in blocks of 50, 100 or 200 pictures or downloaded as video clips for each day (.TLV or .WMV files).

## **2.4 Results**

### ***2.4.1 Cross-shore topographic profiles***

The study site was ideally located to experience storm-induced change during the monitoring programme.

The cross-shore profile development over the 22-month period exhibited a changing but stable beach–dune morphology. It should be noted that the results would have benefitted from surveys extending into winter 2016 and spring 2017 but these were not part of the study design. Figure 2.3 plots the survey data with morphological features evident across the beach face,

for example the distinct berm on the foreshore evident in profiles 2, 3 and 4. This berm is absent in profile 1 on account of the presence of a gravel storm berm and relatively narrow foreshore (Figure 2.4). Profiles 2, 3, 4 and 5 also show the foredune system that dominates the back beach. Profiles 3 and 4 include dune ridges landwards of the foredune. These ridges are man-made using fences from a protection scheme to prevent sand from being deposited on the football field lying inland between profiles 4 and 5 (Figure 2.4a). Profile 5 is also affected by wave reflection processes from the adjacent headland and does not exhibit the prominent berm seen in the middle profiles (Figure 2.3). Throughout the study there was evidence of embryo dune development across profiles 2, 3 and 4. These small dune landforms never exceed 0.50m and never coalesced to form a new foredune but were a sand reservoir during times of extended wave run-up. The middle sections had a very wide foreshore extending 200m during low spring tide. The large tidal range at the site (4.57 m) provides an extensive survey area during low tides. Profile 2 has the widest beach width but is influenced by the stream outlet.



**Figure 2.2. View of time lapse camera (inset) deployed on headland overlooking Golden Strand.**

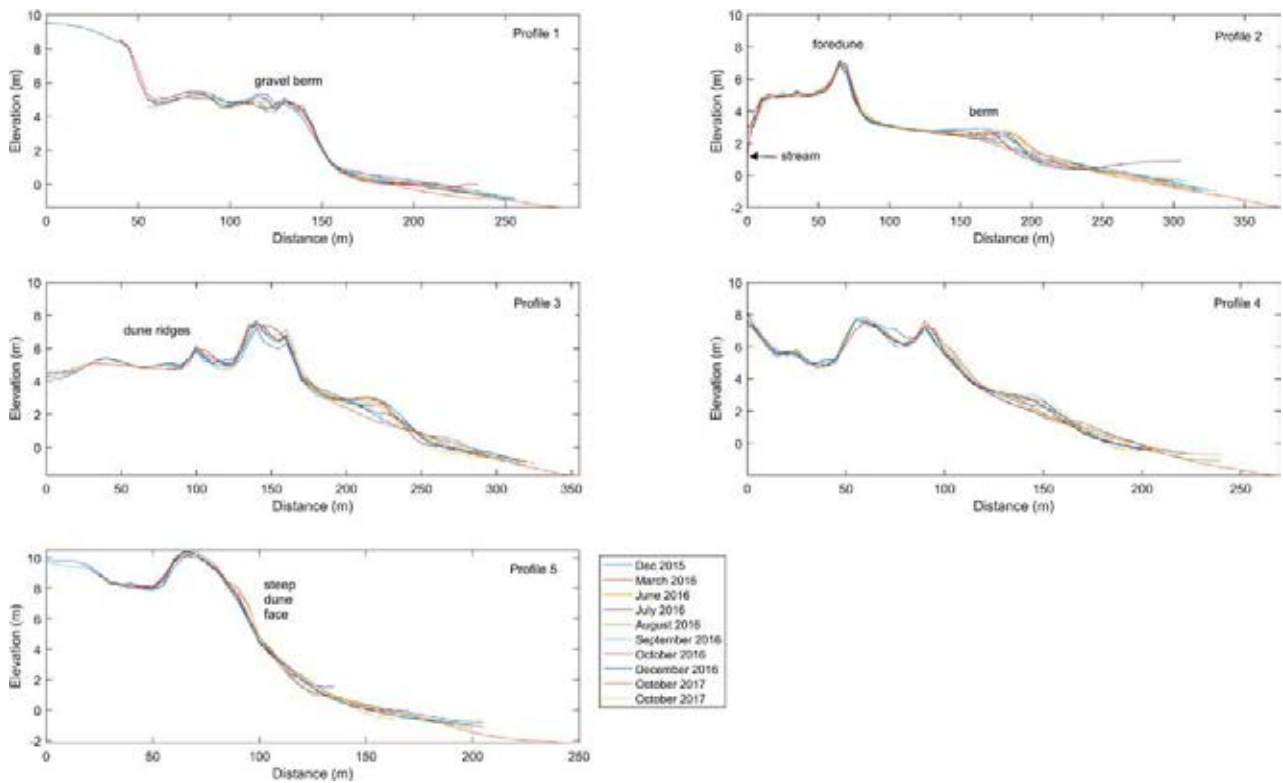


**Figure 2.3. Profiles 1–5 obtained from repeat surveying using a GNSS. See Figure 2.1 for profile locations.**

#### **2.4.2 Sediment exchange between the beach and dune**

The analysis of the morphological changes of the beach–dune system during the study period shows that there is consistent movement of sediment across the beach moving both seawards and landwards. The beach is in constant flux but the primary cross-shore profile shape and elevation was maintained throughout the study period for each profile. The maximum, minimum and average observed changes in elevation are reported in Table 2.2. The average elevation change across the profiles is very low, ranging from 0 to 0.03 m. Each maximum gain and loss is balanced within each profile and is closely linked spatially and temporally (Figures 2.5 and 2.6), i.e. they occur during the same survey period and lie adjacent to each other [e.g. changes in profile 4 between March and June 2016 suggest that the sand lost in the lower foreshore (170–200 m) moved landwards (115–165 m)].

When time-averaged over the complete storm-erosion/post-storm-recovery period there was no net change across the profiles. The total net volume of accretion (erosion) along each profile was insignificant (Table 2.2) and there was no net change, averaged

over the lines, in all seasons. Beach response was mainly manifested in relatively small elevation changes ( $\pm 1$  m) and cross-shore movement of the berm (Figures 2.5 and 2.6). The relatively large change in beach elevation between July and August 2016 recorded in profile 2 is a manifestation of stream migration processes (Figures 2.5 and 2.6). This period had no significant storm surge events. Both the data and qualitative observations show that sand transported from the beach during high-energy conditions was as likely to be deposited in the embryo dunes at the base of the vegetated foredune slope as it was to be deposited over the dune crest, partially burying the marram grass. Profiles 3 and 4 were particularly responsive to minor dune building and dune ramp development, and these deposits are most likely moved seaward during high-energy conditions (Figure 2.6). A longer time series of storm measurements and numerical simulations are required for a comprehensive assessment of the impacts of extreme storm events or storm clustering on the beach profiles. The extent to which the cross-shore profile in Golden Strand would change is not known, but the evidence suggests that the system is resilient and has been modally adjusted to a large swell environment.



**Figure 2.4. (a) Location of the PlotWatcher camera (red filled circle) and football field. (b) Close-up aerial view of man-made dune ridges running oblique to foredune. Note the embryo dune development. (c) View of profile 5 at distal end of beach adjacent to the headland. (d) View of profile 1 with gravel storm berm.**



(c)



(d)



**Figure 2.4. Continued**

**Table 2.2. Observed changes in elevation across each profile**

Profile	Maximum change (m)	Maximum change (m)	Average change (m)
1	-0.53	0.68	0.03
2	-1.83	1.64	0
3	-0.84	1.13	0.01
4	-0.77	0.79	0.03
5	-0.57	1.07	0.01

This assessment is also based on qualitative observations that indicated no evidence of crest lowering and inundation overwash.

### 2.4.3 Storm events

A total of 17 storms were detected after applying the storm detection criteria sensu stricto (Table 2.3; Figure 2.7a). The average  $H_s$  and wave period for these storms ranged from 3.5 m to 4.1 m and from

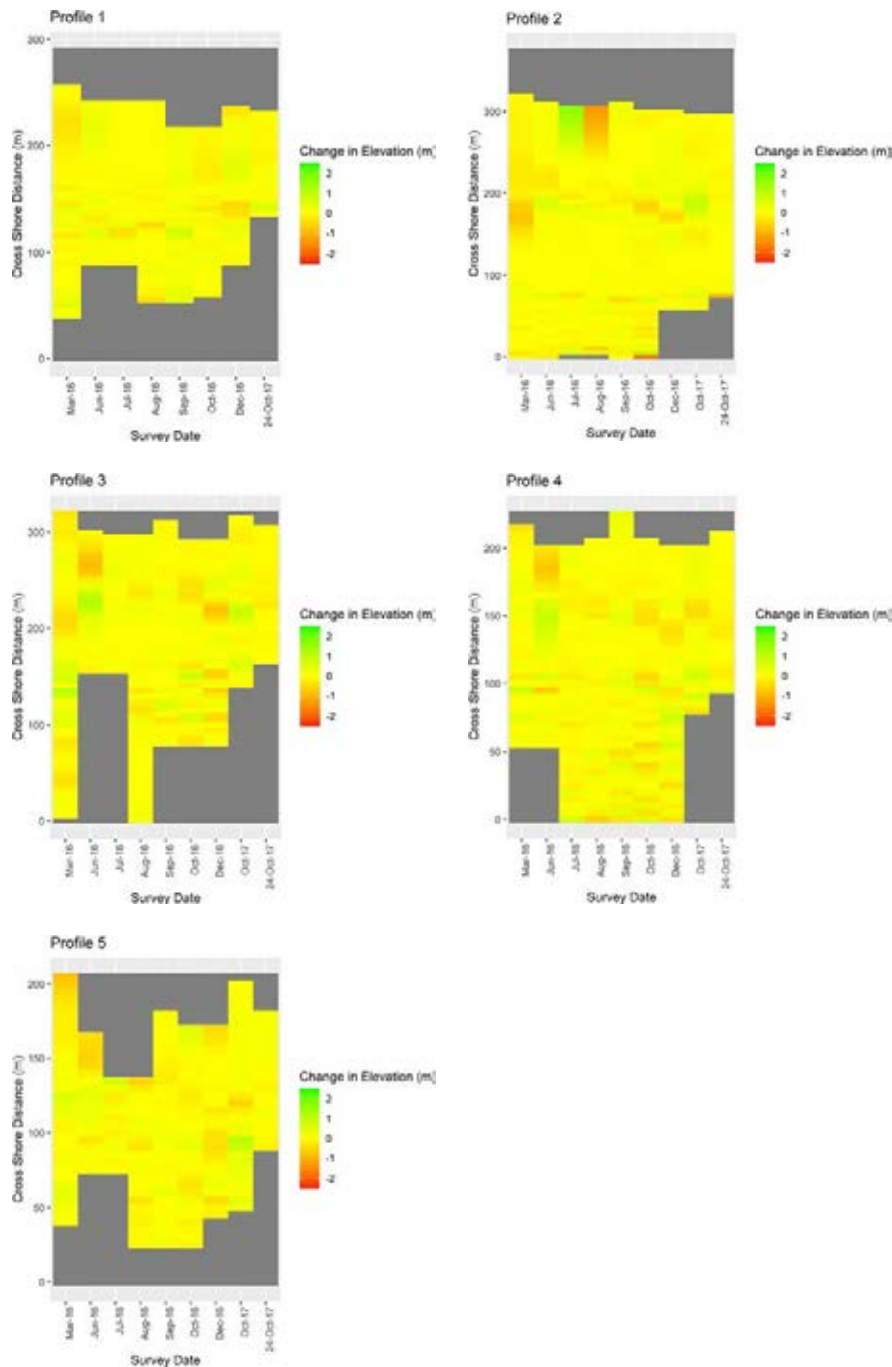


**Figure 2.5. Changes in elevation across each profile for each survey. Positive change signifies accretion; negative change signifies erosion.**

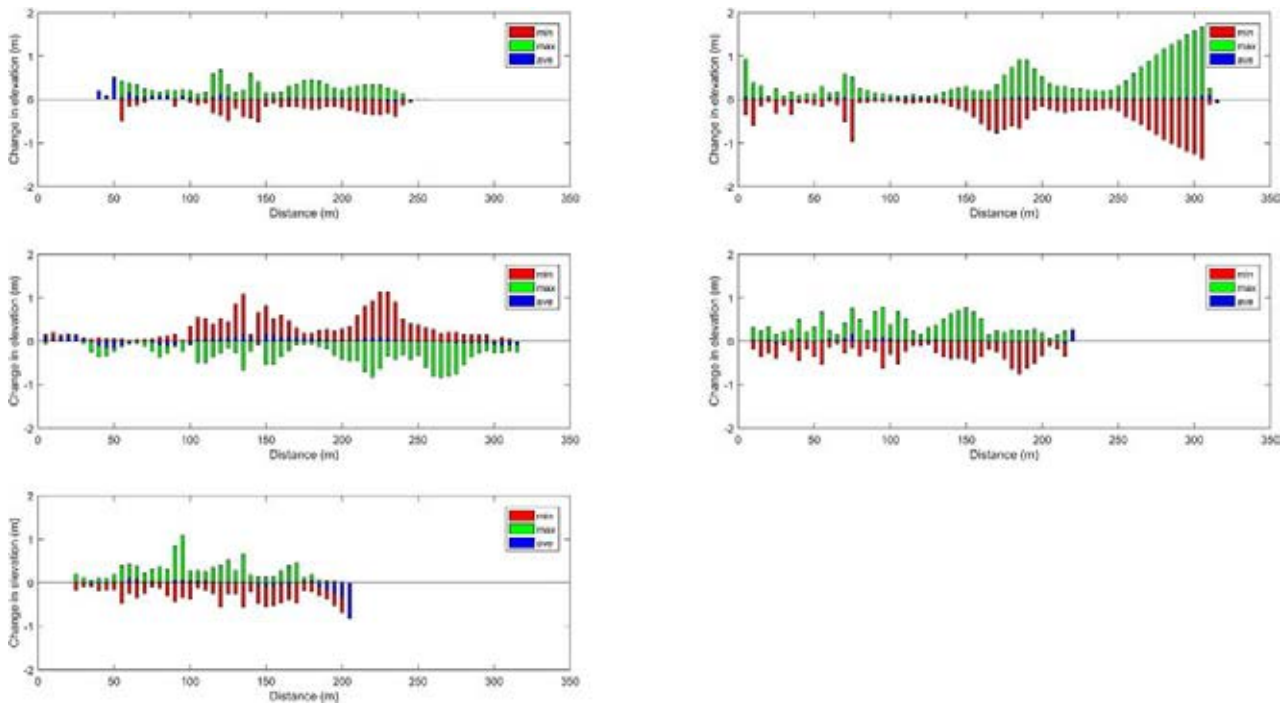


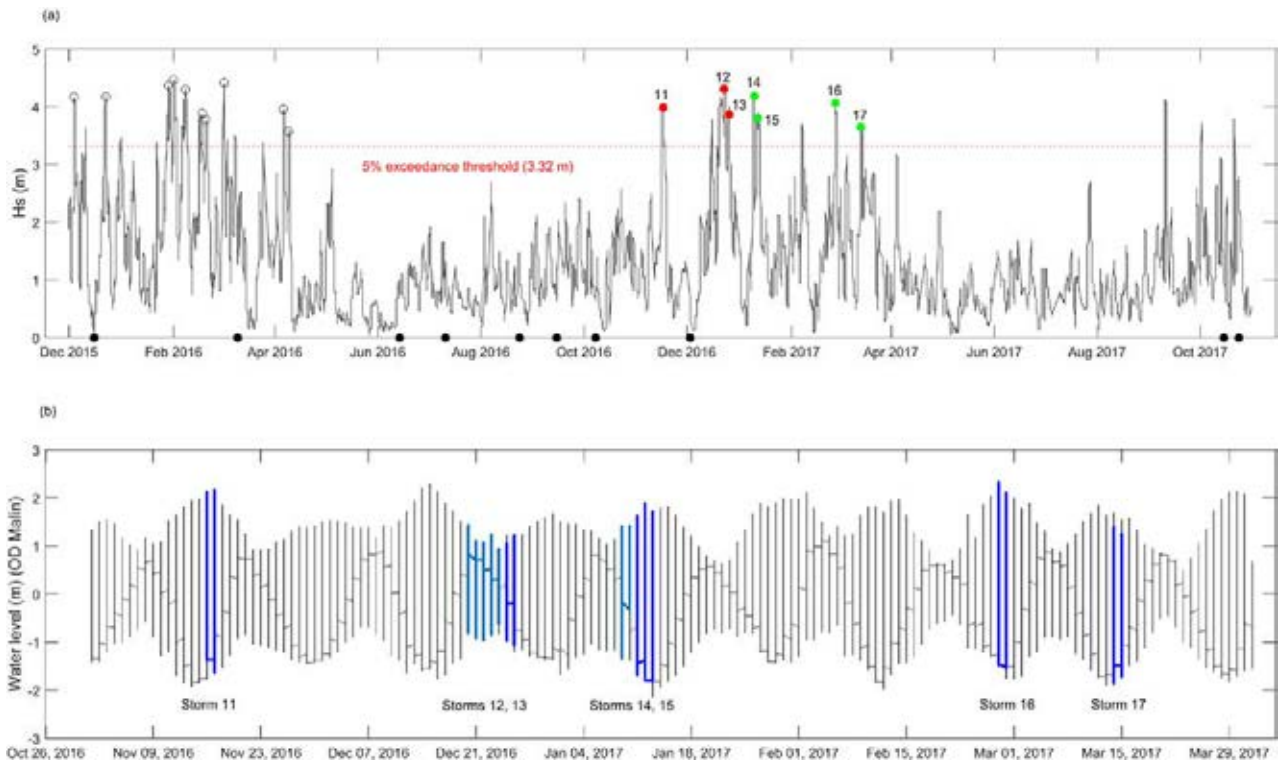
Figure 2.6. The maximum (accretion), minimum (erosion) and average elevations changes across each profile during the monitoring programme. All scales are the same and offsets from 0m occur where profile survey extents differed.

Table 2.3. Details of storm events observed during study. The grey shading indicates storms where wave run-up was observed using time-lapse photography

Storm number	Start date/time	$H_s$ (m)	Period (s)	Wave direction (°)	Duration (h)	Wave run-up to dune
1	4 December 2015 12:00	3.7	9.9	344	18	No camera
2	22 December 2015 12:00	3.9	10.9	343	30	No camera
3	28 January 2016 03:00	3.9	9.9	342	72	No camera
4	1 February 2016 06:00	4.1	9.9	342	51	No camera
5	6 February 2016 18:00	3.8	9.3	342	75	No camera
6	16 February 2016 21:00	3.5	11.3	342	48	No camera
7	20 February 2016 09:00	3.6	10.8	340	27	No camera
8	1 March 2016 21:00	4.1	9.0	341	27	No camera
9	6 April 2016 09:00	3.8	8.5	341	30	No camera
10	9 April 2016 18:00	3.5	13.0	342	12	No camera
11	16 November 2016 15:00	3.7	9.5	340	30	No
12	20 December 2016 09:00	4.0	10.9	342	102	No
13	25 December 2016 12:00	3.7	9.1	342	39	No
14	9 January 2017 12:00	4.1	10.1	341	24	Yes
15	11 January 2017 03:00	3.7	8.3	339	54	Yes
16	27 February 2017 03:00	3.8	11.1	342	36	Yes
17	14 March 2017 09:00	3.5	12.3	342	24	Yes

8.3s to 13.0s, respectively. Storm duration ranged from 12 hours to 102 hours. Wave direction was constant (339–344°) owing to the influence of the coastline configuration. Wave run-up extent during the

storms was observed (during daylight hours only) after August 2016 using the PlotWatcher camera. These data were used to evaluate the frequency when water



**Figure 2.7. (a)  $H_s$  data from the Marine Institute East Atlantic SWAN Wave Model for local conditions (54.047370°, -10.024985°). Data source: Marine Institute. The filled black circles along the x-axis signify topographic survey dates. The circles on the  $H_s$  curve mark where storms were detected (open black: no camera observations; filled red: no dune erosion; filled green: dune erosion). (b) Tide data from Ballyglass Harbour, Co. Mayo, with storm durations overlain.**

levels reached the toe of the dunes, providing an evaluation of dune susceptibility to potential erosion.

Along with storm size, water level is a critical factor in the effectiveness of storms to potentially erode dunes, as shown in Figure 2.7 and previously described in Carter (2013). Storm wave run-up during the study varied depending on the tide stage (e.g. spring versus neap). For example, Storm 12 started on 20 December 2016, lasted 102 hours and had a high  $H_s$  (4.0 m) but did not result in wave run-up reaching the dune toe as it occurred during neap tides. Storm 13 arrived shortly after Storm 12 on 25 December 2016, and lasted 39 hours, but again wave run-up did not extend beyond the back beach, as it occurred within the same tide stage. Conversely, Storm 11 occurred on 16 November 2016, and lasted 30 hours during spring tides, but also failed to cause dune erosion (Figure 2.8a). The most likely explanation is that high tides on that day occurred at 06:00 and 18:00 and the camera did not capture the maximum wave run-up owing to lack of daylight. Conceptually, we could infer a dependency on the antecedent state

of the beach with extended fairweather conditions 7 months prior to this storm. There is evidence that the beach berm grew and moved seaward (Figure 2.3) during this time and was then lowered and moved seawards during Storms 12 and 13. It is not believed that these changes in berm elevation and position were significant enough to prevent wave run-up to the dunes during the high tides of Storm 11.

Storms 14 to 17 all had wave run-up elevations high enough to reach the dune toe. All of these storms occurred during spring tides and lasted long enough to have at least two daily high tides. Similarly, we could infer antecedent conditions related to berm lowering, and seaward migration during Storms 11, 12 and 13 may have increased the potential for dune encroachment by extended wave run-up during subsequent storms.

## 2.5 Discussion

Golden Strand is an accretional beach containing a wide backshore area and a prominent berm.





**Figure 2.8.** Captured images from the low-resolution PlotWatcher camera for Storms 7–14. Dates and times of the maximum observed wave run-up are: (a) 17 November 2016, 09:32; (b) 23 December 2016, 14:36; (c) 25 December 2016, 15:51; (d) 12 January 2017, 17:21; (e) 12 January 2017, 17:21; (f) 7 February 2017, 06:25; (g) 15 March 2017, 08:28. Note that wave run-up in (d)–(g) reaches the dune toe (Storms 14–17 reported in Table 2.3).

Observations in this study illustrated that the impact of high-energy storms is minimal and temporary and the beach is replenished during low-energy conditions as the beach berm grows and moves seaward. Golden Strand’s planform is swash aligned as a result of wave refraction processes and can be considered to be static or metastable equilibrium, similar to other embayed beaches. The beach appears

to be remaining in one state with little morphological variation, and this is not usual for beaches located deep within embayments (20 km from open sea), where waves are refracted and the wave crests arrive parallel to the shore. Figures 2.3, 2.5 and 2.6 illustrate how the cross-shore profiles were maintained within a narrow envelope for the duration of the monitoring programme. This also supports previous findings in

western Ireland, where beaches and dunes exposed to high-energy wave regimes require extreme storms to cause significant morphological change (Cooper *et al.*, 2004; Williams *et al.*, 2015). We would suggest that the observations confirm that Golden Strand behaves like a system that is attuned to the high-energy wave conditions and seems to have been largely insensitive to storms observed during the monitoring programme (see Cooper *et al.*, 2004). This closed-beach system is compartmentalised by two prominent headlands, with sediment being supplied from the offshore and/or adjacent till cliffs that exhibit visual evidence that they are chronically eroding. There is no observed alongshore sediment transport component (with the caveat that nearshore surveying was not conducted).

The episodic movement of sediment across the beach (Figures 2.6 and 2.7) can be best seen in the berm migration and, to a lesser extent, the variability in back beach elevation. This process–response behaviour can be considered to be an attenuated version of the large “cut-and-fill” cycle that has been documented elsewhere. However, it is not to say that extreme waves from the north or north-west cannot act as a trigger to push the system out of equilibrium or initiate a barrier roll-over regime. It is uncertain how much time is needed or what combination of conditions (or “drivers”) needs to occur (wind direction, coastline orientation, tidal stage, water level, antecedent state of the beach) for a substantial volume of sediment to be removed from Golden Strand and trigger severe dune erosion and large-scale system retreat (Cooper *et al.*, 2004; Guisado-Pintado and Jackson, 2018; Loureiro *et al.*, 2016). What we can infer is that the likelihood of these conditions coinciding increases when the number of storms and their intensity increases. This is especially true if we incorporate sea level rise resulting in the number of storm run-up events reaching the dune toe increasing dramatically [e.g. Storms 11–13 in Figure 2.8(a)–(c) would all reach the dune toe if

we applied the mid-range future scenario (+0.5 m) of sea level rise in Ireland]. The extent to which Golden Strand will undergo significant process and domain changes over time (Orford *et al.*, 1996; Jennings *et al.*, 1998) to break the existing “cyclical” operation is difficult to assess because of the uncertainty about the nature of storms required to generate change (Devoy, 2015b; Williams *et al.*, 2015). Currently there is a paucity of long-term observational data in Ireland for coastal forcing and coastal response. These data are required to dismantle local-scale coastal dynamics and to guide numerical coastal change prediction models. This modelling approach can help us move beyond the current state of knowledge (“how much change occurs?”) to develop better insights (“why does change occur?” and “how much change will occur if boundary conditions change?”) and foster new insights into storm climates in Ireland.

The human imprint is not insignificant at the site. The caravan park between beach profiles 1 and 2 (Figure 2.1) has the potential to cause coastal squeeze in the long term, and reports from the local community suggest that the area is already susceptible to coastal surge and pluvial inundation. Immediately landwards of profiles 3, 4 and 5 there are three dune ridges that are oblique (20°, 30° and 50°) to the foredune alignment. Local community input clarified that the dune ridges grew on man-made fences erected to mitigate sand deposition on the adjacent football field (200 m from the back beach). No specific date for installation of the fences was provided, but it is believed to have been approximately 30 years ago. However, these man-made dunes will not limit the accommodation space available for any system rollover should future (larger) storm events exceed the system’s threshold and resilience or the system move landwards (as we would expect) as a consequence of sea level rise and future climate warming.

# 3 WP3 – Tracing Internal Moisture and Salinity Changes in Dunes

## 3.1 Introduction

Moisture and salinity are two key factors that affect dune stability. However, there is a paucity of research on internal dune hydrology and salinity in Ireland. Previous research has focused on the surficial permeability of dunes (e.g. Jungerius and Dekker, 1990) and dune groundwater dynamics (e.g. Bakker, 1990). The vadose zone has been poorly studied, despite evidence of high moisture content variability in this zone (Gardner and McLaren, 1999). Most European coastal dune systems are sediment-supply limited (Carter, 1990), with reduced capacities to respond to significant environmental changes. Given that Ireland is modelled to experience wetter winters with more frequent high-intensity storm events (Nolan, 2015), this is expected to increase erosion rates of coastal dune systems. Baseline environmental data for these systems are required to address coastal dune erosion into the future. This WP presents the results of field experiments that trace internal moisture and salinity dynamics within the vadose zone of a coastal dune system. The overall goal was to collect field observations to characterise the dune system moisture–precipitation behaviour (Table 3.1).

## 3.2 Methods

Sentek EasyAG capacitance probes fitted with TriScan sensors were deployed at four locations within a dune transect: (1) windwards dune face, (2) dune crest, (3) lee slope and (4) transitional dune slacks/machair (Figure 3.1a,b). These sensors measured the relative

volumetric water content (VWC) and volumetric ion content (VIC) every 10 minutes at 0.10 m depth intervals from 0.10 to 0.50 m below the surface over a 3-week period during June and July 2016. The 3-week period was controlled by equipment logistics (periods of failure during the monitoring). Rainfall was measured at a weather station located 200 m from the site (see section 2.1). Rainfall occurred on 18 of 24 data collection days. Precipitation events were classified by magnitude and duration and a random sample of 10 events with intensities greater than 0.5 mm/h was selected for analysis.

## 3.3 Results

### 3.3.1 Moisture activity

Overall, dune moisture increased with distance from the coast. The windwards site displayed a relatively constant, low moisture content (~0.40%), whereas the lee site displayed a consistently high and variable moisture content (Figure 3.2a). The analysis indicates a lag of less than 1 h in moisture response to infiltrating rainfall at depth (Figure 3.2b). The wetting front can be traced as it infiltrates the dune profile, with response to rainfall occurring later with increasing depth. Every site except the lee site demonstrates very little moisture response below 0.30 m depth to infiltrating rainfall. The muted response below 0.30 m also displays a lag following the onset of rainfall. However, for rainfall intensities greater than ~2.0 mm/h, infiltration down to 0.50 m can occur.

### 3.3.2 Salinity activity

Site salinity decreased with distance from the coast (Figure 3.3a). Salinity was consistently high at the crest site, with values between 1600 and 2100 VIC. The machair site showed consistently low salinity at ~1400 VIC. There is no clear relationship between salinity and depth across all sites. The lee site demonstrates greatest salinity at 0.50 m depth, which is probably a result of leaching due to rainfall percolation to this depth. Salinity displays a lagged

**Table 3.1. WP3 objectives**

Objective	Description
Objective 1	Measure moisture flux changes in coastal dunes after sediment erosion and/or deposition
Objective 2	Determine how emplacement (rates and volumes) of moisture from precipitation events affects dunes
Objective 3	Measure the impact of surface water flow, salinity and temperature on dune ecosystem health

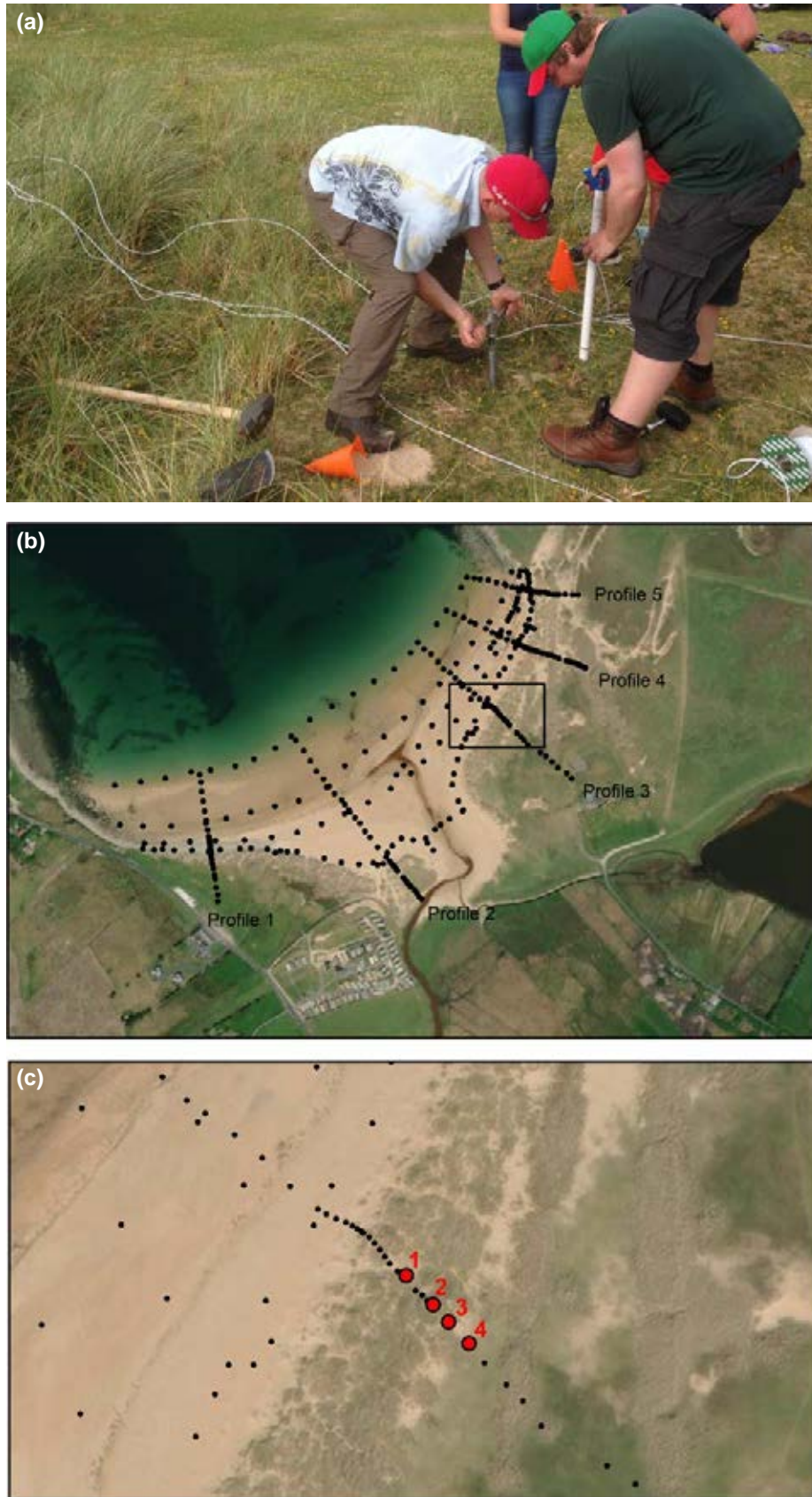


**Figure 3.1.** (a) Installing EasyAG capacitance probes equipped with Sentek TriSCAN moisture and salinity sensors. (b) Approximate location of sensors along profile 3 (WP2). (c) Close up of inset box in (b). Sensors 1–4 relate to the windwards dune face, dune crest, lee slope and transitional dune slacks/ machair, respectively. Map data: Google, CNES, Airbus © 2020.



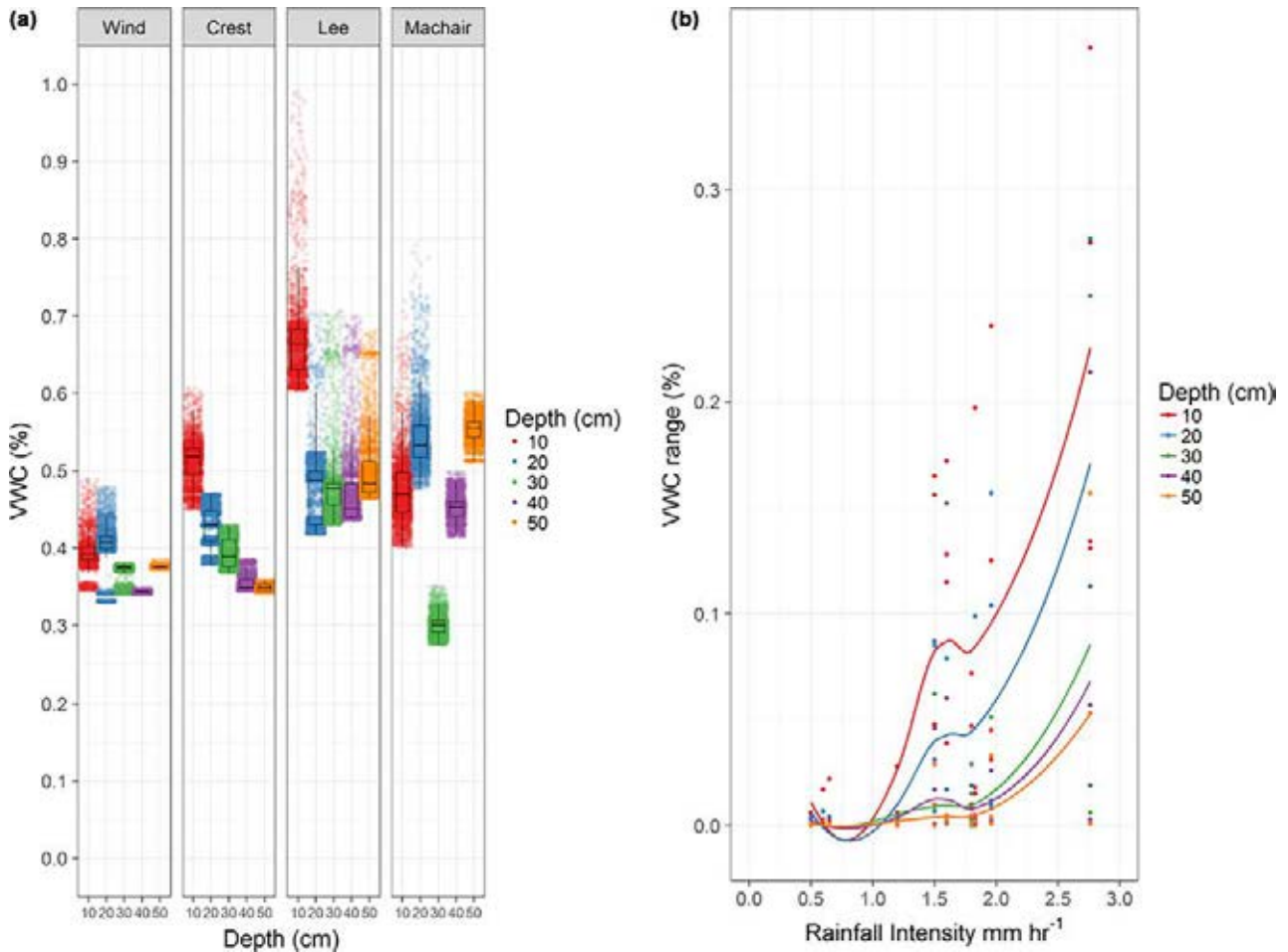


**Figure 3.2. (a) Distribution of moisture values per site and depth. (b) Rainfall intensity (mm/h) plotted against range of moisture per depth for each of the 10 subset rainfall events.**

response to infiltrating rainfall, like moisture. However, the overall distribution of salinity appears chaotic, with an unclear relationship with paired moisture samples. Greatest salinity occurs during the most intense rainfall events but the relationship is not linear (Figure 3.3b).

### 3.4 Conclusions

Moisture and salinity below 0.30 m depth do not typically respond to infiltrating rainfall. However, greater rainfall intensity does result in deeper infiltration. Modelled climatic changes for Ireland

suggest that intense, short-period rainfall events will increase. Our data suggest that the hydrosaline regime within dunes will change as a result of increased infiltrative depth. Salinity in the upper reaches is expected to decrease via rainfall-driven leaching, whereas salinity at the greatest depths will increase. Evolution of the hydrosaline regime within dunes will probably result in changes in vegetation type and coverage. This may alter the stability of the dunes, either towards a more stable condition or a less stable state. Further analysis of vegetation effects on dune stability and salinity is required before we can model dune response.

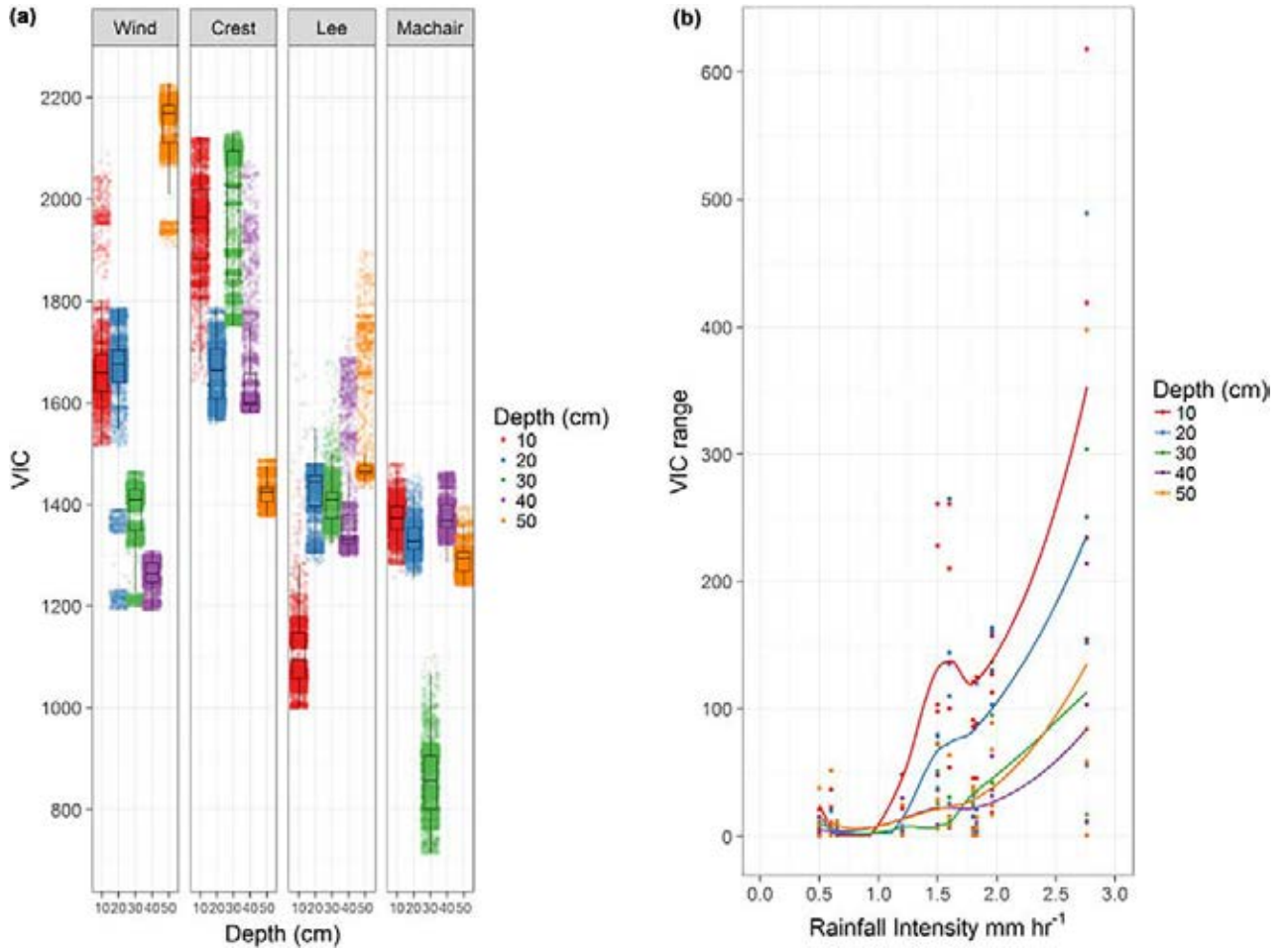


**Figure 3.3. (a) Distribution of salinity values per site and depth. (b) Rainfall intensity (mm/h) plotted against range of salinity per depth for each of the 10 subset rainfall events.**

## 4 WP4 – Groundwater Dynamics in a Coastal Sand Dune

### 4.1 Introduction

In coastal zones, the natural equilibrium between seawater and freshwater is still poorly understood, largely because of the complex mixing processes found in such heterogeneous environments. Saltwater intrusions are driven by the hydraulic gradient, which, in turn, is controlled by the difference in hydraulic heads between the tide and the aquifer (Perriquet *et al.*, 2014). Tidal fluctuations are a major factor in determining variations in boundary conditions. Tidal impacts can modify groundwater discharge in coastal zones, which can lead to slower drainage and potential for flooding of low-lying areas even under modest rainfall events. Under storm conditions the impacts on coastal aquifers can be extreme, both in terms of flooding and in terms of saltwater intrusion (Perriquet *et al.*, 2014). The coastal dune system is an inherently dynamic geomorphological landform that has high sensitivity to water fluxes (groundwater and near-surface flow) through the system and climate shifts. Landform instability is a natural phenomenon in any dune field's evolution. This instability is inherently linked to the ecology, helping to construct species diversity. Jackson and Cooper (2011) have identified a rapid biogeomorphic response on Irish coastal dunes as a result of recent climate change. The storms of winter 2013/2014 perturbed the western coastal dune system, causing erosion, destabilisation and a fresh supply of sediment. The vadose zone of dunes influences species diversity. However, it is unknown how this vadose zone responds to significant erosion and depositional events. This poor understanding has limited our knowledge of the fundamental drivers of change in coastal dune field dynamics. This WP was designed to develop a better understanding of the groundwater regime in the Doogort sand dune system (Table 4.1).

This WP had two primary objectives. Firstly, the spatial distribution of hydraulic conductivity in a coastal dune system was measured and mapped. Secondly, instrumented piezometers were deployed to (1) monitor long-term water level fluctuations in a coastal dune system, (2) determine groundwater flow direction, (3) assess the impact, if any, of tidal

fluctuation on groundwater levels and (4) assess connectivity of dune groundwater with local catchments. The field experiment and data collection was completed over a 2-year period. A source-to-sink approach was used in characterising the study area on the north shore of Achill Island (Figure 1.3). Hydrological data were collected characterising the relationships between stage, discharge and rainfall inputs; these data were integrated with the groundwater results and are reported here.

### 4.2 Geological Setting and Links to Subsurface Flow Dynamics

See section 1.1.4.

### 4.3 Methods

The data collected in this WP related to the spatial distribution of hydraulic conductivity across the dune system and to the long-term groundwater levels in the dune system. Falling head tests were completed to collect the data for determination of hydraulic conductivity values and two instrumented piezometers were installed to record water level changes over an extended period.

#### 4.3.1 Falling head tests

A total of 167 falling head test locations were identified and three discrete tests were completed at each location (501 tests in total) (Figure 4.1). The results from each test site were averaged to provide a total number of 167 values of hydraulic conductivity ( $K$ ). Locations were at 10m intervals on

**Table 4.1. WP4 objectives**

Objective	Description
Objective 1	Determine the relationship between sea water, surface water, groundwater and rainfall in the coastal zone
Objective 2	Determine how groundwater fluxes affect surface sedimentary dynamics or vice versa
Objective 3	Determine how groundwater fluxes affect ecosystem health



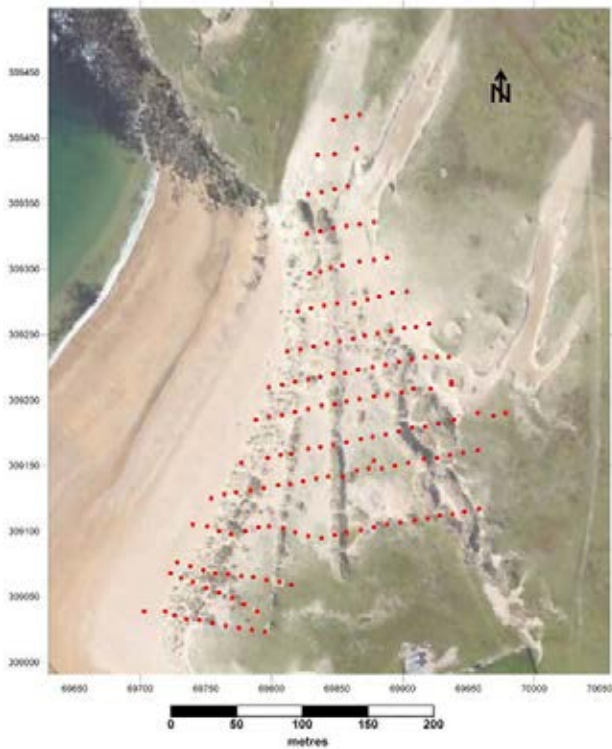


**Figure 4.1. Falling head test locations. Map data: Google, CNES, Airbus © 2020.**

transects running perpendicular to the main direction of the dune structures.  $K$  values were derived using Hvorslev's method (British Standards Institution, 1999; Brassington, 2007). A graduated piezometer was used for the test and the tubing had an internal diameter of 0.04 m and the surface area of the open section was  $2.27 \times 10^{-4} \text{ m}^2$ . Results were mapped to create a distribution map of  $K$ .

#### 4.3.2 Piezometer installation

Two piezometers were installed in the lee of the dune, in the lowest elevation portion. The site was selected following a walkover survey. The piezometer tubes were made from standard Sanbra Fyffe unplasticised polyvinyl chloride (UPVC) pipe (40 mm internal diameter). The pipes were cut to length in the field. Slots were cut in the lower 0.20 m of each pipe to allow water in. A gauze sleeve was taped in place over the slotted section and this was covered by a plastic mesh sleeve. The bottom of each pipe was capped with a blank cover and the top was fitted with a screw top (Figure 4.2).

Two holes were cored into the dune. Freshwater was encountered in both holes within 0.50 m of

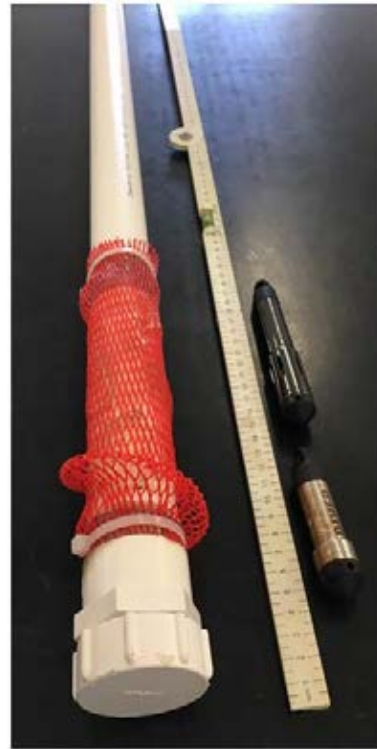


**Figure 4.2. Monitoring well and data loggers.**

the ground surface. When the target depth was reached (1 m in each case), the piezometer tube was installed and the hole was back-filled around it to close to the top. At that point a preprogrammed conductivity, temperature and depth (CTD) data logger was installed in each tube (at the base of the pipe) and a Baro-Diver was installed at the top of one of the tubes (Figure 4.3). The CTD Baro-Diver loggers were programmed to record data on an hourly basis; data recorded included pressure (water depth), temperature and EC. The Baro-Diver was programmed to record air pressure on an hourly basis. This allowed the final output data to be pressure corrected. After the loggers were installed, the depth to water in each standpipe was recorded. This allowed the surface elevation of the water level to be determined as well as the elevation below the surface of the CTD logger. Lockable screw caps were fitted on the top of each pipe. A differential global positioning system (GPS) was used to record the location and elevation of the top of each pipe. The remaining back-filling was completed using a shovel to ensure that each pipe was buried below the surface. A painted stake was hammered into the ground adjacent to each standpipe leaving 0.10 m aboveground.



**Figure 4.3.** Data logger installation at borehole 1 (BH1).

## **4.4 Results**

### **4.4.1 Falling head tests**

The results of the falling head tests are presented in Figure 4.4. The hydraulic conductivity values obtained ranged between  $1.91 \times 10^{-5}$  m/s and  $1.03 \times 10^{-3}$  m/s (falls into the sand range, which is from  $2 \times 10^{-7}$  m/s to  $6 \times 10^{-3}$  m/s). The conductivity was generally much higher in the machair than in the rest of the dunes or on the beach. It was observed that the lowest conductivity values were on the dune crests. This is clearly visible on the map (Figure 4.4), which shows that conductivity values were high between the dune ridges and machair, and low everywhere else. Hydraulic conductivity values were slightly higher on the beach/embryo dunes than on the marram dunes but were still lower than those of the machair.

### **4.4.2 Piezometer data**

Data were recorded for more than a year in each piezometer tube. The recovered data gave the depth of water above each CTD Baro-Diver. The data were corrected for elevation above sea level and are presented in Figure 4.5. Data from both wells were available for the period from 3 February 2017 to

21 October 2017. Additional data were available for borehole (BH) 2 up to 27 April 2018. Unfortunately, BH1 (along with the logger) was removed at some point after 21 October 2017. The data are presented in Figure 4.5. The rainfall data are presented on the secondary y-axis, with the water levels presented on the primary y-axis. This is a standard approach that allows comparison of rainfall depths with water levels.

## **4.5 Discussion**

The distribution of  $K$  values across the dune system is in line with published values for sands. The higher values on the lee of the dune (east side) are probably associated with the increased porosity and connectivity associated with the development of root structures from vegetation. The values derived all refer to the upper portion of the system and reflect  $K$  values at, typically, 0.5–1.0 m below the surface or in the root zone for most vegetation in the area. The water levels in the two piezometers mirror each other, with an approximate difference of 0.2–0.3 m between the two over the life of the project.

The water levels recorded in the two piezometers do not show any tidal influence at all. There is no indication from either dataset that the levels fluctuate

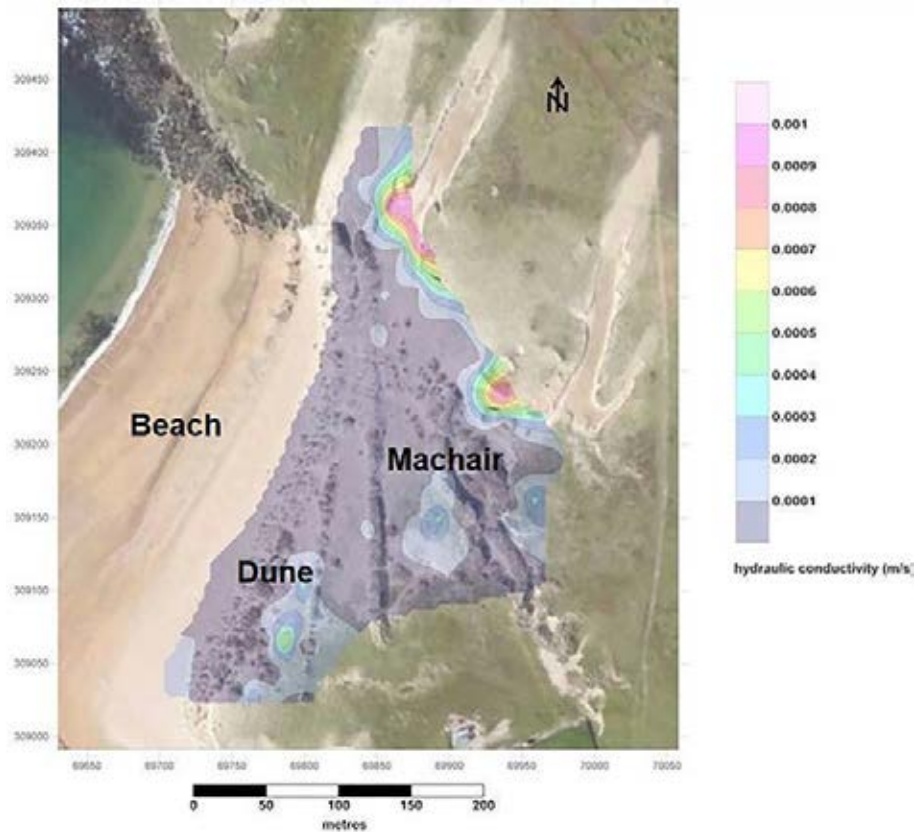


**Figure 4.4.** Distribution of  $K$  values (m/s). Map data: Google, CNES, Airbus © 2020.

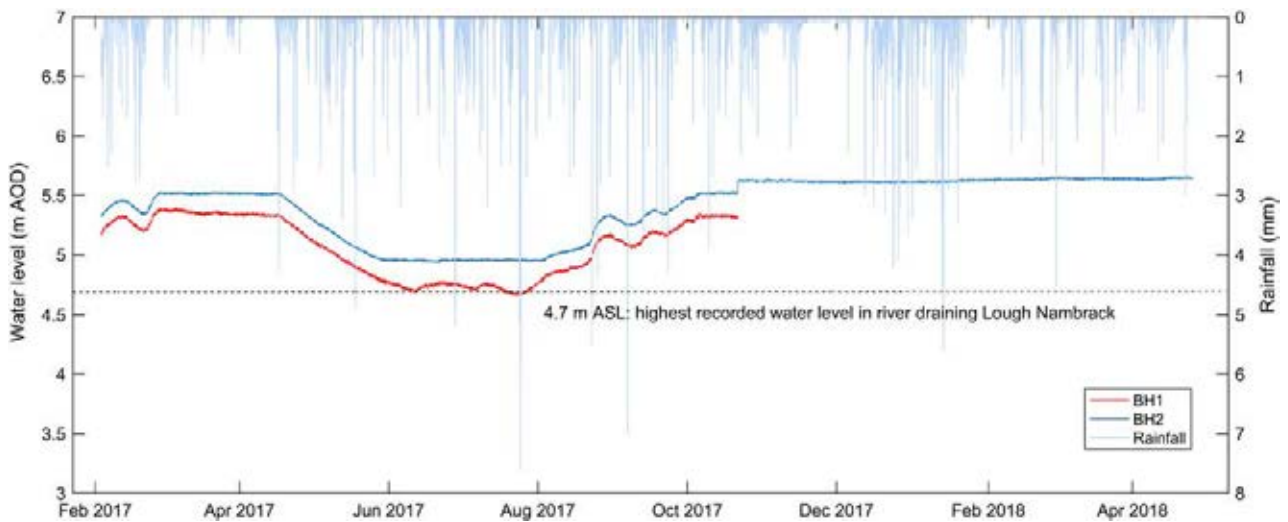


**Figure 4.5.** BH water levels (m) and rainfall (mm). AOD, above ordnance datum.

under any tidal conditions. The water levels are independent of the tides.

The lowest water levels recorded in BH1 are almost all entirely above the highest water level recorded in the stream draining Lough Nambrack (4.70 m). This indicates that the hydraulic gradient is towards the river and not from the river. Drainage from the river

(and from the lake) does not recharge the water stored in the dune. This, in particular, confirms that the dune system is locally recharged from rainfall and is not fed by any other surface or groundwater source. Given the nature of the materials identified in the geophysical survey and given the anecdotal evidence about the drainage of the football field, it would suggest that the



dune is acting like a perched aquifer, sitting on top of very low  $K$  value sediments, which in turn are on top of very low  $K$  value lithologies.

Rainfall data were recorded during the project and these data were added to the borehole data (Figure 4.5). On first inspection there is no clear or discernible pattern relating rainfall to water levels. Water levels in both piezometers started dropping in late April, reaching their lowest levels by the start of June 2017, and they remained depressed until the end of July 2017, when recovery began. During this time, however, rainfall values were not reduced and rainfall amounts were maintained over the summer of 2017.

The rainfall data were grouped in hourly intervals and, using a pivot table, the data were summed to daily and monthly values. The closest Met Éireann synoptic stations are located at Belmullet (30km north-west of the site) and Newport (35km south-east of the site). Monthly rainfall data were sourced for both locations for the duration of the study and plotted against the monthly totals for the site. The broad rainfall patterns are similar, but there is no clear correlation between rainfall at the site and rainfall at the synoptic stations (Figure 4.6a). Potential evapotranspiration (PE) values were calculated at both synoptic stations using the Penman–Monteith method. These data were accessed

and averaged for both locations. Given that these are derived based on energy fluxes they are probably reflective of the general PE values across the entire area and would be appropriate approximations of PE in the study area.

The average monthly PE was subtracted from the monthly rainfall for the site to generate monthly effective rainfall (ER) depths, which were plotted against the site rainfall values (Figure 4.6b). This indicates *negative* ER values for March, April, May and June 2017. These coincide with the reduction in water levels in the two piezometers. As ER values increase in July and August 2017, the water levels start recovering in both piezometers.

#### 4.6 Conclusion and Recommendations

It would appear from these data that water level fluctuations in the dune system are primarily controlled by PE losses. In the spring, later summer, autumn and winter, PE values are low and losses are low (water levels remain at their highest). In the summer of 2017 the depression of the water levels coincided with strong PE losses.

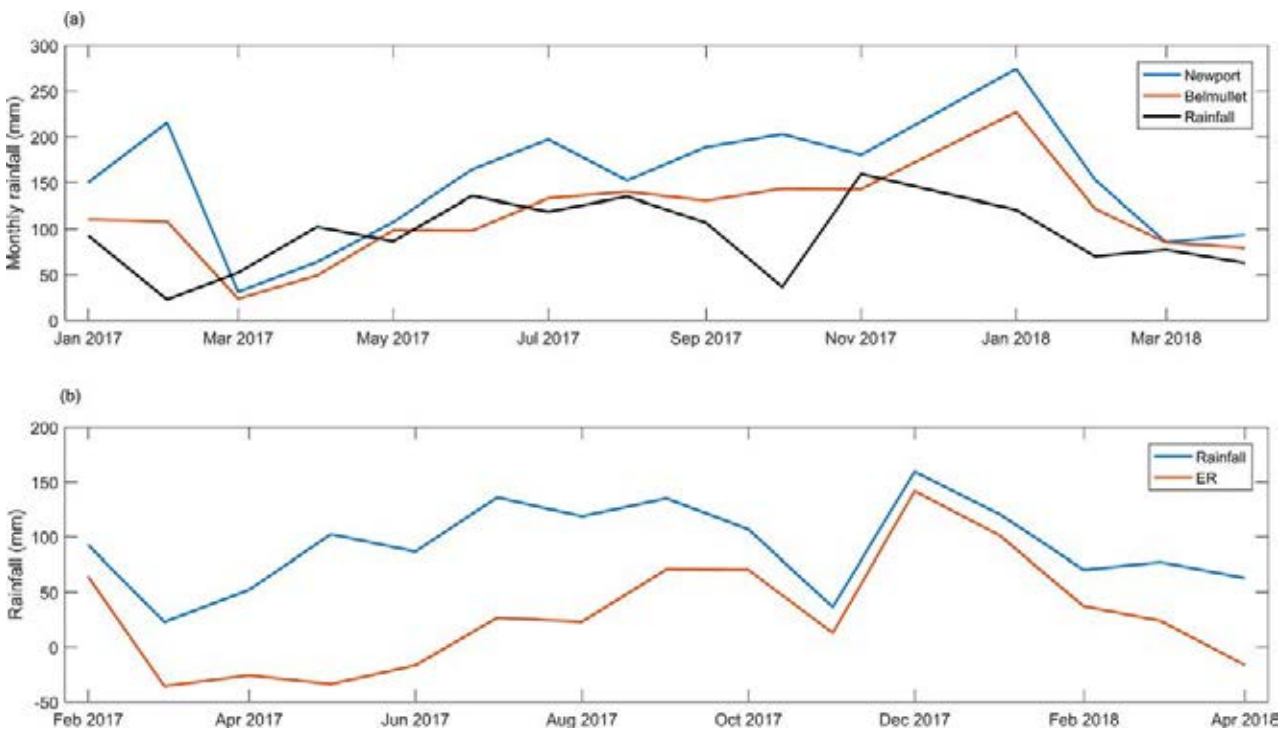


**Figure 4.6. (a) Monthly rainfall totals (mm). (b) Site rainfall (mm) versus site ER (mm).**

Future work in this area or similar areas should take a four-dimensional approach, considering the physical make-up of the site in terms of location and depth (seating it in a geological context) and in terms of time.

Recovery of groundwater samples for isotope analysis would also be really useful to assess short-term and long-term recharge and storage.

## 5 WP5 – Plant Functional Diversity and Habitat Change in a Machair System

### 5.1 Introduction

Coastal sand dunes are considered extremely resourceful in terms of their ecological and economic functions. Their role in coastal defence is among their most significant, as they have the ability to absorb energy from high wind velocity as well as from tide and wave movement, protecting the more inland habitats from exposure to the elements of the coast (Everard *et al.*, 2010). Plant species also play an important role in ecosystem functions such as nitrification and nutrient cycling. For example, *Trifolium repens* (white clover), abundant in many coastal grassland communities, is capable of fixing nitrogen. Current threats to coastal systems, such as erosion, have been intensified by human interference via recreational and exploitive activities, and in some cases have resulted in the stabilisation of dune habitat (Kindermann and Gormally, 2010) via soil compaction and increased erosion susceptibility via vegetation openings (blowouts) that exposed larger areas to erosion (Liddle and Grieg-Smith, 1975; Cooper *et al.*, 2005). The main effect of this is a loss of important vegetation structure and habitat that reduces the system's ability to absorb energy from storm events.

Characteristic plant communities reflect both past and current environmental pressures and conditions. Plant community assessment and management has historically focused on species diversity and richness components. However, more recently, research in plant functional traits to determine functional diversity has gained significant attention (Diaz and Cabido, 2001). Plants can be grouped into functional groups characterised by sets of species with similar roles within an ecosystem. Plant functional types (PFTs) play a role in the performance of plants within ecosystems based on a set of similar biological attributes and their ability to respond to alterations in environmental variables (Gitay and Noble, 1997). Specific response groups are mainly associated with a species' ability to cope with disturbance regimes. An area of particular interest is within herbaceous-dominated grasslands, such as a machair system, that

are especially accustomed to land use change and alteration of the disturbance regime.

Machair is a highly diverse ecological grassland habitat that exists only on the western coasts of Ireland and Scotland (Basset and Curtis, 1985). Since 1996, there has been a total loss of 66.4 ha of machair, or 2.35% of the total area, in the west of Ireland, mainly attributed to increased agricultural practices of cultivation and grazing, changes in patterns of land holdings and anthropogenic stressors (Ryle *et al.*, 2009). As a result, only 8% of machair is classed as "favourable". The condition of machair in most locations was described as "unfavourable – inadequate" at 62% of locations, with just 10% achieving "favourable" conservation status (NPWS, 2013b). The remainder was rated as "unfavourable–bad", which is attributed to poor management practices and increased intensity of agricultural use. Current machair management relies on the adjustment of grazing intensity. This method maintains biodiversity by controlling the height of vegetation to facilitate the growth of herb-rich grassland (Kent *et al.*, 2003). As grazing by cattle and sheep is a common occurrence on machair, the proper level of grazing is crucial to prevent overgrazing, which can lead to erosion. Thus, through an analysis of plant vegetation community change, we may offer insights to current and past environmental and anthropogenic pressures on this system.

Machair can be split into two very different sub-communities: dry machair and wet machair (Gaynor, 2006). Dry machair communities are typically characterised by species such as *Plantago maritima* (sea plantain), *Rumex acetosa* (garden sorrel) and *Ctenidium molluscum* (comb-moss) and contain numerous salt-tolerant species and an absence of moisture-loving plants. Wet machair communities contain higher abundances of moisture-loving plants and herbs, such as *Carex nigra*, *Juncus articulatus*, *Hydrocotyle vulgaris* and *Potentilla anserina*. Several species, such as the sand sedge (*C. arenaria*), can cope in both systems (Crawford *et al.*, 1998). It is likely

that these highly versatile species may play a major role in the future functioning of the machair ecosystem. With the expected increased storminess and projected sea level rise of approximately 3.4 mm per year for Ireland (Devoy, 2008, 2015a), it is likely that the resilience and adaptiveness of dry machair plant communities will be tested as a result of increased inundation and flooding.

The assessment of habitat changes over time, together with an assessment of habitat quality and investigation of current land use and threats, can be used to determine appropriate site management. Based on the overall understanding of dune processes, the main aim of this WP is to assess the changes of a coastal system containing machair habitat over a 20-year period and investigate possible causes, both anthropogenic and natural, of plant community and functional change (Table 5.1).

## 5.2 Site Description and Methodology

This WP assesses habitat and plant functional changes in coastal sand dune habitats over time in Doogort, Achill Island, County Mayo. The site, about 3 km east of the village of Doogort, is located on the northern side of Achill Island, facing the North Atlantic and sheltered by Slievemore Mountain. Approximately 2 km<sup>2</sup>, the site is used primarily for sheep and cattle grazing on a largely unenclosed dune habitat, which covers most of the site, and also for recreational purposes, such as camping, swimming and water sports (e.g. kayaking and surfing). Facilities present include a camping and caravan park on the southern part of the site and a football pitch. Access points to the site include a road into the camp site and a road to the soccer club. The most northern part of the site is fenced by private owners.

The site is designated as Doogort Machair/Lough Doo SAC (IE0001497) (NPWS, 2013a), as it contains Annex I-listed priority habitat machair, which is protected under the EU Habitats Directive (92/43/ECC) and requires particular protection on account of its limited distribution and risk from habitat loss (O’Keeffe, 2008). In addition to the Annex I-listed habitats machair and grey dune, an Annex II species, petalwort (*P. ralfsii*), has been recorded at this site and alongside machair is one of the qualifying interests of the site (NPWS, 2013b).

A baseline habitat map was produced for the sand dune habitats in the Lough Doo sub-site during the Coastal Monitoring Project (CMP) (Ryle *et al.*, 2009). This map lists the total area of machair habitat to be 96.9 ha, 88.2 ha of which is contained within the boundary of Doogort Machair/Lough Doo SAC (NPWS, 2017).

### 5.2.1 Objective 1 – habitat mapping

This objective aimed to identify and map current coastal and sand dune habitats and interpolate past habitat change via aerial imagery interpretation. We used *A Guide to Habitats in Ireland* (Fossitt, 2000) to classify habitats in the field and we followed standard best practices to map habitats and habitat mosaics as per Smith *et al.* (2011) by adding both habitat types to the polygon and putting the most dominant habitat label first, e.g. CD6/CD3. We identified habitats to a minimum mappable area of 20 m × 20 m (Smith *et al.*, 2011); however, smaller areas of notable habitats were noted and included in the maps if they were visible in the aerial photographs.

For this objective, we replicated the 1996 Biomar Irish machair vegetation survey (Crawford *et al.*, 1998) at Doogort. Using 2 × 2 m quadrats, we recorded the percentage cover of each species within the quadrat in the same location as the previous study using Garmin ETrex Venture GPS units. Using the sand dune habitat keys, we noted any indicator species for a particular habitat, as listed in Fossitt (2000), to aid identification of the habitat in which quadrats were located. The field visits to the sites were spread out over the course of 3 months in the summer, from June to August 2016.

We transferred the data collected in the field into ArcMap (10.2) and we used aerial photographs from 1995, 2000, 2005 and 2010 to create digital habitat

**Table 5.1. WP5 objectives**

Objective	Description
Objective 1	Assess plant functional traits to assess ecosystem function by constructing a species abundance matrix with a species trait matrix
Objective 2	Observe the response of beach–dune vegetation, machair and blanket bog biodiversity to large (preferably) perturbations in the system (e.g. bog burst, coastal and/or inland flooding, drought)



maps showing past habitat distributions within the site boundary. Habitats were identified using the 2016 habitat maps as aids and by observing signature vegetation patterns to determine the size and shape of the habitat polygons. The same approach for recording habitats and mosaics was used as for the 2016 habitat maps, using Fossitt (2000) codes. As the aerial photographs from 1995 were in black and white, any vegetation visible from the aerial photographs represented by the black and grey shading of the aerial photos was given the label of “VEG”. Any unvegetated sandy areas, such as sand dunes and blowouts, were represented by any white colouring in the aerial photo and were given the label “open sand”.

### 5.2.2 Objective 2 – plant functional traits

We also gathered data for plant functional trait analysis using the 1996 Biomar survey (Crawford *et al.*, 1998), which provided the species and physical property data for various machair plots. The species data were recorded using the Domin scale of abundance and required transformation into percentage cover using the mid-range value in line with the National Grasslands Survey guidelines (O'Neill *et al.*, 2010; Table 5.2). Furthermore, to better place the study site machair into proper context, we chose six additional machair sites for reference. Species that were present at fewer than five plots in each of the sites were removed from the study, consistent with the methodology outlined by Lewis *et al.* (2014a). Bryophytes were excluded on account of a lack of accessible trait data.

**Table 5.2. Transformation of Domin scale values in the Biomar study to percentage cover values. Mid-range values were used, in line with the National Grassland Survey guidelines**

Domin scale	Range (%)	Mid-value used (%)
10	91–100	95
9	76–90	83
8	51–75	63
7	34–50	42
6	26–33	30
5	11–25	18
4	4–10	8
3	<4 frequent	3
2	<4 occasional	0.5
1	<4 rare	0.3

Trait data are based on the LEDA traitbase, a database of life-history traits of the Northwest European flora (Kleyer *et al.*, 2008), and the traits used by Lewis *et al.* (2014b). Quantitative variables, such as canopy height (CH), seed mass (SM), terminal velocity (TV), leaf dry matter content (LDMC) and specific leaf area (SLA), were chosen, adapted from Lewis *et al.* (2014b), but the majority of the data were obtained from the LEDA database (Kleyer *et al.*, 2008, Table 5.3). In most cases, values were available for species based on studies all across Europe and, when this was the case, we used the value from studies relating to the UK. Where data gaps occurred, for example where species had no values for certain traits, we used values for a similar species of the same genus. In one case, we lacked species data on a specific trait and, as there were no studies on any species of this genus available for this chosen trait, an average was taken of all the other values for that trait and inserted into the matrix. Other traits, such as age of first flowering, plant lifespan, plant growth form, seed bank and dispersal type, were also chosen as suitable traits to investigate based on their prominence throughout the literature.

We also assessed Ellenberg values for light (L), moisture (M), reaction (R), nitrogen (N) and salt (S). The values used here were adapted from the ECOFACT research programme in the UK, where researchers used Ellenberg publications to provide a full set of Ellenberg values for selected plant species across the British Isles (Hill *et al.*, 1999). Where no values were provided, the researchers used their own calculations to provide a more complete outlook of species within the British Isles.

We calculated functional diversity measures following Leps *et al.* (2006) and a macro-enabled Excel file

**Table 5.3. Plant functional traits used to assess machair sites**

Variable	Source
SM	LED A (Kleyer <i>et al.</i> , 2008)
TV	LED A (Kleyer <i>et al.</i> , 2008; Lewis <i>et al.</i> , 2014b)
SLA	LED A (Kleyer <i>et al.</i> , 2008; Lewis <i>et al.</i> , 2014a)
LDMC	LED A (Kleyer <i>et al.</i> , 2008; Lewis <i>et al.</i> , 2014b)
CH	LED A (Kleyer <i>et al.</i> , 2008)
Ellenberg L	Hill <i>et al.</i> (1999)
Ellenberg N	Hill <i>et al.</i> (1999)

(FunctDiv.xls). The macro can be used to calculate the Rao index for species and traits (Leps *et al.*, 2006), functional diversity indices (Mason *et al.*, 2005), community-weighted means based on traits and the relative abundance of a species in a plot. The Rao index has the ability to indicate many useful properties associated with the functional diversity of a community. In general, it reflects the probabilities of choosing two random individuals in a community that are, in fact, different (Leps *et al.*, 2006). When dealing with trait diversity, the Rao index measures the likelihood that they are in some way functionally different. The Rao coefficient offers useful properties for analysing the functional diversity of a community and is indeed a more generalised form of the Simpson index of diversity (Leps *et al.*, 2006) and has the form:

$$FD = \sum_{i=1}^S \left| \sum_{j=1}^S d_{ij} p_i p_j \right| \quad (5.1)$$

The proportion of  $i$ th species in a community is  $p_i$  and dissimilarity of species  $i$  and  $j$  is  $d_{ij}$  and  $s$  is the number of species in a community (Leps *et al.*, 2006).

## 5.3 Results

### 5.3.1 Objective 1 – habitat maps

The replication of the Biomar Irish machair vegetation surveys (Crawford *et al.*, 1998) carried out at Doogort resulted in a resurvey of five quadrats at the site (Table 5.4). This yielded a minimum of four and a maximum of six machair habitat indicator species, all ranging from 5% to 70% cover of a quadrat. Other quadrats could not be resurveyed, as these were on private land (e.g. trailer park) for which access permission could not be obtained, or the plot was destroyed. These findings are compared with the presence ( $P$ ) or absence ( $A$ ) of the 1995 results species within the quadrats.

The vegetation height at Doogort was between 3 and 5 cm, with the difference between the 2016 and 1995 surveys ranging from 2 to 3 cm. The overall vegetation and individual habitat cover at the site shows an increase of 18.7% over 20 years, with a substantial increase between 2005 and 2010 (Table 5.5).

The sand dune habitats present are machair (CD6), marram dune (CD2), fixed dune (CD3) and dune slack (CD5). We estimate that the Doogort machair

**Table 5.4. Plant species composition cover in Doogort machair, County Galway, as recorded from the Biomar 1995 surveys and our 2016 resurveys<sup>a</sup>**

Species	Frequency of quadrats (of 5) (%)	Mean cover 1995 (%)	Mean cover 2016 (%)
<i>Bellis perennis</i>	100	16	16
<i>Festuca rubra</i>	100	26	55
<i>Galium verum</i>	100	4	28
<i>Lotus corniculatus</i>	100	11	18
<i>Luzula campestris</i>	100	3	5
<i>Plantago lanceolata</i>	100	13	27
<i>Trifolium repens</i>	100	13	40
<i>Achillea millefolium</i>	80	0	8
<i>Carex arenaria</i>	80	2	9
<i>Carex flacca</i>	80	14	10
<i>Cerastium fontanum</i>	80	2	8
<i>Leontodon autumnalis</i>	80	7	26
<i>Climacium dendroides</i>	60	5	15
<i>Euphrasia officinalis</i> sp.	60	9	20
<i>Poa pratensis</i>	60	3	5
<i>Prunella vulgaris</i>	60	13	10
<i>Rhytidadelphus squarrosus</i>	60	2	20
<i>Cerastium semidecandrum</i>	40	4	5
<i>Cynosurus cristatus</i>	40	2	8
<i>Leontodon taraxacoides</i>	40	18	13
<i>Potentilla anserina</i>	40	4	25
<i>Agrostis stolonifera</i>	20	1	5
<i>Carex nigra</i>	20	0	15
<i>Cirsium vulgare</i>	20	1	5
<i>Ditrichum flexicaule</i>	20	30	5
<i>Fissidens adianthoides</i>	20	0	30
<i>Homalothecium lutescens</i>	20	3	5
<i>Koeleria macrantha</i>	20	0	40
<i>Linum catharticum</i>	20	3	5
<i>Sagina nodosa</i>	20	3	5
<i>Taraxacum officinale</i>	20	1	5
<i>Thymus</i> sp.	20	0	5
<i>Thymus praecox</i>	20	0	10
<i>Tortula ruralis</i>	20	63	15

<sup>a</sup>Species ordered according to frequency of occurrence.

cover ranged from 24.7% to 32.0% over our survey period. These percentage covers include both dry and wet machair (CD6, CD6 wet) on their own, as well as mosaics with other habitats (e.g. CD6/CD5). The

**Table 5.5. Habitat cover change (%) at Doogort from 1995 to 2016**

Parameter	1995 (%)	2000 (%)	2005 (%)	2010 (%)	2016 (%)
Total vegetation cover	56	57	65	75	75
Open sand	30.02	21.96	14.00	4.14	4.86
<b>Habitat</b>					
Buildings and artificial surfaces (BL3)	0.26	0.3	0.3	0.38	0.38
Car tracks	0.19	0.02	0.08	0.5	0.4
Embryonic dune (CD1)		0.13	1.02	1.49	0.9
Marram dune (CD2)		0.55	1.94	4.59	5.19
Fixed dune (CD3)		12.66	14.6	10.28	12.1
Dune slack (CD5)		0.71	1.04	2.65	2.54
Machair (D6)		20.48	23.87	28.37	28.1
Marram/machair mosaic (CD2/CD6)		0	0	0.18	0.12
Dune slack/fixed dune mosaic (CD5/CD3)		10.94	10.4	13.55	14.41
Dune slack/machair mosaic (CD5/CD6)		0	0.21	0.59	0.47
Machair/fixed dune mosaic (CD6/CD3)		4.08	4.44	3.55	2.66
Machair/fixed dune mosaic (CD6/CD3)		0.14	0.22	0.11	0.12
Dystrophic lake (FL1)	0.37	0.43	0.5	0	0
Eroding river (FW1)	0.15	0.22	0.2	0.28	0.56
Depositing river (FW1)	0.39	0.71	0.83	1.78	0.35
Amenity grassland (GA2)	3.33	3.4	3.5	3.5	3.5
Marsh (GM1)		0.9	0.8	0.8	1.11
Wet grassland (GS4)		4.09	3.91	4.26	4.3
Shingle and gravel shores (LS1)	1.76	1.28	1.39	3.58	4.37
Sand shores (LS2)	15.1	14.8	14.9	10.42	11.2
Archaeological features	0.12	0.22	0.16	0.3	0.3

percentage of cover of dry and wet machair increased by 7.1% from 2000 to 2016.

At Doogort, fixed dune (CD3) covered on average 12.9%. The marram dune vegetation (CD2) increased by 4.6% between 2000 and 2016. Dune slacks (CD5) increased between 2000 and 2016. Including mosaics, there was a total percentage area of 11.6% in 2000 and 17.5% in 2016. Closer to the sea in the intertidal zone of the sites, the sand shores (LS2) have decreased over the past 20 years (3.9%).

Digital maps of the habitats observed during field studies were created to display the distribution and size of habitats over time (Figure 5.1a–e).

### 5.3.2 Objective 2 – plant functional traits

#### 5.3.2.1 Community-weighted mean and Mason indices

Community-weighted mean (CWM) and Mason index values (functional richness) of selected traits

indicate several traits with differences between Lough Doo Dry and Lough Doo Wet, which are highlighted by the figures relating to SLA, LDMC and SM. CH values are highest at Lough Doo Wet, whereas the traits of TV, L and N varied only slightly among the sites (Tables 5.6 and 5.7). CWM values for LDMC are the most variable across all sites. Lough Doo Dry has the highest value for LDMC across all sites (265), with the value at Keel Lough much lower, at 226. Relatively high values also occur at Mannin Bay (248) and Dooaghtry (247), with lower values at Lough Doo Wet (238) and Dogs Bay (237).

The Mason index of functional diversity is shown in Table 5.7. For SLA, the Mason functional diversity index highlights a large difference between Lough Doo Wet (12.0) and Lough Doo Dry (7.0) plots, Dogs Bay (8.4) and Dooaghtry (9.9) rank higher than both Keel Lough (7.7) and Mannin Bay (7.7) sites.

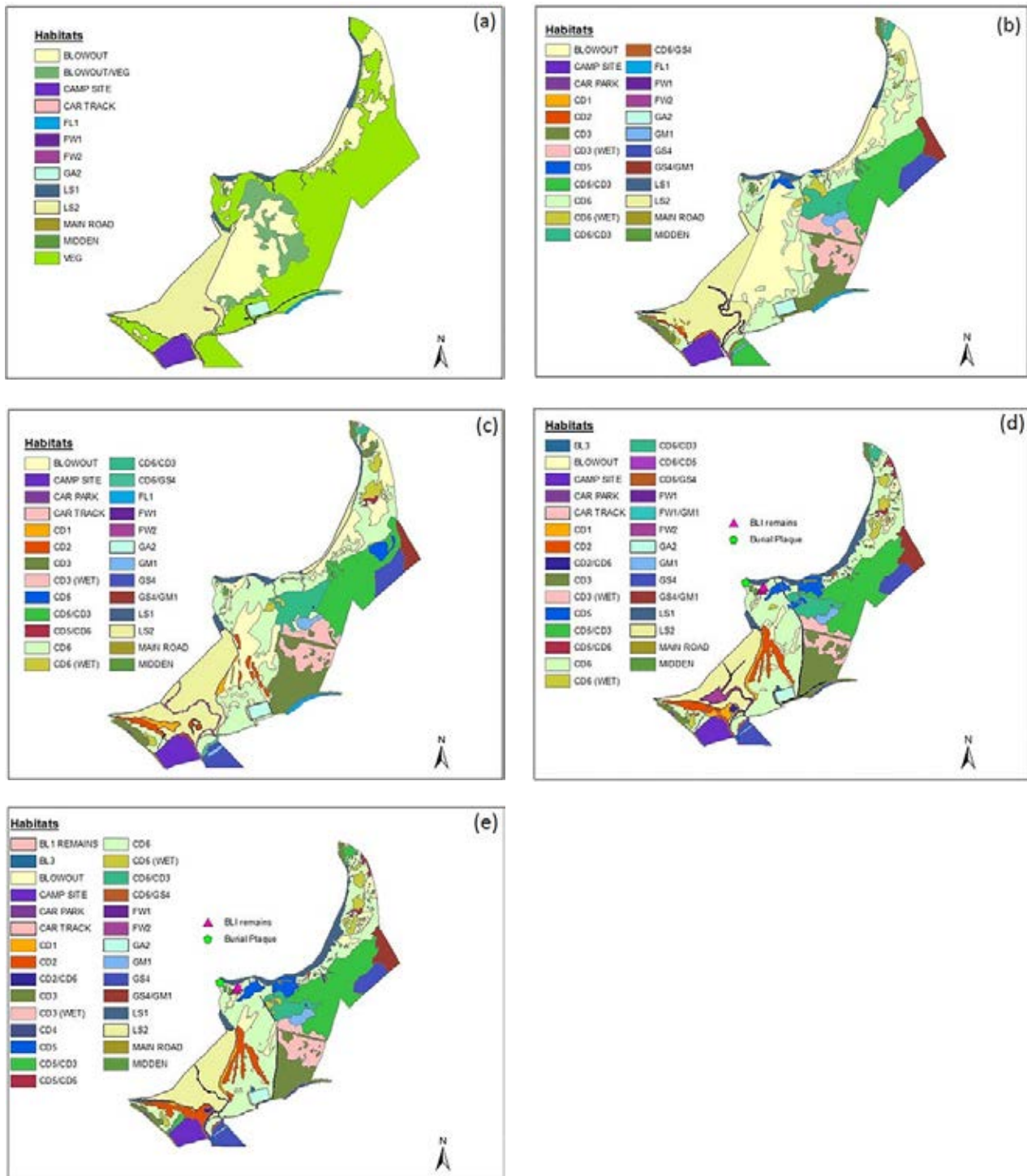


**Figure 5.1. Habitat map showing the identified sand dune habitats using Fossitt (2000) codes for (a) 1995, (b) 2000, (c) 2005, (d) 2010 and (e) 2016. See Figures 1.1, 1.2 and 2.3 for geographic reference.**

#### 5.3.2.2 Plant functional diversity – Rao

Overall all the machair sites exhibit similar Rao functional diversity measures (Table 5.8). Keel Lough is the most functionally diverse site (0.39), whereas Lough Doo Dry (0.36) and Dogs Bay (0.36) are the least diverse; however, the functional diversity varies by only 0.03 among the sites.

## 5.4 Discussion

### 5.4.1 Objective 1 – habitat mapping

Habitat changes from 1995 to 2016 in terms of vegetation cover at Doogort showed an increase of 19.3%, with a substantial increase of 18.3% occurring between 2000 and 2010. This site was shown to be

**Table 5.6. CWM trait values for SLA, CH, LDMC, SM, TV, Ellenberg L and Ellenberg N across all six sites**

Trait	Dogs Bay	Dooaghtry	Keel Lough	Lough Doo Dry	Lough Doo Wet	Mannin Bay
SLA	22.5	23.8	21.7	18.6	27.4	22.5
CH	0.3	0.3	0.3	0.3	0.4	0.3
LDMC	237.5	247.3	226.4	265.4	238.3	248.0
SM	1.0	0.7	0.7	1.6	0.6	0.9
TV	2.6	2.5	2.6	2.9	2.6	2.8
L	7.5	7.5	7.6	7.5	7.4	7.5
N	3.2	3.9	4.0	4.0	4.2	4.0

**Table 5.7. Mason index of functional diversity for SLA, CH, LDMC, SM, TV, Ellenberg L and Ellenberg N across all six sites**

Trait	Dogs Bay	Dooaghtry	Keel Lough	Lough Doo Dry	Lough Doo Wet	Mannin Bay
SLA	8.4	9.9	7.7	7.0	12.0	7.7
CH	0.2	0.2	0.2	0.2	0.2	0.2
LDMC	78.7	78.5	76.1	60.0	79.3	58.8
SM	0.7	0.6	0.6	1.8	0.6	0.7
TV	0.8	0.9	0.8	0.8	0.9	0.7
L	0.5	0.4	0.5	0.5	0.5	0.5
N	1.2	1.3	1.3	1.5	1.5	1.4

**Table 5.8. Mean values for the Simpson index, SLA, CH, LDMC, SM, TV, Ellenberg L, Ellenberg N and functional diversity across all six sites**

Trait	Dogs Bay	Dooaghtry	Keel Lough	Lough Doo Dry	Lough Doo Wet	Mannin Bay
Simpson	0.76	0.77	0.81	0.71	0.78	0.76
SLA	0.66	0.68	0.71	0.63	0.69	0.67
CH	0.07	0.07	0.08	0.07	0.07	0.07
LDMC	0.75	0.76	0.80	0.66	0.77	0.74
SM	0.25	0.21	0.20	0.29	0.18	0.21
TV	0.30	0.32	0.33	0.27	0.33	0.28
L	0.16	0.15	0.17	0.16	0.17	0.17
N	0.36	0.40	0.45	0.43	0.47	0.42
FD	0.36	0.37	0.39	0.36	0.38	0.37

FD, functional diversity.

potentially the most susceptible to erosion in 1995, with 30% of the site taken up by open sand. In 1991 and 1997 there were recorded windstorms, and in 1998 hurricane winds that affected the north and north-west of Ireland. These conditions could have been responsible for the areas of open sand, which are highly susceptible to erosion, seen in 1995 and 2000. It is possible that, prior to 1995, the areas of open sand observed were occupied by stable dunes and that the high wind power of storm activity then caused them to migrate inland by mobilisation of

dune sand (Tsoar, 2005). Therefore, the increasing vegetation cover occurring since 1995 suggests that the semi-stable habitats such as machair and marram dune will continue to become more fixed and develop into more stable habitats in the future. Based on the observed increase in vegetation cover compared with the amount of open sand, it can be said that the rate of succession corresponds to the extent of open sand. Furthermore, the vegetation that succeeded these areas of open sand in Doogort appears to show a swift response in highly disturbed areas.



Habitat changes throughout the site appear to be primarily attributable to shifts in the embryonic dune habitats between 2000 and 2016, all ranging from 0.1% to 1.4%. This is a highly mobile dune habitat and fluctuations in this habitat, are common. The natural progression of embryonic dune to marram dune was detected between 2010 and 2016 in Doogort, when the embryonic dune decreased and the marram dune increased, i.e. where there were once patches of embryonic dune in 2010, there is now marram dune.

Throughout the site, fixed dune is found in more inland areas and also in mosaic with other habitats. This is attributed to the fact that inland areas are sheltered from sea spray, allowing a greater variety of vegetation to grow (Ryle *et al.*, 2009). In Doogort, the average percentage cover of fixed dune remained 12% between 2000 and 2016. The lack of fluctuation in cover could be because of the heavy grazing of sheep and cattle; the land is unable to stabilise any further as a result of the constant removal of vegetation, erosion and the pressure exerted by treading, thus increasing the disturbance regime and inhibiting dune succession (Ritchie, 1974). The presence of grey dunes in Doogort, defined as fixed coastal dunes with herbaceous vegetation (Houston *et al.*, 2001), indicates that the fixed dune is further protected from erosion; therefore, there is no considerable decrease in percentage cover. These trends indicate that no further succession of fixed dune has occurred, as the next stage of fixed dune transformation (dune scrub and woodland) would not normally occur in Irish dune systems as a result of grazing and agricultural improvements (Fossitt, 2000).

Another trend for all sites is the increase in the wetter sand dune habitat dune slack. Doogort experienced an increase in dune slack, including its mosaic habitats of 5.9%. Between 2005 and 2010, overall dune slack cover increased from 11.6% to 16.9%. This could be a factor of the time of year when the aerial photographs were taken. For example, the 2010 image was taken in October, a particularly wet month, with 80.8 mm of rain and 148.6 mm of rain the previous month, whereas the photos for 1995, 2000 and 2005 were taken in the summer months.

The watercourse habitats, such as eroding and depositing rivers, have displayed fluctuating patterns throughout the years, which could be attributed to the amount of rainfall in a particular year or the time of

year when the aerial photograph was taken as well as to the natural course of the water changing over time. Built lands, such as those with roads or buildings on the site, remained the same throughout the years. There were small differences in area calculations, and these were probably the result of discrepancies in map drawing. Car tracks appear to have decreased on all sites, which may reflect the change in attitude of drivers driving on the machair grassland or the establishment of an overview parking area near the north-western edge of the site.

## **5.4.2 Objective 2 – functional traits**

### *5.4.2.1 Community-weighted mean and Mason indices*

The CWM for traits and the Mason index of functional diversity are measures of functional richness. The CWM trait value identifies the most dominant traits in a community and is linked to the mass ratio hypothesis (Grime, 1998), which states that the traits of the most abundant species are likely to dominate the formation of ecosystem processes (Ricotta and Moretti, 2011). Comparing the results of the various compositions of traits of communities enables inferences about the dominant land use strategies. For example, in a grazing-intensive machair environment, one would expect species to exhibit a lower CH and to invest fewer resources per unit area, with the opposite occurring in areas with a less grazing-intensive management regime (Lewis *et al.*, 2014a).

After the analysis, at Lough Doo Wet machair habitat the niche trait space appears to be taken up largely by plants with larger SLAs, with a higher average CH and a higher Ellenberg N value, which is a good indicator of soil fertility. Therefore, the community composition at this site is dominated by larger leaved and taller species. These characteristics would also be consistent with competitive species. An Ellenberg N value of 4 is indicative of more fertile soils representative of fixed dune habitats. This is not positive for the future prospects of machair at this site. Higher SLA values are associated with plants that have a tolerance for grazing (Zheng *et al.*, 2010). This would be expected because of the high levels of sheep grazing that occur at Lough Doo (Crawford *et al.*, 1998). The contrast between the Lough Doo Wet and Lough Doo Dry is noticeable in the CWM

results, particularly for the traits of SLA, LDMC and SM. The variability of community composition and CWM values is indicative of the highly diverse nature of the machair grassland, as these large differences occur in areas less than 1 km apart. Higher levels of SLA and CH, coupled with lower values of LDMC, are consistent with results outlined by Lewis *et al.* (2014b) on Scottish machair grasslands. The results for Lough Doo Wet agree with the findings of Lewis *et al.* (2014b) that LDMC declines with increasing disturbance. This also complements the results of Pakeman *et al.* (2011), who linked lower levels of LDMC to increased productivity and disturbance gradients.

A higher SLA and a lower LDMC is a strategy undertaken by plants in higher productivity areas, where higher SLA is associated with plants that are competitive in nature, whereas LDMC is an indicator of efficiency of nutrient conservation (Bochet and García-Fayos, 2015). The Bochet and García-Fayos (2015) findings are related to the scenario occurring at Lough Doo Wet, where the SLA values are relatively higher and LDMC is relatively lower. This is an indication that the competitive nature of plants there is vital for their survival. This finding is consistent with CSR results for the site, where competitive species are dominant (data not shown).

Lough Doo Dry is characterised by significantly lower SLA, which indicates a resource-poor environment; the need to retain captured resources is greater (Wilson *et al.*, 1999). The lower SLA at the site, taken in conjunction with a higher mean vegetation height, indicates a lower level of disturbance frequency. Differences in SM values between the two sites are worth noting, with higher seed mass values associated with Lough Doo Dry, which are associated with the harsh conditions at the site. The significant threat of erosion, by both the Aeolian transport of sand and strong onshore Atlantic winds, means that plants produce more seeds as a survival mechanism. The slightly more sheltered region of Lough Doo Wet could help explain the disparity in SM values between the two sites.

Across all six sites there are very few differences between trait values of TV and Ellenberg L. Prior to analysis, functional richness was much lower than expected, which is in most cases indicative of functional convergence. Lewis *et al.* (2014a) state that functional convergence can be tied to the process of

environmental filtering, whereby filters based on an environmental setting, or indeed on anthropogenic factors, reduce the potential array of traits in the niche space, resulting in similar traits dominating across various sites and environments.

#### *5.4.2.2 Functional diversity Rao*

The Rao functional diversity results offered little in terms of difference among the sites for all traits except for SM. This can be explained by a correlation of both the Simpson and Rao indices of functional diversity. Leps *et al.* (2006) claim that, when more dominance occurs in a sample, the likelihood increases that there will be a correlation between the Simpson and Rao functional diversity indices. *Festuca rubra* is the most relatively abundant in five of the six sites (Lough Doo Wet is the exception), in line with the suggestion by Leps *et al.* (2006). It could be argued that 10–15% abundance is not dominance. However, when the top five most relatively abundant species are taken from each of the sites, their composition as a group could be considered dominant, and this is the factor that results in this correlation.

SM values at Lough Doo Dry would indicate the presence of ruderal species that generate large quantities of seeds to combat high levels of grazing. However, an analysis of Lough Doo Dry plant strategies indicates that ruderals are the least prominent of the CSR strategies. This may indicate that these plants are producing large quantities of seeds in response to another variable. This would appear to be the result of the high threat associated with wind and sea erosion (Crawford *et al.*, 1998). Therefore, because of this high stress at this location, plants are producing more seeds as a survival mechanism in response to these harsh environmental conditions. This strategy is common not only in machair grasslands, but also in harsh landscapes, such as a plant tolerating increasing temperatures by producing more seeds (Bita and Gerats, 2013).

According to the results, the most functionally diverse site is that of Keel Lough; however, this finding should be interpreted with caution because of the high standard error. However, being more functionally diverse will be an advantage to the Keel Lough ecosystem function. Functional diversity is now widely accepted as a more favourable surrogate



for assessing ecosystem function (Diaz and Cabido, 2001). Therefore, Keel Lough's high functional diversity can be explained by its intensive grazing regime, the levels of ruderals being the highest of all the sites. Any potential shift in anthropogenic or environmental conditions would put pressure on an ecosystem if it did not have a widespread array of vital functional traits to ease this shift. Despite having a similar species composition to the other sites, some species exclusive to Keel Lough are likely to provide important traits that play a major factor in ecosystem function.

The role played by grazing in maintaining functional diversity is highlighted by Komac *et al.* (2015), who studied Andorran grasslands and found that functional diversity was maintained and enhanced through grazing, which also played a role in improving functional richness. Carmona *et al.* (2012) also note the vital role of grazing in increasing functional diversity in grasslands; however, note the limiting factor of water availability. In areas where there is not an unlimited supply of water, grazing intensity actually has the opposite effect, as it reduces functional diversity. Functional diversity is likely to be more affected by the grazing regime in place in wetter areas (Cingolani *et al.*, 2005). This is of particular interest for Lough Doo Wet, where wetter conditions are likely to help increase functional diversity in response to the grazing level. This is supported by the relatively high functional diversity value for Lough Doo Wet, in comparison with Lough Doo Dry, Dogs Bay, Dooaghtry and Mannin Bay, in spite of similar levels of grazing.

The relatively poor result for functional diversity is not uncommon in the literature. Pakeman (2011) found that functional diversity was not a good indicator for grassland productivity in his study based on LDMC of grasslands. The low levels of functional diversity across all sites, as a result of high land use intensity (grazing), are consistent with the results of Flynn *et al.* (2009), Pakeman (2014) and Laliberté *et al.* (2010).

## **5.5 Conclusions**

Coastal dune systems, including machair, are characterised by disturbance and change. However, using historical aerial imagery, field surveys and plant functional assessment we find that anthropogenic activities exert an overriding influence on the resilience of this coastal system by changing the capacity of these systems to respond to natural and anthropogenic stressors. At Doogort, we find a machair system that is unimpeded by hard engineering structures. This helped maintain the cover of machair vegetation and allow for an adequate supply of sand necessary for the maintenance of this system. However, our plant functional assessment indicates a shift towards nutrient-adapted species, suggesting an increase in organic matter content and a greater likelihood of a transition to a fixed dune or wet machair system. Management of anthropogenic stressors, such as reducing the existing grazing regime, a shift towards more cattle grazing and a reduction in soil compacting practices, will ensure machair stability and longevity.

## 6 WP6 – Hydrology, Water Quality and Catchment Exports

### 6.1 Introduction

WP6 focused on hydrology, water quality and the export of waterborne sediment and pathogens from the catchment draining into the Golden Strand area of the study catchment. The principal aim of this WP was to investigate how catchment exports influenced the coastal zone under a range of flow conditions, including extreme events. A subsidiary aim was to explore process interactions through the high-resolution monitoring of a range of water quality parameters and explore linkages to field observations from the coastal and dune surveys and ecological investigations in the machair zone. The water quality parameters that were selected for monitoring were temperature, pH, EC, DO, turbidity (as a proxy for SSC) and tryptophan fluorescence (as a proxy for faecal-based coliforms). According to Lawlor *et al.* (2012), long-term, high-resolution multiparameter monitoring of water quality has been limited in an Irish context but offers the potential to capture short-term fluxes and trends that can be missed by traditional discrete sampling methods (Dawson *et al.*, 2001; Wetzel, 2001), such as those adopted under the Water Framework Directive (WFD) (Blaen *et al.*, 2016; Dick *et al.*, 2016). This higher level of temporal precision is important, as many parameters may exhibit more complex patterns than those captured through periodic sampling (Campbell *et al.*, 2005; Lawlor *et al.*, 2012; Blaen *et al.*, 2016). This is particularly important when seeking to understand catchment dynamics in more remote settings that are subject to extreme weather events, such as those associated with Atlantic storms on the west coast of Ireland (Wang *et al.*, 2008), which are predicted to increase with climate change (Charlton and Moore, 2003).

### 6.2 Water Quality Parameters

The main water variables investigated in this study (temperature, pH, EC and DO) are some of the most commonly examined parameters in water quality monitoring (e.g. Prabu *et al.*, 2011; Lawlor *et al.*, 2012; Wade *et al.*, 2012) and collectively they

can provide a basic overview of river health. Many are interdependent and so it is sensible to monitor them together to identify trends and relationships. In addition, this study employed a tryptophan fluorescence sensor, which is a relatively novel technique that has shown potential as a surrogate measure for monitoring faecal coliforms associated with effluent from municipal and agricultural sources (Baker and Inverarity, 2004). Hereafter follows a brief synopsis of each parameter including some examples of former research in Ireland.

#### 6.2.1 Temperature

Temperature in degrees Celsius (°C) refers to the thermal energy of a substance and expresses how hot or cold it is (EPA, 2001). Temperature is measured using a thermistor sensor (YSI, 2017) and is easy and relatively inexpensive to continuously monitor (Webb *et al.*, 2008). It is a highly useful, yet undervalued, parameter, given that it affects both the chemical and physical composition of water (Caissie, 2006). The temperature of rivers and streams is dependent on many physical characteristics, the most obvious being climate and weather; however, it is also dependent on in-channel characteristics as well as on the type and quantity of the riparian zone (Webb *et al.*, 2008). Deeper sections of a channel will typically experience cooler conditions than surface water temperatures (Webb, 1996). A riparian zone can provide shading to keep river conditions cool, but can also act as insulation and cause more stable conditions in comparison with more exposed reaches (Webb *et al.*, 1996). Most aquatic biota have their own temperature range for survival; for example, some fish, such as trout, prefer cooler, shaded conditions (Caissie, 2006). Changes can also occur from other water sources, such as those from groundwater or the hyporheic zone (Story *et al.*, 2003). Heat is derived from radiation, evaporation, bed friction or conduction and atmospheric heat transfer (Webb *et al.*, 2008). Anthropogenic influences have been the recent focus of research in this area, focusing largely on the impacts of urban areas, industrial and

wastewater effluent on heat influxes in rivers (Poole and Berلمان, 2001). While temperature has an impact on the physical aspect of rivers, it also affects the chemical composition of water. For example, it affects the solubility of certain chemicals and substances, such as oxygen and salt, thereby influencing the way in which they are measured (EPA, 2001). As a result, these sensors must correct the data collected to a certain temperature so that they may be standardised and therefore may be comparable. No temperature standard in Irish rivers exists, as temperatures typically range between 0°C and 25°C (EPA, 2001). Results change seasonally, but mean values have been found to range between 7°C and 13°C (Regan *et al.*, 2011; Tedd *et al.*, 2017). The average stream temperature in the Glennamong river, a peatland stream in County Mayo, was found to be 10°C (O'Driscoll *et al.*, 2013). However, after trees were removed for harvesting purposes, the average temperature rose to approximately 13°C (O'Driscoll *et al.*, 2013). The forest clear-felling exposed the stream to more warmth and light, which in turn affected the aquatic biota residing within this reach.

### 6.2.2 pH

The parameter pH is a measure of the activity of hydrogen ions in a water sample (Hem, 1985; Tedd *et al.*, 2017). It is measured on a logarithmic scale of 0 to 14, with a pH of 7 considered as neutral and pH values below 7 being classified as acidic and those above 7 classified as basic (EPA, 2001). Most pH sensors consist of a glass membrane filled with a reference neutral liquid that experiences a constant and consistent binding of hydrogen ions, while the outside is exposed to the sample liquid (YSI, 2015). With the use of two electrodes within the probe, the difference in hydrogen ion activity is used to calculate a pH score for the water sample (YSI, 2015). As pH is influenced by temperature, the score is corrected to a temperature of 25°C (EPA, 2001). Most living organisms within rivers require the pH to be within the range of 6–9 for survival (EPA, 2001). The pH of water also strongly influences the solubility of many compounds, including metals, with lower pH levels generally increasing solubility and water toxicity as a result (Perlman, 2016). The most common cause of acidity in surface waters is dissolved CO<sub>2</sub> stemming from processes such as respiration, decomposition and acid rain (Hem, 1985). Water samples from

peatland catchments also tend to have lower pH values on account of the presence of humic acid and dissolved Fe (Hem, 1985; St-Hilaire *et al.*, 2004; Dick *et al.*, 2016). Seawater is more basic than freshwater because pH increases in the presence of dissolved salts (Perlman, 2016). According to the Irish EPA (2001), the optimum pH for water for drinking and bathing and for freshwater fish is between 6 and 9. In the River Boyne, County Meath, beside the M3 motorway, an average pH of 8.1 was found between January and June 2000; in 2010, over the same period, the pH ranged between 7.9 and 8.35. Values between 6.0 and 6.95 were found in the River Lee, County Cork (Lawlor *et al.*, 2012), and Tedd *et al.* (2017), in several studies around Ireland, reported values between 6.7 and 7.8. Donohue *et al.* (2006) reported a marginally higher range for a larger number of 290 sites within Ireland. However, lower pH values are typically recorded for rivers draining peatland catchment areas (Lawlor *et al.*, 2012). For example, O'Driscoll *et al.* (2013) reported pH ranges between 4.0 and 6.7, but pH values below 4 are rare and considered fatal to aquatic species (EPA, 2001).

### 6.2.3 Electrical conductivity

The EC of water refers to its ability to conduct an electrical current (Hem, 1985). It is linked to the ionic content of water, which in turn is related to the total dissolved solids (TDS) (EPA, 2001). The TDS content that is ionised is usually associated with dissolved salts (Miller *et al.*, 1988). EC is relatively easy to monitor (Schleppi *et al.*, 2006). Monitoring sensors measure the conductivity by generating an electrical current and gauging the response of the water sample to this current (Miller *et al.*, 1988). Results are usually given in microsiemens per centimetre (µS/cm) (YSI, 2015). Temperature has a direct influence on EC, which increases by 2% with a 1°C rise in temperature (EPA, 2001). For this reason, results are standardised to a temperature of 25°C (previously 20°C in some Irish and UK models). EPA (2001) suggests there is a difference of 10% in the results gathered via devices that correct the temperature to 20°C. The EC of water can reveal crucial information regarding its chemical composition, including salinity, which can be determined from EC and temperature (Miller *et al.*, 1988). As EC is linked to the TDS content of water, it is also a useful metric for monitoring pollution levels (Kuusisto, 1996). There normally

exists a positive correlation between pH and EC; however, there are specific conditions in which this relationship deteriorates, such as when there is a high content of dissolved organic matter (DOM) (Wetzel, 2001). Recommended values, as per drinking water regulations, are limited to 2500  $\mu\text{S}/\text{cm}$ . Measurements of EC from four stations along the River Lee, County Cork, showed an increase in EC downstream, because of urban and later tidal influences (Regan *et al.*, 2011). At the furthest upstream site in this study, in the peatland countryside of Gougane Barra, the EC ranged between 34.04 and 36.82  $\mu\text{S}/\text{cm}$  (Regan *et al.*, 2011). Further downstream, ranges of 83–144.11  $\mu\text{S}/\text{cm}$  were reported, with peaks of 40,000  $\mu\text{S}/\text{cm}$  in the Lee estuary (Regan *et al.*, 2011). An average range of 45–1029  $\mu\text{S}/\text{cm}$  was found for 244 sites located across Ireland between the years 1999 and 2002, featuring a variety of different catchment characteristics (Donohue *et al.*, 2006). Sites with higher conductivity were said to drain calcareous areas and/or catchments in which intensive farming practices occurred (Donohue *et al.*, 2006). According to Tedd *et al.* (2017), the natural baseline for EC is lower in Ireland than in the UK, with the former reporting values below 1000  $\mu\text{S}/\text{cm}$ , whereas the UK reports an average of 3055  $\mu\text{S}/\text{cm}$ . This, however, may be because of the more extensive water quality monitoring undertaken in the UK, creating a broader database. Table 6.1 gives empirical ranges reported for freshwater to seawater studies in Ireland and shows the marked difference in EC between freshwater and full marine conditions.

#### 6.2.4 Dissolved oxygen

Dissolved oxygen refers to the concentration of unbonded oxygen anions in a water sample. It is a very important and useful water quality parameter, as high DO is essential for aquatic life (Hem, 1985). There are several processes that produce DO in rivers and streams, including reaeration, which is common

in fast-flowing and turbulent water. Aquatic plants can convert  $\text{CO}_2$  into DO through photosynthesis during daylight hours (Wetzel, 2001). However, aquatic biota can also consume DO, depleting the content available, as can processes that involve decomposition (Hem, 1985; Wetzel, 2001). Rivers and streams containing higher concentrations of organic matter have been shown to produce lower rates of DO, as it is consumed during decomposition (O'Driscoll *et al.*, 2013). The oxidation of iron (e.g. during precipitation) has also been found to deplete DO in streams (Hem, 1985; Vuori, 1995). These factors may be important in peatland catchment areas where the sediment type transported by rivers in these regions contains humic-rich and Fe-bearing compounds (St-Hilaire *et al.*, 2004). The DO content is also highly influenced by both temperature and salinity. Temperature affects the solubility of oxygen in a non-linear capacity, as it increases in colder water (Wetzel, 2001). Conversely, the solubility of oxygen decreases with an increase in salt water (Wetzel, 2001). Oxygen is approximately 20% less soluble in seawater than in freshwater at the same temperature (Miller *et al.*, 1988), which is important to consider in brackish or transitional waters. Continuous, in situ monitoring is the most accurate method of measurement of this parameter, owing to the various influences affecting it at a high temporal rate (Guasch *et al.*, 1988; Wade *et al.*, 2012; Dick *et al.*, 2016). DO sensors use luminescence to examine the intensity of oxygen present in a sample of water and findings are reported in milligrams per litre (mg/L). Percentages can also be given to indicate how close DO is to 100% air saturation levels (YSI, 2015). According to the EPA (2001), results should be greater than or equal to 9 mg/L in at least 50% of samples taken within a single study or greater than 7 mg/L in all samples taken. These specifications are based on several water quality regulations, including the Freshwater Fish Directive (2006/44/EC) and the Surface Water Regulation. Lawlor *et al.* (2012) found DO to have a mean range between 9 and 10 mg/L in four sample areas along the River Lee, County Cork. Similarly, along the River Boyne and two tributaries in County Meath, they recorded an average of 12.0 mg/L between January and June in 2000 and found that over 77% of their samples, from the same period in 2010, were  $\geq 9$  mg/L (Purcell *et al.*, 2012). Although a motorway had been constructed between the two sampling periods, these findings suggest that this

**Table 6.1. Typical values for EC**

Type of water	EC ( $\mu\text{S}/\text{cm}$ )
Freshwater	0–2500
Brackish water	2500–40,000
Seawater	c.50,000

Compiled from SWRCB (2002), Donohue *et al.* (2006) and Lawlor *et al.* (2012).

did not have a negative impact on the DO content at this site.

### 6.2.5 Turbidity

Turbidity is related to the optical properties of water and is a measure of the degree of light scatter or absorbance of emitted light caused by suspended particles in the sample (Lawler, 2016). Turbidity describes the cloudiness of an environmental sample that stems from the presence of sediment and other particulate materials in suspension (Tedd *et al.*, 2017). The cloudiness is caused by the effect that suspended particles have on the scattering of light, which means the greater the volume of floating particles, the cloudier the water. This can have an impact on the process of photosynthesis, affecting DO levels, and impair the visual range of fish and other sighted species (Davies-Colley and Smith, 2007). For this reason, the use of turbidity as an indicator of detrimental levels of suspended and colloidal matter in freshwater systems is common.

Turbidity is often used as a surrogate measure for SSC, as it is not the quantity of sediment that causes the most problems, but rather the quality (EPA, 2001). Clear water cannot guarantee good-quality conditions, just as cloudy water may not necessarily indicate poor status. Although it is not the perfect measure for suspended sediment, turbidity has proved to be an excellent proxy, particularly in an in situ, quasi-continuous monitoring capacity (e.g. Uhrich and Bragg, 2003; Jastrom *et al.*, 2010). It is more practical and less costly than the long-term monitoring of SSC using acoustic backscatter instruments. However, there exists no standardised method for measuring turbidity, and this raises issues when comparing data collected using different sensor types and set-ups (Rymaszewicz *et al.*, 2017). For this reason, high-resolution turbidity records should always be calibrated against known SSCs to produce SSC time series that are comparable between sites and studies.

Turbidity is reported in either nephelometric turbidity units (NTUs) or formazin nephelometric units (FNUs) depending on the method of sampling. In practice, there is very little difference in the unit scales (Lawler, 2016). High-frequency monitoring of turbidity is one of the most reliable methods for capturing high temporal variability in SSC, often observed during storm events (Wade *et al.*, 2012). Because of the lack of

standardised measuring units, there are no definitive guidelines restricting quantities in rivers (EPA, 2001). Turbidity largely varies between rivers and even between reaches in the same river. For example, monitoring of the Owenabue and Bandon in County Cork gave ranges of 1–210 NTU and 1–71 NTU, respectively (Harrington and Harrington, 2013). Large floods were experienced during this study, one with a return period of 1 in 10 years, in which a turbidity peak of 410 NTU was experienced at the Owenabue site (Harrington and Harrington, 2013). The catchment consists largely of peat and podzols, with significant areas of calcareous and non-calcareous bedrock and sandstone (Harrington and Harrington, 2013). Although no exact values are given, turbidity ranged between 5 and 110 formazin turbidity units (FTU) for a section of the River Boyne, County Meath, downstream of the M3 motorway (Purcell *et al.*, 2012). During the construction period, when there was very little vegetation cover, turbidity reached peaks of over 100 NTU, mainly after precipitation events. However, values were reduced after vegetation cover was again established (Purcell *et al.*, 2012). It can be difficult to find values for turbidity in an Irish setting, as many studies convert and report their results in SSC (e.g. May *et al.*, 2005; Thompson *et al.*, 2014).

### 6.2.6 Tryptophan fluorescence

Fluorimetry (fluorescence spectroscopy) is widely employed in water quality monitoring to look at DOM, chlorophyll and algae (Baker *et al.*, 2015). Sensors work by detecting the wavelength of substances that fluoresce when receiving light. Data are reported in relative fluorescence units (RFUs). High-resolution monitoring of tryptophan-like fluorescence (TLF) to assess human influence on water quality is a relatively new and novel approach in the field of fluorimetry (Baker and Inverarity, 2004). TLF peaks are associated with the input of reactive/labile organic carbon (e.g. sewage or farm waste) and its microbial breakdown. Hence, real-time measurement of TLF can be used to monitor water pollution associated with faecal bacteria (Sorensen *et al.*, 2015) and, more broadly, as a surrogate for biological oxygen demand (BOD) (Khamis *et al.*, 2015a). Recent research has demonstrated that sensors operating in the TLF region do experience interference or “quenching” associated with temperature and turbidity (Khamis *et al.*, 2015a). In laboratory and field experiments, Khamis *et al.*



(2015b) demonstrated an inverse relationship with temperature, together with turbidity effects associated with specific particle size fractions (although in this study these did not require corrections).

The three main objectives for WP6 are described in Table 6.2.

### 6.3 Description of the Study Area

See section 1.1.3.

### 6.4 Materials and Methods

#### 6.4.1 Field monitoring equipment

##### 6.4.1.1 YSI EXO2 sonde

Stream water quality was monitored using a YSI-manufactured EXO2 Multiparameter Sonde (Figure 6.1). This instrument permits the deployment of multiple sensors and is equipped with an integrated depth recorder and central antifouling wiper for automated cleaning of the optical sensor heads. The six water quality sensors deployed in this study were temperature, pH, EC, DO, turbidity and a beta-tested tryptophan fluorescence sensor that was new to the YSI sensor pool (Table 6.3).

Automated field measurements for all sensors were recorded at 15-minute intervals via a YSI Storm 3 data logger. Readings were transmitted via a 3G Vodafone telemetry link to the YSI Storm Central platform every hour to allow remote website viewing of the datastream and facilitate data download at any time.

**Table 6.2. WP6 objectives**

Objective	Description
Objective 1	Measure hydrology and sediment flux to coastal dune systems from terrestrial surface drainage
Objective 2	Measure and determine associated dissolved and sediment-borne contaminant fluxes, including nutrients (N+ phosphorus) and pathogens (faecal coliforms). This will include application of the tryptophan sensor as a proxy for <i>Escherichia coli</i> in water
Objective 3	Develop process–response models linking sediment/nutrient/pathogen flux (surface hydrology) to meteorology (WP2) and coastal water quality metrics



**Figure 6.1. YSI EXO2 Multiparameter Sonde.**  
© 2020 YSI, a Xylem brand (reproduced with permission).

##### 6.4.1.2 Teledyne ISCO Autosampler

In tandem with the EXO2 sonde, an ISCO storm water autosampler (Figure 6.2) was installed to capture water samples during high-flow events for the purpose of calibrating the continuous turbidity data (Bruen, 2017). The ISCO sampler (Model 6712) that was available to the project team was integrated with the Storm 3 data logger, so bottles were set up to fire on a designated water level. The programme thereafter filled the carousel of 24 bottles in 12 hours, collecting an 800 mL sample every 30 minutes. The initial water level was set to 0.6 m but was increased to 0.8 m and then 0.9 m during the project in an attempt to capture major storm events. The ISCO sampler was powered by a 12 V battery, which was later augmented with a solar panel trickle feed supply. Despite these efforts, the project team encountered problems with repeated power failures, which are further discussed in section 6.4.3.

A summary of date and times when ISCO automated sampling was initiated is given in Table 6.4.

Programme initiation was monitored using the EXO2 depth readings on the Storm Central website. Bottles were collected as soon as possible after firing and stored at <4°C before being analysed in-house using standard methods. Details of the calibration, including problems that were encountered by the project team, are given in section 6.4.3.

##### 6.4.2 Site installation

The monitoring site was set up on the downstream side of a road bridge, approximately 500 m from the coast (54.009566°, -9.988230°) (Figures 6.3 and 6.4).

**Table 6.3. EXO sensors specifications**

Sensor	Units	Range	Accuracy	Resolution	Sensor type
Depth	PSI, depth (m)	0 to 10 m	±0.04% FS (±0.004 m)	0.001 m	Stainless steel strain gauge
Temperature (T) <sup>a</sup>	°C	−5°C to 50°C	−5°C to 35°C ±0.01°C 35°C to 50°C ±0.05°C	0.001°C	Thermistor
EC <sup>a</sup>	µS/cm	0 to 200 mS/cm <sup>c</sup>	0 to 100 mS/cm: ±0.5% of reading or 0.001 mS/cm, whichever is greater; 100 to 200 mS/cm: ±1% of reading	0.0001 to 0.01 mS/cm, range dependent	4-electrode nickel cell
pH	pH units	0 to 14 units	±0.1 pH units within ±10°C of calibration temperature; ±0.2 pH units for entire temperature range	0.01 units	Glass combination electrode
DO	% saturation (mg/L)	0% to 500% air sat., 0 to 50 mg/L	0 to 200%: ±1% reading or 1% air sat., whichever is greater; 200 to 500%: ±5% reading 0 to 20 mg/L: ±1% of reading or 0.1 mg/L; 20 to 50 mg/L: ±5% reading	0.1% air sat., 0.01 mg/L	Optical, luminescence lifetime
Turbidity	FNU <sup>b</sup>	0 to 4000 FNU	0 to 999 FNU: 0.3 FNU or ±2% of reading, whichever is greater; 1000 to 4000 FNU: ±5% of reading	0 to 999 FNU: 0.01 FNU 1000–4000 FNU: 0.1 FNU	Optical, 90° scatter
Tryptophan fluorescence	RFU, QSU	0 to 100 RFU	Not reported	0.1 RFU	Pumping cell. T channel (excitation 280 nm, emission 340 nm)

<sup>a</sup>Temperature and EC sensors are integrated in a single device.

<sup>b</sup>The EXO turbidity sensor employs a near-infrared light source and detects scattering at 90° of the incident light beam. According to the ASTM D7315 method (ASTM International, 2017), this type of turbidity sensor has been characterised as a nephelometric near-infrared turbidimeter, non-ratiometric. This method calls for this sensor type to report values in FNUs, which closely correspond to NTU.

<sup>c</sup>EC was calibrated and logged as specific conductivity in this project.

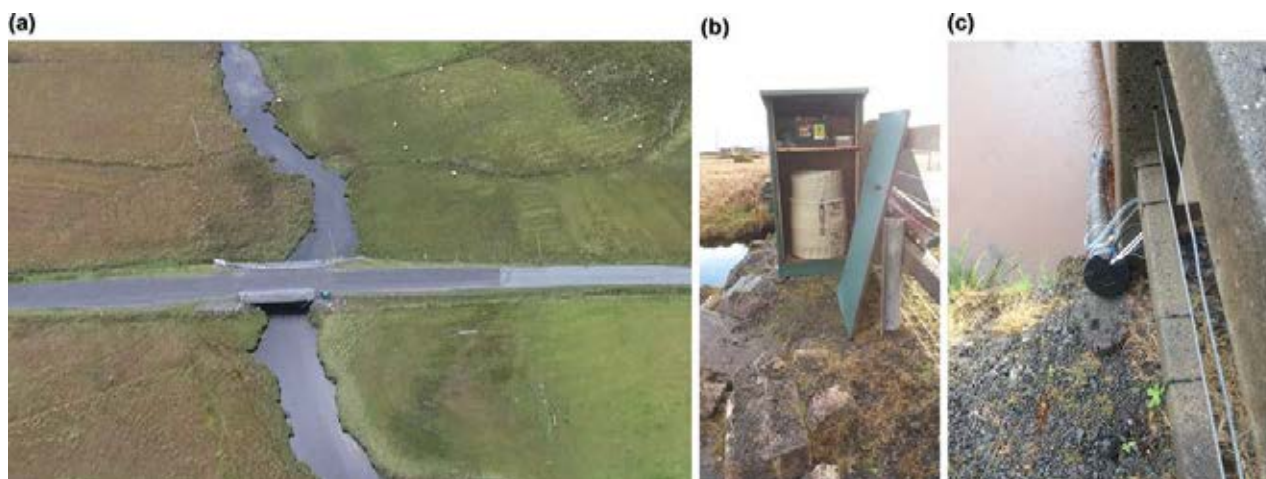


**Figure 6.2. (a) Location of Teledyne ISCO autosampler in custom-built box beside bridge. (b) Close-up view of ISCO sampler containing sampling bottles. (c) The PVC pipe housing the EXO2 sonde.**

This site was chosen because of the ease of access and because it provided solid ground and secure mountings for the weatherproof, custom-made casings that housed the Storm 3 data logger and ISCO autosampler and protected the equipment from

theft. The EXO2 sonde was housed in a 5 m PVC pipe, which was secured to the bridge and river bed. The PVC pipe had a padlocked metal bolt at the top for security and was perforated at the position of the sonde to allow the stream water to flow freely past the

**Table 6.4. ISCO programmes run during the monitoring period**

No.	Programme start date (time)
1	10 June 2016 (09:21)
2	14 June 2016 (13:30)
3	9 July 2016 (12:45)
4	23 September 2016 (23:27)
5	5 February 2017 (08:15)

sensors. A metal bolt was positioned near the base of the pipe to ensure that the sonde remained in a fixed position c.0.4m above the river bed for the duration of the study. A rope tied to the top of the sonde ensured that it could be removed and returned safely after each on-site check.

#### **6.4.3 Site maintenance and troubleshooting**

##### *6.4.3.1 Calibration of sensors*

Sensor calibration was carried out as per the manufacturer's guidelines (YSI, 2015). The dates of

calibration are summarised in Table 6.5 and resulted in short (up to 24 hours) breaks in the data stream.

##### *6.4.3.2 Power supply issues and solutions*

To avoid initial concerns regarding theft and vandalism at the site, rather than using solar panels, power supply was provided through two deep-cycle, 12V batteries. The sonde and data logger power supply typically lasted for c.3 months, while an independent 12V battery to the ISCO sampler typically provided sufficient power for 1–2 months of operation, plus the running of the programme once initiated. The project team, however, encountered issues with the ISCO batteries, resulting in loss of power and the failure to capture a number of large events during the monitoring period. To resolve power supply issues, both batteries' set-ups were augmented with 5V solar panels in the second year of monitoring.

##### *6.4.3.3 Calibration of the turbidity data*

A total of 144 ISCO water samples were collected to develop a field calibration between the continuous,



**Figure 6.3. Location of monitoring site at the road bridge on the unnamed stream, south of Doogort beach and dune area. See also Figure 1.3. Map data: Google, CNES, Airbus © 2020.**





**Figure 6.4. Monitoring site set-up showing (1) the PVC pipe housing the EXO2 sonde, (2) the custom-made box housing the Storm 3 data logger and (3) the box housing the ISCO autosampler.**

**Table 6.5. Dates of sensor calibration**

No.	Calibration date
1	9 June 2016
2	9 October 2016
3	4 February 2017
4	10 July 2017
5	10 February 2018

high-resolution (15 minutes) turbidity data and SSCs. The majority of these samples contained negligible sediment, so a subset of 30 water samples, which visually contained the highest suspended sediment, were analysed to determine total suspended solids (TSS) following the APHA Standard Method 2540D, using standard glass microfibre filters with a particle retention of 1.2  $\mu\text{m}$  (see Bruen, 2017). The results, however, showed a poor correlation between NTU and SSC values (Figure 6.5). Given that instrument calibration indicated that the turbidity sensor was performing correctly, the poor correspondence was most likely to be the result of particle size effects.

The poor fit precluded the use of an ISCO-based SSC versus NTU rating relationship. Instead, samples of sediment were collected manually from the river bed

to develop a rating relationship through the creation of in-house standards in the final phase of the project. Two very distinctive types of sediment were evident on the river bed, as shown in Figure 6.6. The first was a dark-grey, organic-rich, minerogenic sediment and the second was an orange-brown, very fine sediment that was observed in layers along some sections of the stream, believed to be Fe-bearing minerals that have precipitated from the bog water draining the peatland.

Sample preparation involved oven drying at 105°C, manual disaggregation and sieving to <90  $\mu\text{m}$  to more closely reflect the sediment fraction transported in suspension (Walling, 1983). Using the EXO2 sonde in “run” mode, turbidity values were determined for prepared sediment concentrations in deionised water, ranging from c.20 mg/L to >1000 mg/L. Sediments were kept in suspension using a magnetic stirrer. Both sediment types were tested, together with a sediment mix comprising 10% and 30% of the bog Fe by weight. The results in Figure 6.7 show a significant difference between the minerogenic sediment and sediment containing progressively higher proportions of the Fe-rich sediment, although there was only a marginal difference in turbidity values between sediment containing 30% and 100% Fe-rich sediment.

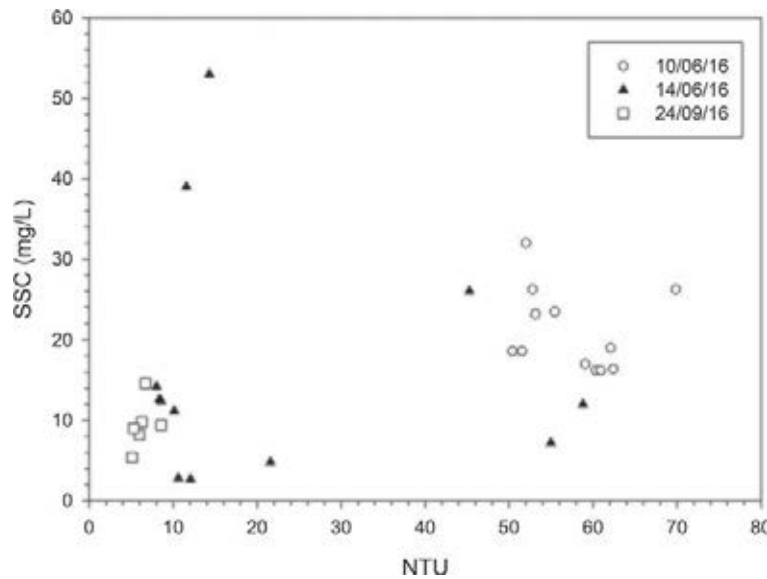


**Figure 6.5. SSC–turbidity relationship for field samples ( $n=30$ ).**



**Figure 6.6. Laboratory set-up for the preparation of the in-house standards. Inset shows close-up of the two sediment types with Fe-rich sediment on the left.**

Figure 6.8 plots the ISCO field sediment samples with the in-house standards models and supports the hypothesis that the different turbidity values of the field samples are the result of very distinctive sediment types moving under different flow and flood conditions in the catchment. For example, the lower FNU/SSC values recorded for some of the field samples lie between the 100% and 90% organic-mineral sediment curves, while the higher FNU/SSC values for the water samples (collected on 10 June 2016) plot beyond the 100% Fe-rich sediment curve. This could be because this suspended sediment was finer than the sediment collected from the bed or because some of the sediment had returned to aqueous solution during

storage. Irrespective of the reasons for the variable turbidities shown by the field and laboratory testing, the marked differences in turbidity values shown by these tests emphasises the importance of capturing water samples in the field for calibration of the continuous turbidity data and made determination of SSC from the turbidity data problematic.

#### *6.4.3.4 Flow reconstruction*

The remote location of the field site meant that manual direct measurement of discharge for sufficient flows to develop a robust stage-discharge rating would present challenges to the project team. As an alternative a continuous flow record for the project period was to be reconstructed using a channel rating derived from a Hydrologic Engineering Center – River Analysis System (HEC-RAS) model of the river channel and bridge, in combination with the water level record recorded at the bridge monitoring station. HEC-RAS is a one-dimensional link and node river model that continues to be developed by the US Army Corps of Engineers. The HEC-RAS model itself was based on channel cross-section and bridge geometries (Figure 6.9) determined from a topographical survey of the study site and it was intended that the model would be executed using observed water levels over the downstream sand bar as the downstream boundary condition. In the course of analysis, however, mismatches between observed water levels at the location of the downstream sand bar and those at the



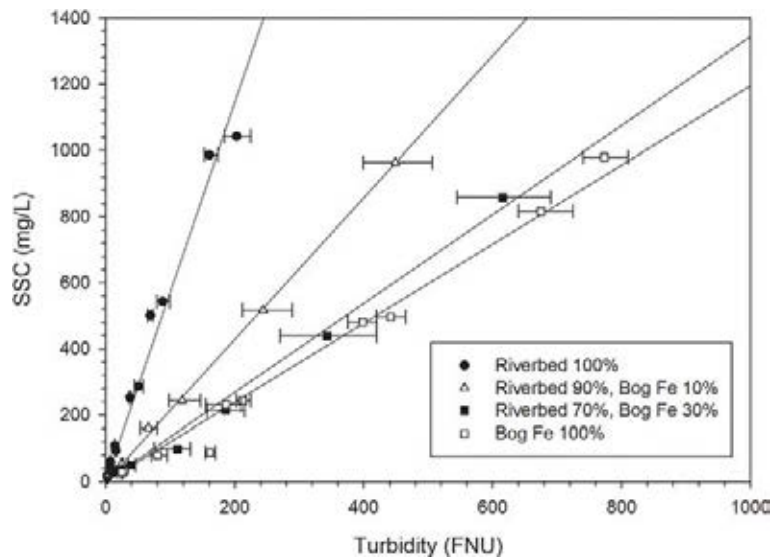


Figure 6.7. Linear calibration models for in-house standards for sediments collected from the river bed in the unnamed stream (riverbed 100%:  $y=5.7178x$ ,  $r^2=0.98$ ; riverbed 90%:  $y=2.142x$ ,  $r^2=0.99$ ; riverbed 70%:  $y=1.3436x$ ,  $r^2=0.99$ ; bog Fe:  $y=1.2074x$ ,  $r^2=0.98$ ).

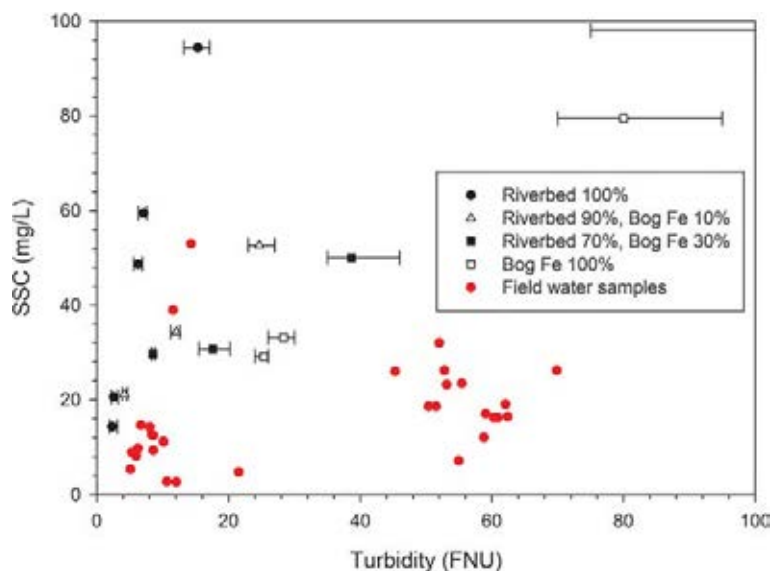


Figure 6.8. Comparison of the field samples and in-house standards.

monitoring station emerged and it was not possible to correlate monitored levels with reliable flows. The analysis of the recorded data suggests that the water was leaving the channel through the boundary (bed, banks and/or the downstream sand bar). A verified measured ADCP (acoustic doppler current profiler) flow of  $0.487 \text{ m}^3/\text{s}$  at a depth of 1.4 m, which was below the minimum elevation of the sand bar, confirmed this loss of water. In the absence of a reliable record of river discharge, it was not possible to determine sediment fluxes from the catchment as was first intended.

#### 6.4.3.5 Data cleaning and analysis

Aside from the depth sensor, which malfunctioned prior to calibration in February 2017, the sonde sensors produced stable data streams and showed no evidence of significant drift following calibration. Continuous and high-resolution turbidity data, however, are rarely free from data spikes or other defects and therefore turbidity records often require data quality checks and cleaning (Bruen, 2017). Data were first screened to identify dubious singular peaks that were five times higher than the preceding



**Figure 6.9. Map showing relative positions of cross-sections and long-profile surveys for flow reconstruction. Map data: Google, CNES, Airbus © 2020.**

and subsequent data values. Thereafter the study employed the methods adopted in the EPA SILTFLUX project (Bruen, 2017) by overlaying turbidity data with water levels to identify spurious data not associated with higher flows. Such data should be treated with caution and, as noted by SILTFLUX, knowledge of the catchment and surroundings of the monitoring point is important to identify potential point source sediment inputs that could be contributing to short-duration turbidity peaks. Reconnaissance fieldwork revealed no evidence of bank instability or other such point sources, so significantly elevated values were assumed to be the result of sensor fouling, outliers, sensor sensitivity or malfunction. Where spurious spikes were removed, the data were linearly interpolated using the ROW function in Excel.

## **6.5 Results**

### **6.5.1 Summary of results**

Summary statistics for water depth and each of the EXO2 sonde water quality parameters are shown in Table 6.6. These do not include spurious peaks that

were removed during data cleaning (section 6.4.3.4). A total of 806 days of data (at 15-minute resolution) were collected for all sensors, with the exception of the tryptophan fluorescence sensor, which was installed later in the project. The percentage recovery for all sensors was >90% with data loss resulting from sensor calibration and an extended period between May and June 2017, when the sonde was not operating as a result of the power failures mentioned earlier.

### **6.5.2 Sensor data time series**

Time series are presented for each water quality parameter in Figures 6.10–6.16. These data are plotted with EXO2 water depth (as noted in section 6.4.3.3, flow could not be modelled for the site) and tidal data from the most local buoy at Ballyglass, County Mayo. In addition, hourly rainfall data from Dooagh, Achill Island, which is located c.10 km south-west of the monitoring site, are plotted above each plot. Given the length and resolution of the datasets, the results are presented for each monitoring year of the project.

**Table 6.6. Descriptive statistics and summary of data collected for each water parameter**

Sensor	Statistics	Monitoring period	Data days	Recovery (%)
Depth (m)	Max: 1.18 Min: -0.25 Med: 0.55 LQ: 0.31 UQ: 0.68	10 June 2016 to 24 April 2018	806	93.9
Temperature (°C)	Max: 20.35 Min: 1.87 Med: 10.21 LQ: 6.99 UQ: 13.83	10 June 2016 to 24 April 2018	806	93.9
Specific conductance (µS/cm)	Max: 49,175.17 Min: 9.35 Med: 125.47 LQ: 99.58 UQ: 177.66	10 June 2016 to 24 April 2018	806	93.9
pH	Max: 7.77 Min: 4.64 Med: 5.71 LQ: 5.45 UQ: 5.97	10 June 2016 to 24 April 2018	806	93.9
DO (mg/L)	Max: 12.67 Min: 0.88 Med: 8.63 LQ: 7.2 UQ: 10.04	10 June 2016 to 24 April 2018	806	93.9
Turbidity (FNU)	Max: 674.14 Min: 0.06 Med: 3.13 LQ: 2.06 UQ: 6.39	10 June 2016 to 24 April 2018	806	93.9
Tryptophan fluorescence (RFU)	Max: 4.26 Min: -1.57 Med: -0.54 LQ: -0.8 UQ: -0.27	06 February 2016 to 24 April 2018	565	90.2

**LQ, lower quartile; Max, maximum; Med, median; Min, minimum; UQ, upper quartile.**

#### 6.5.2.1 Rainfall, water level and tidal data

Hourly rainfall data for the monitoring period were obtained from the Dooagh water treatment plant. High-resolution (6 minutes) tidal data are plotted for Ballyglass, County Mayo, which is the nearest monitoring buoy to the study site. The tidal data showed the classic semi-diurnal tidal pattern experienced on the west coast of Ireland (Marine Institute Ireland).

In terms of the flow data, the calibration of the sonde carried out on 4 February 2017 resulted in a shift in the water level because the sensor had become clogged. Therefore, data for the preceding 2 weeks (and possibly up to 2 months) may be unreliable. Overall, however, the water depth showed good correspondence with observed depths in the field during site visits.

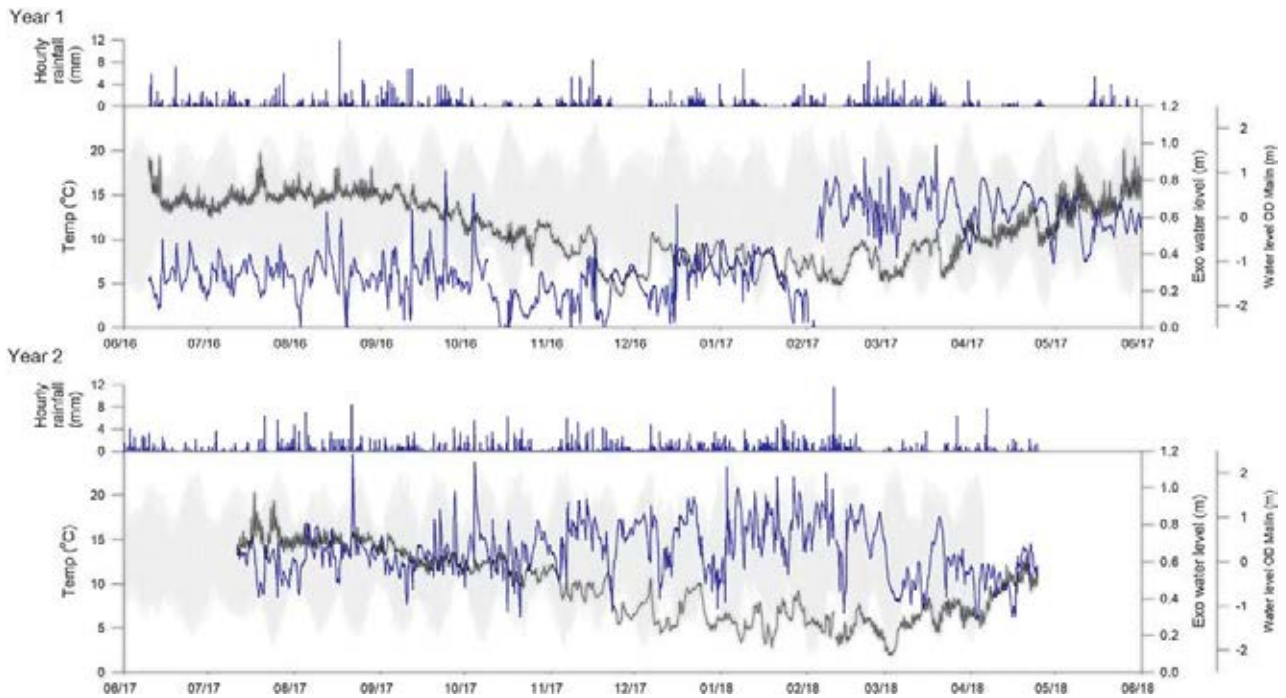


**Figure 6.10.** High-resolution (15 min) temperature time series (black) plotted with EXO2 water level (blue) and tidal data from Ballyglass tidal gauge (grey). The hourly rainfall data above each plot (also in blue) are from the Dooagh water treatment plant, south-west Achill Island.

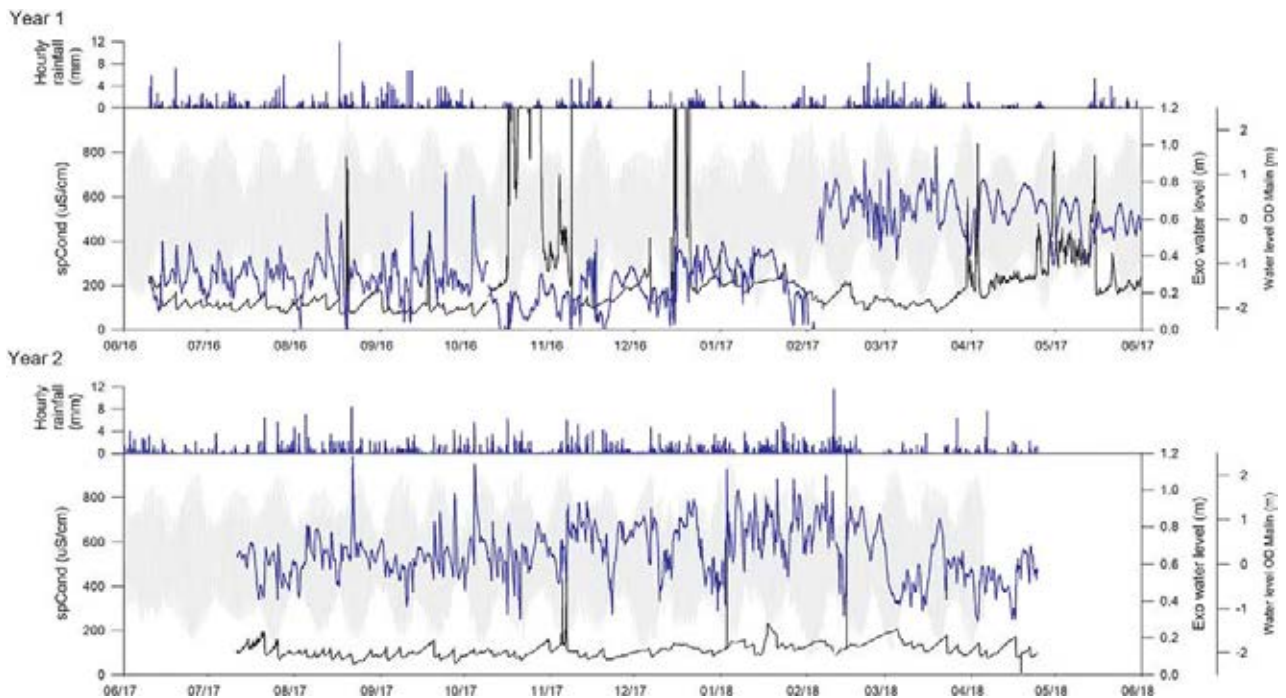


**Figure 6.11.** High-resolution (15 min) SC time series (black) plotted with EXO2 water level (blue) and tidal data from Ballyglass tidal gauge (grey). The hourly rainfall data above each plot (also in blue) are from the Dooagh water treatment plant, south-west Achill Island.

Flow data showed considerable variability but no consistent pattern or trends, although throughout the second year of monitoring water levels were higher.

Negative values recorded during October 2016 could be the result either of the sensor being out of the water (this was during a dry period) or of sensor malfunction,



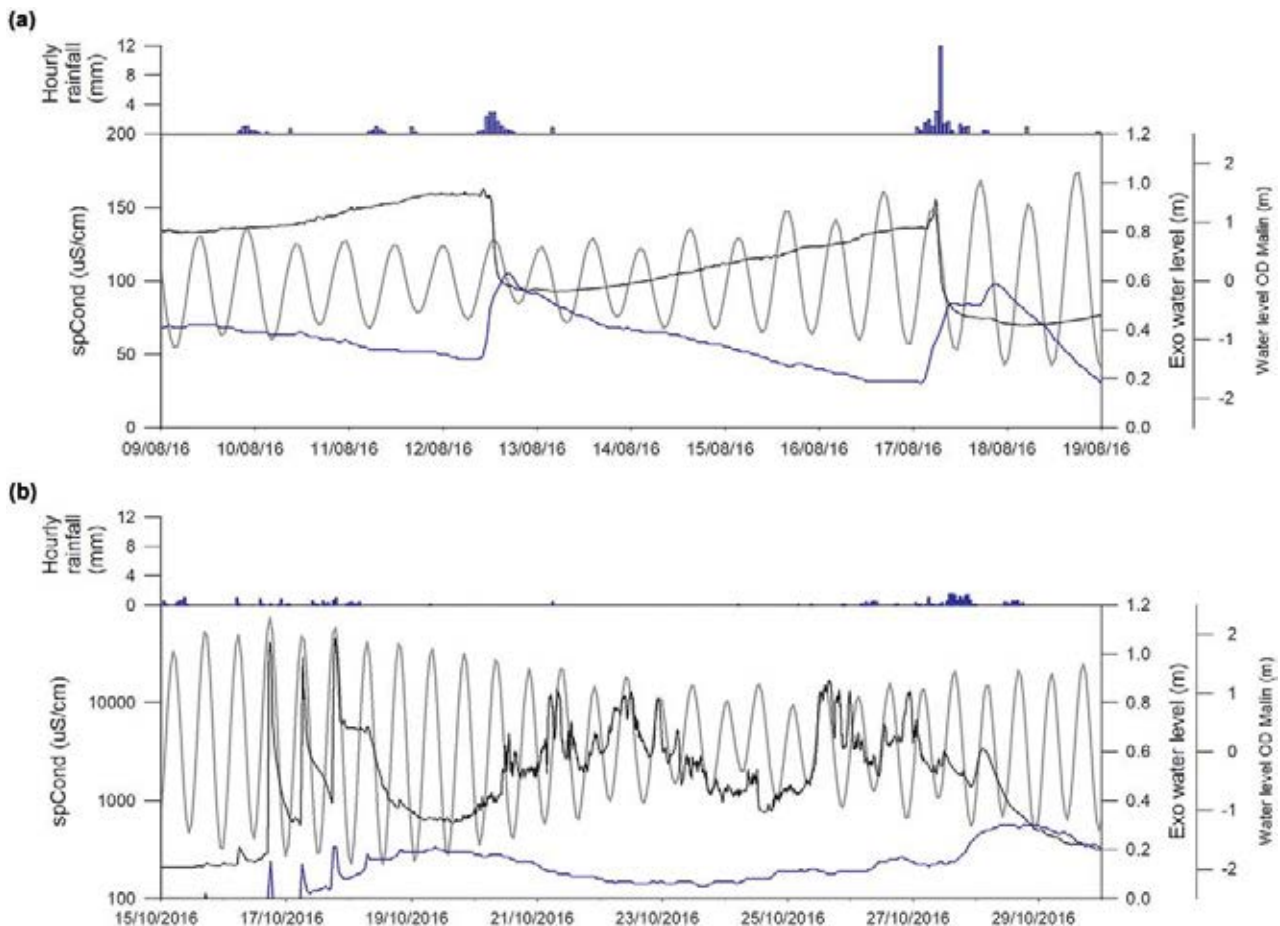


**Figure 6.12. High-resolution (15 min) SC (black) plotted with EXO2 water level (blue) and tidal data from Ballyglass tidal gauge (grey) for two specific periods. (a) The asymmetrical SC pattern that is inversely related to water level. (b) The timing of SC spikes and high tides. The hourly rainfall data shown above each plot (also in blue) are from the Dooagh water treatment plant, south-west Achill Island.**

as discussed. Short-duration peaks in flows, which typically corresponded to changes in the water quality parameters, are interpreted as catchment flood events, although in some cases the change in water level at the site was relatively minor ( $<0.3$  m). For some periods of the record, when there was relatively little or no rainfall, water levels still displayed clear fluctuations (e.g. between April 2017 and June 2017) that were not in phase with the spring tide cycle.

#### 6.5.2.2 Temperature

Long-term temperature variations at the monitoring site reflected characteristic seasonal and diurnal patterns (Figure 6.10). Summer values peaked at  $c.20^{\circ}\text{C}$ , when water levels dropped, and were consistently  $>15^{\circ}\text{C}$ ; this reflects the predominantly lentic conditions found at the site. Winter lows were  $c.3^{\circ}\text{C}$  in December 2016

and  $<2^{\circ}\text{C}$  in March 2018 during the winter cold snap ("Beast from the East"). Diurnal ranges did not exceed  $4^{\circ}\text{C}$ , with the lowest values typically recorded in the morning, following dissipation of the previous day's heat (Wetzel, 2001). Median values are similar to those found in other research (e.g. Regan *et al.*, 2011), which is consistent with the general mild temperatures found along the west coast of Ireland.

#### 6.5.2.3 Electrical conductivity (specific conductance)

EC, reported here as specific conductance (SC), typically ranged between 100 and  $200\ \mu\text{S}/\text{cm}$  (Figure 6.11) and corresponds to freshwater conditions. Many of these baseline readings also displayed a particular asymmetrical pattern of values gradually increasing before sharply declining. The



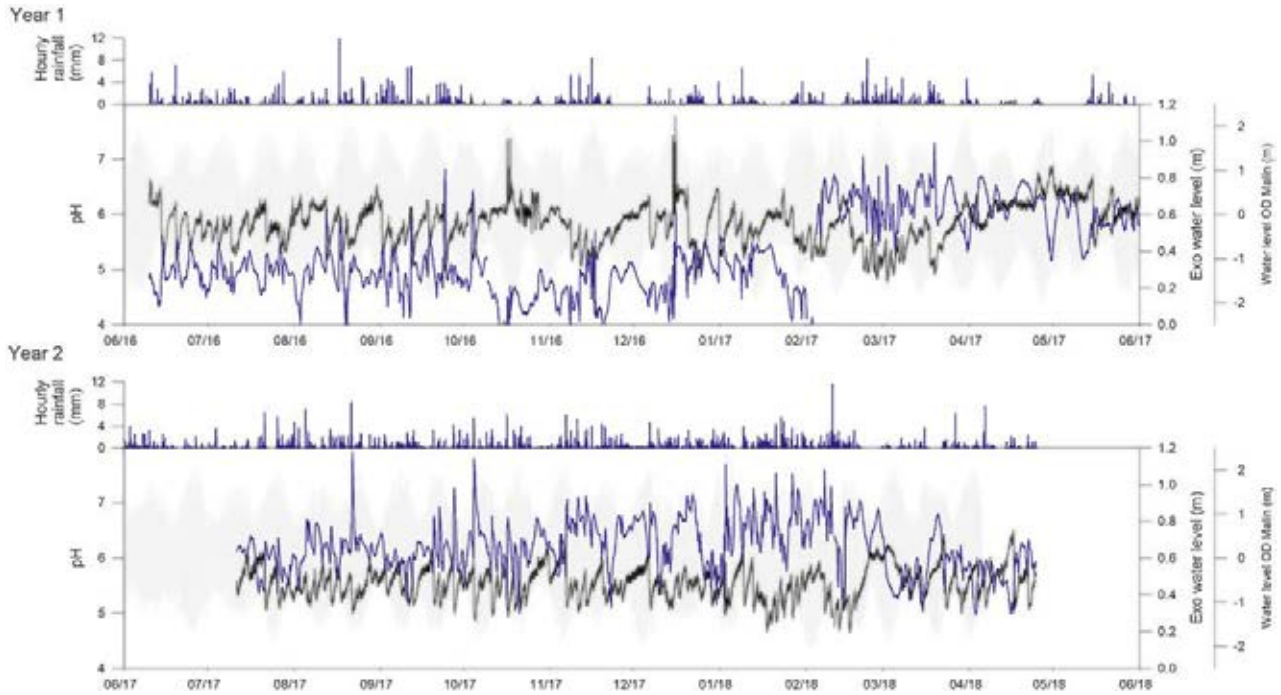


**Figure 6.13.** High-resolution (15min) pH time series (black) plotted with EXO2 water level (blue) and tidal data from Ballyglass tidal gauge (grey). The hourly rainfall data above each plot (also in blue) are from the Dooagh water treatment plant, south-west Achill Island.

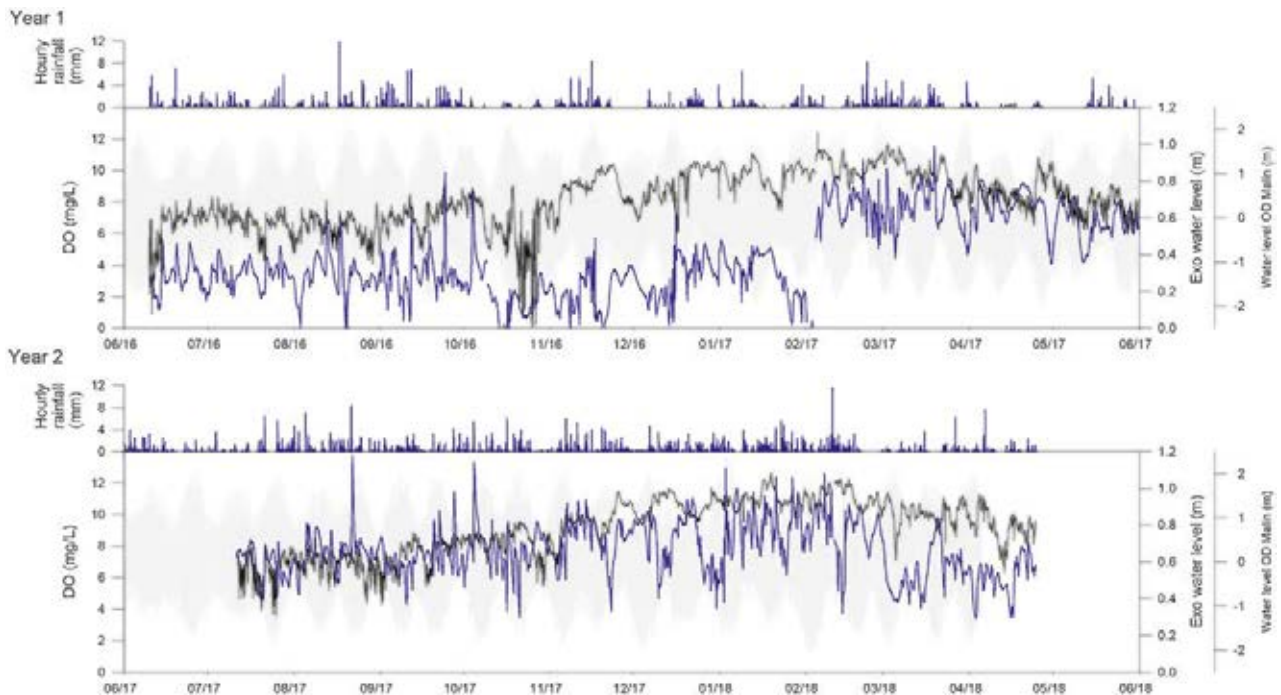


**Figure 6.14.** High-resolution (15min) DO time series (black) plotted with EXO2 water level (blue) and tidal data from Ballyglass tidal gauge (grey). The hourly rainfall data above each plot (also in blue) are from the Dooagh water treatment plant, south-west Achill Island.

periodicity of these patterns was variable, ranging from a few days to > 2 weeks, and is therefore not clearly correlated with daily or monthly tidal cycles. However,

for much of the record, this pattern is inversely related to water levels, for example for 2 weeks in August 2016 (Figure 6.12a). Here, the rapid fall in SC

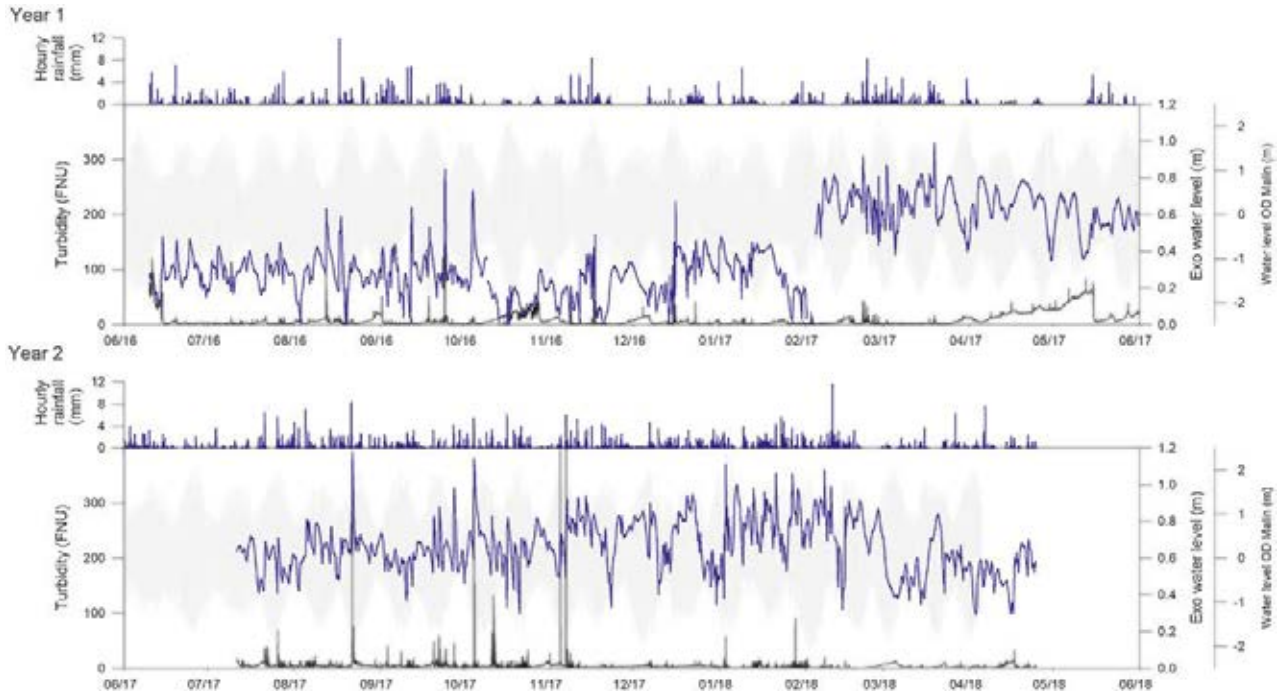


**Figure 6.15.** High-resolution (15min) turbidity time series (black) plotted with EXO2 water level (blue) and tidal data from Ballyglass tidal gauge (grey). The hourly rainfall data above each plot (also in blue) are from the Dooagh water treatment plant, south-west Achill Island.

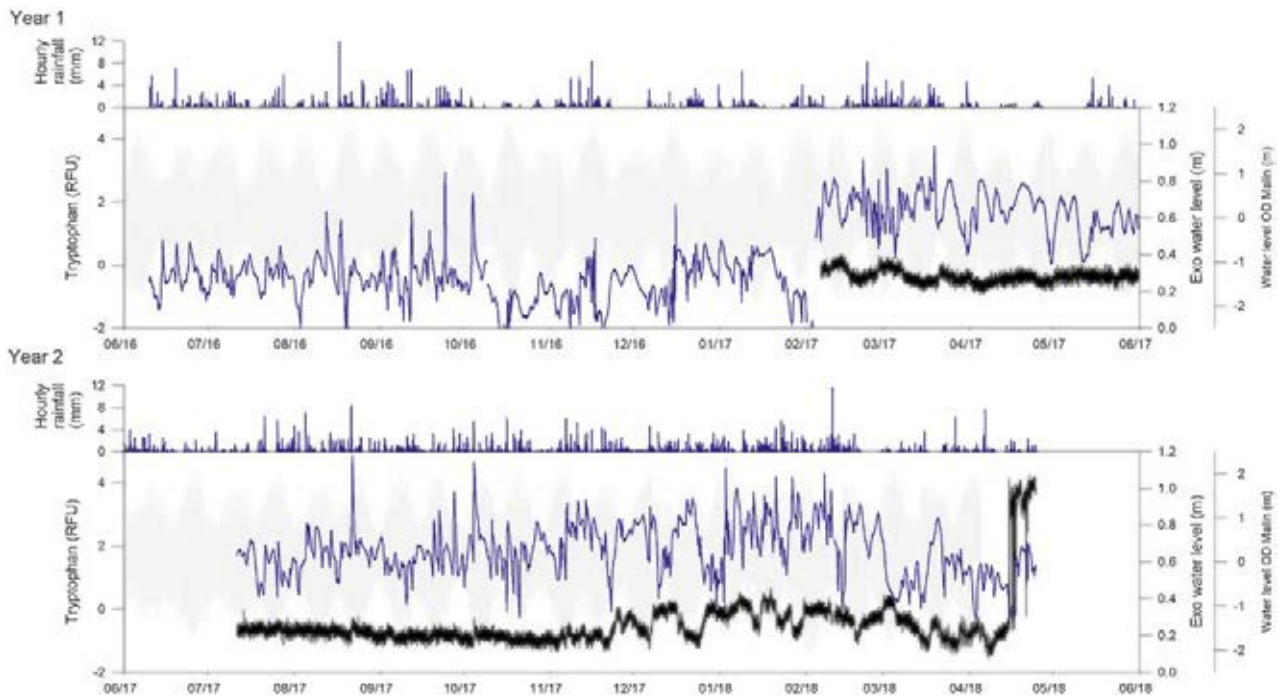


**Figure 6.16.** High-resolution (15min) tryptophan fluorescence time series (black) plotted with EXO2 water level (blue) and tidal data from Ballyglass tidal gauge (grey). The hourly rainfall data above each plot (also in blue) are from the Dooagh water treatment plant, south-west Achill Island.

coincided with an increase in water levels that appears to be related to rainfall events (this was not the case for the entire record). Alongside this baseline pattern

were 13 occasions when the SC rose sharply above the median value and two short-lived episodes when SC repeatedly peaked at  $c.45,000 \mu\text{S}/\text{cm}$ , indicating

temporary seawater conditions at the site. The first and most complex of these events, which occurred in the final 2 weeks of October 2016, is shown in Figure 6.12b. Although this episode coincided with a possible fault in the level sensor (which was recording anomalous low values), the three significant peaks on 16 October 2016 are all detected by short (<1 hour) peaks in the level sensor. Furthermore, these peaks occur immediately before or after (within 15 minutes) the spring high tides, supporting the hypothesis that this was a seawater incursion. What is also evident, however, is that the waning limb of these conductivity peaks did not follow the tidal cycle, and the lower amplitude, more protracted peaks that continued to the end of the month were also only intermittently in phase with the tidal cycle.

#### 6.5.2.4 pH

The pH at the site typically ranged from 5.5 to 6, which is consistent with acidic values found in other peatland catchments (O'Driscoll *et al.*, 2013) (Figure 6.13). Values peaked above pH 7 for short periods (30–75 minutes) on only five occasions during the monitoring period, coinciding with the highest EC readings (section 6.5.2.3). In contrast, more acidic waters below pH 5 were recorded almost 1000 times, with the lowest pH value, of 4.64, recorded on 16 February 2018 at 23:00. The patterns observed by pH show a gradual build-up and sharp decline, mirroring (for the most part) those displayed by the baseline conductivity readings. In a similar manner to conductivity, this pattern was erratic in places, in terms of the response to fluctuating water levels, but more often than not pH dropped when water levels showed a marked increase. This would be expected with an influx of the acidic water draining the peatland catchment.

#### 6.5.2.5 Dissolved oxygen

DO as a concentration (mg/L) is shown in Figure 6.14. Although there was some evidence of gradual build and sharp decline shown by conductivity and pH (e.g. between 3 December and 10 December 2016), the short-term DO patterns are inconsistent, possibly reflecting multiple influences within the stream. Clear seasonality was observed, with DO values increasing during the winter months, probably because of increased solubility in colder water. The median value was 8.63 mg/L and the maximum value was

12.67 mg/L, recorded on 19 January 2018 at 12:45. In the first year of monitoring there was a 5-day episode characterised by intermittent hypoxic conditions (DO <2 mg/L) between 21 October 2016 at 04:30 and 26 October 2016 at 23:30, with the minimum DO value of 0.08 mg/L recorded on 25 October 2016 at 16:15.

#### 6.5.2.6 Turbidity

Turbidity data are shown in Figure 6.15. The scale has been adjusted to 400 FNU; the single recording above this value, which occurred on 6 November 2018 at 21:15, peaked at 617.14 FNU and corresponds to a flood event. The median turbidity reading was 3.13 FNU, and 90% of values lie between 1.4 and 14.8 FNU.

Qualitative analysis of the turbidity data revealed two distinctive patterns. The first was characterised by a gradual build-up of FNUs, followed by a rapid fall. In this pattern the peaks were of variable duration and amplitude, with the longest lasting 41 days in 2017: the FNU rose from 4.35 on 4 April 2017, peaked at 76.8 on 15 May 2017 at 09:00 and dropped to 6.8 on 15 May 2017 at 21:15 (over c.12 hours). In turbidity monitoring, this pattern is typically associated with sensor fouling following wiper malfunction, resulting from a build-up of material on the optical lens (Bruen, 2017). The marked drop in turbidity occurs when the lens is wiped. Although wiper failure cannot be completely ruled out at this site, the EXO2 sonde employs an integrated wiper, which showed no evidence of malfunction during each calibration test. The fact that this pattern was also displayed by some of the other sensors, including EC, which does not operate on optical principles, strongly suggests that the data reflect genuine trends in turbidity.

The second pattern was more characteristic of turbidity data collected in Ireland and elsewhere and was characterised by short duration peaks ranging from 45 minutes to >12 hours. These peaks occurred when water levels rose, marking a high-flow event in the catchment and resulting in the flushing of sediment. The majority of these flushing events displayed positive hysteresis, with peaks occurring on the rising limb of the hydrograph, but there were also events (e.g. on 8 November 2016) when turbidity peaked after water level. In terms of frequency and magnitude, the majority of these flushing events occurred from late August 2017 to February 2018 (particularly

from October and November) in the second year of monitoring and corresponded to rainfall events on Achill. It is worth noting that not all flood hydrographs were associated with elevated turbidity.

Given the aforementioned uncertainties with the NTU versus SSC calibration, the full time series for SSC have not been plotted for the monitoring period. However, based on the four laboratory models reported in section 6.4.3.3, the peak turbidity of 674 FNU (recorded on 6 November 2017 at 21:15) would equate to 3900 mg/L, 1400 mg/L, 900 mg/L and 800 mg/L. Based on former studies in Ireland (reviewed in Lawler *et al.*, 2017), a sediment concentration of 3.9 g/L would be exceptionally high and is almost certainly an overestimate. A sediment concentration of 1.4 g/L is more realistic, but would itself potentially translate to a significant flux from the catchment (dependent on discharge at that time).

#### 6.5.2.7 Tryptophan fluorescence

The time series for tryptophan fluorescence showed very little variation in RFU between February 2017 (when the sensor was installed) and November 2017, with values fluctuating marginally below zero for this period (Figure 6.16). From December 2017 to April 2018 the patterns changed slightly, with the amplitude of changes increasing to  $\pm 0.5$  RFU. On 15 April 2018 at 05:15, values stepped up to between c.3 and 4, with RFU values oscillating at the start of this change to c.0 RFU.

Following consultation with instrument manufacturers these data are interpreted as noise, with variations reflecting variations in sunlight levels (effectively background). The step-up in RFU found at the end of the monitoring period did not correspond to a change in any of the other parameters, and the data are deemed unreliable. This may be the result of the instrument becoming unstable, and this is currently being explored with YSI.

The lack of evidence for labile organic carbon shown by the tryptophan signal at the site is not unexpected given the absence of municipal and agricultural sewage and wastewater upstream of the monitoring location.

### 6.5.3 Correlations between water parameters

Preliminary statistical analysis of the water quality data using the Kolmogorov–Smirnov test and Q-Q

plots using SPSS IBM Statistics 24 showed that none of the datasets conformed to a normal distribution and that not all relationships were linear, making them unsuitable for principal components analysis. Exploration of the relationship between the parameters is presented in Appendix 1 (Tables A1.1 to A1.9) using two-tailed Spearman's rank correlation coefficients (rho coefficients) for the full dataset and for datasets corresponding to seasonal subsets (Table A1.9). This approach is more robust for handling non-parametric data with outliers (Hauke and Kossowski, 2011), which are clearly evident in the turbidity and conductivity distributions. Although a significant relationship does not imply process linkages, it is sufficient for assessing correlations between water parameters from which inferences and hypotheses can be developed. Correlations were carried out using SPSS IBM Statistics 24 with significant rho coefficients marked with one or two asterisks at the  $p < 0.05$  or  $0.01$  level, respectively. Significant positive and negative correlations above  $\pm 4$  have also been highlighted in blue and red, respectively.

Results for the full dataset are shown in Table A1.1. The most significant relationship is shown between temperature and DO ( $r = -0.825$ ,  $p < 0.01$ ). This inverse relationship is widely reported in the literature because of the increased solubility of oxygen ( $O_2$ ) in cold water. This pattern is more evident in lentic systems, where water bodies can build up heat, aeration is lower and biological activity can consume oxygen. Typically, these conditions are found during the spring and especially summer months, but correlations for the seasonal data do not show a consistent seasonal pattern.

The strong inverse relationship ( $r = -0.497$ ,  $p < 0.01$ ) between temperature and TLF confirmed the role of temperature, widely reported in the literature, but, again, this was not consistent through the different seasons and was strongest in the final 3 months of monitoring.

A more consistent inverse relationship was shown between DO and turbidity. For the full dataset  $r = -0.418$  ( $p < 0.01$ ) and rho values were similar for all seasons with the exception of the final 3 months of monitoring. This inverse relationship between DO and turbidity may reflect the oxidation of ferrous iron ( $Fe^{2+}$ ) exported in the solution from the peatland catchment.

Another consistent, but in this case positive, relationship was shown between pH and conductivity ( $r=0.671$ ,  $p<0.01$ ). This pattern can be seen in Figure 6.12, alongside the EXO2 water level at the monitoring site, which was negatively correlated with all three variables (albeit not as strongly). Water pH and turbidity also showed a positive relationship ( $r=0.575$ ,  $p<0.01$ ), although the strength of this relationship decreased during much of the second year of monitoring. EC is controlled by the ionic content of the water, so the positive correlations suggested that the EC was controlled by ions contributing to higher pH (e.g. bases or salts) rather than  $H^+$  ions associated with lower pH.

Neither water level nor tidal cycle showed consistently strong correlations with the dependent variables. Overall, the water level was inversely and significantly correlated with temperature ( $r=-0.235$ ,  $p<0.01$ ), conductivity ( $r=-0.233$ ,  $p<0.01$ ), turbidity ( $r=-0.078$ ,  $p<0.01$ ) and pH ( $r=-0.319$ ,  $p<0.01$ ) and positively with DO ( $r=0.426$ ,  $p<0.01$ ) and tryptophan fluorescence ( $r=0.082$ ,  $p<0.01$ ). The tidal data showed no correlation with the dependent variables, aside from temperature ( $r=0.068$ ,  $p<0.01$ ). The relationship between water level and tides was weakly negatively correlated throughout the monitoring period ( $r=-0.045$ ,  $p<0.01$ ). This was not anticipated and implies some reversal of the hydraulic head from upstream to downstream, resulting in the movement of water into the channel when tides were ebbing.

## 6.6 Discussion

The results from this single-site monitoring study were complex, and the difficulties in establishing a robust SSC versus turbidity relationship and reliable flow data undermined the objective of establishing sediment flux from the catchment. The high-resolution data, however, revealed interesting and unexpected patterns that provided insights into the hydrodynamics and process interactions in this low-gradient, peatland catchment. Fundamentally, there appear to be two distinctive patterns of catchment behaviour emerging from the water quality data.

The first was related to sustained base flow conditions when turbidity, pH and EC all gradually increased, until such a time when the site was perturbed by a high-flow event (although it is noted that water levels did fluctuate during these trends). This trend is

interpreted as showing a physico-chemical exchange between dissolved and particulate constituents in the water. This exchange resulted in the accumulation of particulate, chemically precipitated Fe-rich sediment in the water. Blanket peat is known for the production of Fe, especially pristine *Sphagnum*-rich bogs (Krachler *et al.*, 2016), when Fe is mobilised in soluble complexes, often in association with DOM. This river-borne Fe will precipitate at the mouth of these systems in low-salinity estuarine settings (e.g. Sholkovitz *et al.*, 1978), and this appears to be occurring at the monitoring site in this study. The, albeit modest, increase in pH that corresponded to an increase in turbidity and EC (illustrated in Figure 6.15) suggests interaction and mixing with either groundwater from the calcareous machair zone and/or marine waters moving inland through the dune system. The gradual build-up of Fe-rich sediment leads to relatively high FNUs, but low SSC concentrations, because these sediments are extremely fine. Similar colloidal material in the form of Fe(III) oxyhydroxides draining from peatlands have been reported in marine settings (e.g. Hirst *et al.*, 2017; Jilbert *et al.*, 2018). Flocculation of Fe-rich colloids has also been observed in these settings and is evidenced in this study by the layers of Fe-rich sediment deposited on the stream bed. These Fe flocs produced lower FNUs than the ultra fine sediment in the ISCO bottles, which is almost certainly related to particle size (Rymaszewicz *et al.*, 2017). When these flocs reach settling velocity they will fall out of the water column (Dietrich, 1982), and this clearly occurs in this system. However, at the monitoring site, the fall in FNUs corresponded to a drop in pH and EC from the input of bog water during a high-flow event. This input of bog water resulted in either the dilution or flushing of the colloidal Fe or, alternatively, the redissolution of the Fe as a result of the fall in pH. Where this pattern is dominant in the monitoring record, discussion of particulate flux is not meaningful because this sediment was originally moving as part of the solute load.

The second pattern identified in this study was related to flood events and was observed far more frequently during the second year of monitoring, which was characterised by more sustained periods of rainfall. During this phase, which was most evident during the late autumn and early winter of 2017/2018, the data showed no evidence of the gradual build-up of turbidity associated with Fe precipitation, but rather



short-duration pulses of sediment were observed. Based on the limited ISCO bottle samples that were collected, this sediment was dominated by particulate organic matter, but also contained variable quantities of remobilised Fe-rich sediment, leading to highly variable SSC versus FNU relationships. The flushing events, in some cases, produced much higher FNUs and could potentially reflect significant carbon flux events although quantification is uncertain and estimated concentrations of >1000 mg/L appear to be overly high given the absence of fines trapped on vegetation downstream.

Increasing evidence of climate change in Ireland emphasises the urgent need to build datasets that will support future management and decision-making (e.g. Charlton and Moore, 2003; Hall and Murphy, 2011). Although models have been developed, the outcomes of climate change are highly uncertain, and predicted effects from the analysis of current trends can be subject to both under- and overestimation (Charlton and Moore, 2003; Murphy and Charlton, 2008; Hall and Murphy, 2011), and show high spatial temporal and spatial variability, even within a small country such as Ireland (Sweeney *et al.*, 2003). In the context of current climate non-stationarity, Hall and Murphy (2011) argue that data gathered over the last few years, as opposed to historical data over 30 years, should be used in forecasts and modelling predictions to improve accuracy. Despite some of the challenges posed in this study, in situ water quality monitoring devices offer huge potential to capture complex patterns ranging from short-term activities

(storm events, diurnal fluctuations) to long-term activities (seasonal observations) (Blaen *et al.*, 2016; Dick *et al.*, 2016). Long-term deployment of these devices, working in collaboration with other monitoring techniques, can help establish data to inform current management practices and for modelling purposes (Garner *et al.*, 2017).

## 6.7 Concluding Remarks

This study reveals complex time- and flow-dependent patterns in water quality and sediment flux, which appear to be controlled by the delivery of Fe-bearing water from the peatland catchment and its interaction with water derived locally from the coastal zone.

The limited measurements of water quality parameters at a single site, however, contributed to uncertainty in the interpretation and analysis of the measured datasets. Furthermore, monitoring in this study was insufficiently long to capture seasonality, which may be the result of the contrasting conditions (dry and wet) during the 2 years of monitoring.

Reconstructing flows based on water level and hydraulic models (as was done in the SILTFLUX project) is appropriate under certain conditions. However, the monitoring site in this study was not suitable for reconstruction of the flow field. Unexpected time-averaged inverse relationships between water level and tides also suggested secondary and/or time-dependent hydraulic influences that are not fully understood.

## 7 WP7 – Recommendations

Golden Strand is an accretional beach containing a wide backshore and a prominent berm. Observations in this study have shown that the impact of high-energy storms appears to be minimal and temporary. The results from WP2 illustrate how the beach berm is replenished during low-energy conditions as sand that was lost during storms moves landward. In Ireland, coastal response to storms is site specific (complete recovery; no recovery; partial recovery; excess recovery), but understanding these changes at local and regional scales is limited by the quantity and quality of monitoring data. Currently, there is a paucity of long-term, large-scale, coastal change observational data in Ireland for coastal forcing and coastal response. The Irish coastline is highly compartmentalised and varies significantly in terms of static (geology, orientation, sediment size and abundance) and dynamic (wave, tide) conditions (Scott *et al.*, 2011; Masselink *et al.*, 2015, 2016a; Devoy *et al.*, 2021), resulting in very diverse coastal environments (beaches, dunes, cliffs, barriers, lagoons, estuaries, embayments, mudflats, saltmarshes) that respond differently to storms. Cycles of erosion/recovery on sandy beach–dune systems can be sub- to multi-annual (Golden Strand) or even multi-decadal or longer (Dooagh beach on the south side of Achill Island). The research community is cognisant that one validated model of coastal change may be valid for only a relatively small stretch of coastline or a small number of beaches.

We recommend that stronger links and research structures be developed between academic institutions, government departments, local authorities and research agencies (EPA, Marine Institute, An Teagasc, Geological Survey Ireland, Office of Public Works and NPWS) to develop and sustain long-term, field-based monitoring projects of coastal systems.

The sediment flux of Golden Strand has geological controls that have forced it to behave as a closed system, with sediment sources most likely from

glacigenic sediment lying offshore, and from the eroding cliffs. Over the last centuries, a sediment budget deficit has forced many coastal systems in Ireland, and elsewhere in north-west Europe, to self-cannibalise as they retreat landward by rollover and seek new equilibrium states (Devoy, 2015b; Stéphan *et al.*, 2015). One of the biggest threats to the continued existence of beaches and dunes in Ireland, and elsewhere, is coastal defence structures that limit their ability to migrate landward (Pilkey and Cooper, 2014). Historically, coastal planning and management practices in Ireland, and north-west Europe, have relied first and foremost on engineering solutions to reduce climate risks. These hard structure, “one-off” coastal management interventions (at least on the timescales of engineering design life expectancy), have real value in site-specific locations, but can equally have unintended consequences in adjacent coastal locations. The geomorphological (beach lowering; blocking of natural littoral drift) and ecological (habitat loss; decreasing biodiversity; coastal squeeze and loss of accommodation space) impacts of engineering structures are well known. At Golden Strand the beach–dune system is free to migrate landward owing to the availability of backbeach accommodation space. The one exception is the caravan park located in the dunes immediately west of the main stream at the site. The park is protected by a large cement wall, but will be susceptible to storm surge inundation, pluvial floods and erosion over the coming decade(s).

We recommend that coastal risk reduction strategies and levels of protection are incorporated in the local authority Local Area Plan via an Integrated Coastal Zone Management process that embraces local specificity.

To mitigate the short- and long-term risks of coastal hazards and their drivers, monitoring programmes and early warning systems are needed. Large-scale (regional) coastal modelling is being used successfully

to mitigate coastal risks in south-west England, where multiple government and academic institutions collect and analyse monitoring data, such as repeat light detection and ranging (LiDAR) (Environment Agency) and real-time kinematic (RTK) GPS (Plymouth Coastal Observatory, Plymouth University) surveys, offshore (Sevenstones Lightship) and inshore wave buoys (Plymouth Coastal Observatory), and water levels (British Oceanographic Data Centre). Ireland would benefit tremendously from an equivalent multidisciplinary coastal observation system to reduce climate risks; strengthen links between academic institutions, government departments and research agencies; and showcase the application of science and technology for societal needs. The existing nearshore buoy networks around Ireland, such as the SmartBay test facility (SmartBay, 2020) or the Irish Marine Buoy Data Observation Network (Marine Institute, 2020), need to be expanded substantially and integrated into large East Atlantic-scale infrastructure such as JERICO-RI (Joint European Research Infrastructure of Coastal Observatories – Research Infrastructure). The “real” map of Ireland includes our marine territory of over 220 million acres (880,000 km<sup>2</sup>), which is 10 times the size of the island of Ireland. Thus, it is a real challenge to simultaneously address requirements for in-depth environmental information and coverage of this large ocean extent. However, post Brexit, Ireland should aim to become the main hub for north-east Atlantic coastal and marine monitoring and research, with the potential to be at the heart of a blue growth agenda. An ambitious coastal–ocean observation infrastructure provides the necessary data to validate state-of-the-art high-resolution coastal change models to test impact scenarios (best case; worst case; no change) related to storminess and/or rising sea levels (EPA, 2017). This modelling approach also helps researchers and decision-makers move beyond the current state of knowledge (“how much change occurs?”) to develop better insights (“why does change occur?”, “how much change will occur if we account for climate projections of rising sea levels and increased storminess?”) and foster new insights into storm impacts in Ireland.

The results from WP2 and WP6 highlight the variability of controls or sediment dynamics existing within catchment subsystems and the different spatial and temporal scales of behaviour. For example, the sediment flux of the stream observed in WP6 is controlled by upper peatland catchment dynamics.

We recommend that the Irish government leverage the EU for peripheral regional stimulus funding based on our unique geographical and, post Brexit, political location. These funds will support our research agencies and academic institutions to develop and sustain a comprehensive coastal observing and modelling infrastructure to build early-warning systems, validate coastal change models and monitor essential ocean variables for physical, biogeochemical, and biological processes, which contributes to the remit of JERICO (Farcy *et al.*, 2019).

The resilience of our catchment systems is dependent on land management techniques for managing flood waters, through managing soil, wetlands, woodlands and floodplains to retain water strategically at times of flood risk (Murray, 2017). Catchment exports can influence the coastal zone but traditional discrete sampling methods such as those adopted under the WFD are not specifically designed to identify complex, short-lived catchment dynamics. The results from WP6 illustrate why any period of monitoring should be longer (at least 10 years) to more effectively capture inherent environmental variability. Replicated studies in similar hydrodynamic settings, where water levels and flows are controlled by complex hydrological and hydraulic interactions, must be provided with resources to directly monitor flow (discharge) and, furthermore, include an additional control location outside these effects (e.g. upstream). Resources should also be made available to monitor a broader range of parameters (e.g. surface, subsurface, hyporheic zone interactions) to understand the complex process–response systems emerging from these exploratory investigations. Notwithstanding the greater cost implications, the research design should also include a reference dataset from an upstream location for all water parameters measured. Where suspended solids are compositionally complex and temporally variable (as was the case with the eroded detritus and chemically precipitated Fe-rich sediment in this study), discrete water sampling must be carried out through controlled, systematic firing of autosampler bottles (e.g. through text messaging) to capture the full range of sediment types and range of turbidities for calibration models. Resources should be provided for

these integrated systems. Although SSCs reported in this study carry high uncertainty, potentially short-lived, elevated fluxes of carbon-rich sediment from peatland catchments warrant further investigation and this should be carried out alongside quantification of DOM loads.

We recommend that multidecadal-scale catchment monitoring programmes be adequately resourced to dismantle the complex hydrological and hydraulic interactions between catchment subsystems (surface water, groundwater, aerated zone) and quantify the impact of extreme climate events.

The results from WP3 indicate that an analysis of vegetation effects on dune stability and salinity would be beneficial in order to model dune evolution. It is still unknown how the vegetation cover (type and distribution) of dunes in Ireland will respond to changing climate patterns and increased storm surge inundation. Longitudinal dune surveys, such as the CMP (NPWS, 2013b) and sand dunes monitoring project (SDM) (Delaney *et al.*, 2013), are invaluable to provide snapshots in time (every 6 years) of the state of dune habitat health in Ireland. However, these surveys do not provide insight into (1) the processes (natural and/or human impacts) that are causing short- and long-term changes or (2) the spatial and temporal characteristics of the changes via system thresholds and feedbacks manifested through patterns of response and recovery over large (small) and long (short) spatial and temporal scales (Farrell and Bourke, 2018). These critical questions are best resolved via long-term monitoring programmes (years to decades) that deploy state-of-the-art sensors to collect high-frequency environmental data. It is also recommended that a longer monitoring period be designed (a 3-week snapshot is reported herein on account of equipment logistics). Furthermore, the results from WP4 highlight the need for future work in groundwater and surface flows in or adjacent to coastal dunes and machair to take a four-dimensional approach and consider the physical make-up of the study site in terms of location and depth (seating it in a geological context). Recovery of groundwater samples for isotope analysis would also be very useful to assess short- and long-term recharge and storage processes.

We recommend that long-term (subdecadal) field experiments be designed to monitor the changing ecohydrological and hydrogeological drivers of dune and pond ecosystems, and that this is used this information to assess their structure, conservation status and vulnerability to climate change.

The development of coastal dune management strategies also needs to be considered in the context of increased usage of coastal zones for social and economic purposes (Cooper and McKenna, 2008; Farrell, 2018; Farrell *et al.*, 2020). Human-induced pressures include grazing (including overgrazing and undergrazing; see WP5), recreation (sports and leisure structures and activities), urbanisation, sand and gravel mining, pollution, invasive species, erosion and trampling. For example, Delaney *et al.* (2013, p. 105) highlight how the drainage of wetlands or the erection of sea walls disturbs the natural processes that underpin dune ecosystems and argue that “interrupting the natural transitions between sand dunes and other habitats also reduces the ecological value of sand dunes as fauna from the wider landscape is no longer able to access the dunes”. WP5 illustrates the impact of humans on a machair system. At Doogort, the machair system was unimpeded by hard engineering structures, which helped maintain the cover of machair vegetation and permitted the adequate supply of sand necessary for the maintenance of this system. Many coastal dune systems, including machair, are characterised by disturbance and change, and we find that human activities exert an overriding influence on the resilience of these coastal systems by changing their capacity to respond to natural and/or anthropogenic stressors. The results from WP5 suggest that the machair system at the study site is already showing evidence that it is transitioning to a new state more representative of a fixed dune or wet machair system. These types of land cover response need to be closely monitored and managed, especially as we have legal obligations to protect them under the EU Habitats Directive.

We recommend reducing and/or changing the existing grazing regime (e.g. transition from sheep to cattle) and reducing soil compacting practices to enhance machair stability and longevity.

The increase in frequency of extreme weather events and sea level rise is now locked in for Ireland on account of human-induced climate changes over the past century. The results from this project highlight the need for substantial investment to support longitudinal, multidisciplinary (geomorphology, ecology, hydrology, climatology, oceanography) monitoring programmes to build an inventory of case studies. Concurrently, it is critical that policymakers understand how the ecosystem services provided by coastal ecosystems benefit society and prioritise policy mechanisms to conserve and protect them. The recommendations from the project will be made available to the EPA-funded Ireland's Climate Information Platform

([www.climateireland.ie](http://www.climateireland.ie)) as part of the case study directory to guide decision-makers for climate adaptation.

We recommend that the degradation and loss of our ecosystems is framed within the new climate policy (Climate Action Plan 2019, National Adaptation Framework) as a loss of an integral element of local and regional natural heritage that is of considerable scientific, conservation and recreational value.



# References

- Adger, W.N., Hughes, T.P., Folke, C., Carpenter, S.R. and Rockström, J., 2005. Social-ecological resilience to coastal disasters. *Science* 309(5737): 1036–1039.
- ASTM International, 2017. *Standard Test Method for Determination of Turbidity Above 1 Turbidity Unit (TU) in Static Mode*. ASTM Designation D7315 – 17. ASTM International, West Conshohocken, PA.
- Backstrom, J., Jackson, D., Cooper, J.A.G. and Loureiro, C., 2015. Contrasting geomorphological storm response from two adjacent shorefaces. *Earth Surface Processes and Landforms* 40: 2112–2120.
- Baker, A. and Inverarity, R., 2004. Protein-like fluorescence intensity as a possible tool for determining river water quality. *Hydrological Processes* 18: 2927–2945.
- Baker, A., Cumberland, A.A., Bradley, C., Buckley, C. and Bridgeman, J., 2015. To what extent can portable fluorescence spectroscopy be used in the real-time assessment of microbial water quality? *Science of the Total Environment* 532: 14–19.
- Bakker, T.W.M., 1990. The geohydrology of coastal dunes. In Bakker, T.W., Jungerius, P.D. and Klijn, J.A. (eds), *Dunes of the European Coasts*. Catena, Stuttgart, Germany, pp. 109–119.
- Bassett, J. and Curtis, T.G.F., 1985. The nature and occurrence of sand dune machair in Ireland. *Proceedings of the Royal Irish Academy* 85B: 1–20.
- Beyers, J.H.M., Jackson, D.W.T., Lynch, K., Cooper, J.A.G., Baas, A.C.W., Delgado-Fernandez, I. and Pierre-Olivier, D., 2010. Field testing and CFD LES simulation of offshore wind flows over coastal dune terrain in Northern Ireland. Fifth International Symposium on Computational Wind Engineering (CWE2010), Chapel Hill, NC, 23–27 May.
- Bitá, C. and Gerats, T., 2013. Plant tolerance to high temperature in a changing environment: scientific fundamentals and production of heat stress-tolerant crops. *Frontiers in Plant Science* 4: 273.
- Blaen, P.J., Khamis, K., Lloyd, C.E.M., Bradley, C., Hannah, D. and Krause, S., 2016. Real-time monitoring of nutrients and dissolved organic matter in rivers: capturing event dynamics, technological opportunities and future directions. *Science of the Total Environment* 569: 647–660.
- Bochet, E. and García-Fayos, P., 2015. Identifying plant traits: a key aspect for species selection in restoration of eroded roadsides in semiarid environments. *Ecological Engineering* 83: 444–451.
- Brassington, R., 2017. *Field Hydrogeology*. John Wiley & Sons, Hoboken, NJ.
- Brenner, O., Lentz, E., Hapke, C., Henderson, R., Wilson, K. and Nelson, T., 2018. Characterizing storm response and recovery using the beach change envelope: Fire Island, New York. *Geomorphology* 300: 189–202.
- British Standards Institution, 1999. *BS 5930:1999 Code of Practice for Site Investigation*. British Standards Institution, London.
- Burningham, H. and Cooper, J., 2004. Morphology and historical evolution of north-east Atlantic coastal deposits: the west Donegal estuaries, north-west Ireland. *Journal of Coastal Research* 41: 148–159.
- Burvingt, O., Masselink, G., Russell, P. and Scott, T., 2017. Classification of beach response to extreme storms. *Geomorphology* 295: 722–737.
- Caissie, D., 2006. The thermal regime of rivers: a review. *Freshwater Biology* 53: 1389–1406.
- Campbell, C.G., Laycak, D.T., Hoppes, W., Tran, N.T. and Shi, F.G., 2005. High concentration suspended sediment measurements using a continuous fibre optic in-stream transmissometer. *Journal of Hydrology* 311: 244–253.
- Carmona, C., Azcarate, F., de Bello, F., Ollero, H., Leps, J. and Peco, B., 2012. Taxonomical and functional diversity turnover in Mediterranean grasslands: interactions between grazing, habitat type and rainfall. *Applied Vegetation Science* 495: 1084–1093.
- Carter, R., 1975. Recent changes in coastal geomorphology of Magilligan Foreland, Co. Londonderry. *Proceedings of the Royal Irish Academy B: Biological Geological and Chemical Science* 75: 469–497.
- Carter, R., 1980a. Longshore variations in nearshore wave processes at Magilligan Point, Northern Ireland. *Earth Surface Processes and Landforms* 5: 81–89.
- Carter, R., 1980b. Vegetation stabilisation and slope failure of eroding sand dunes. *Biological Conservation* 18: 117–122.

- Carter, R., 1982. Recent variations in sea-level on the north and east coasts of Ireland and associated shoreline response. *Proceedings of the Royal Irish Academy B: Biological Geological and Chemical Science* 82: 177–187.
- Carter, R.W.G., 1990. The geomorphology of coastal dunes in Ireland. In Bakker, T.W., Jungerius, P.D. and Klijn, J.A. (eds), *Dunes of the European Coasts*. Catena, Stuttgart, Germany, pp. 31–40.
- Carter, R.W.G., 2013. *Coastal Environments: An Introduction to the Physical, Ecological, and Cultural Systems of Coastlines*. Elsevier, Cambridge, MA.
- Carter, R. and Wilson, P., 1991. *Chronology and Geomorphology of the Irish Dunes*. European Union for Dune Conservation and Coastal Management, Dublin.
- Carter, R.W.G., Johnston, T.W., McKenna, J. and Orford, J.D., 1987. Sea-level, sediment supply and coastal changes: examples from the coast of Ireland. *Progress in Oceanography* 18: 79–101.
- Carter, R.W.G., Forbes, D.L., Jennings, S.C., Orford, J.D., Shaw, J. and Taylor, R.B., 1989. Barrier and lagoon coast evolution under differing relative sea-level regimes: examples from Ireland and Nova Scotia. *Marine Geology* 88: 221–242.
- Carter, R.W.G., Nordstrom, K.F. and Psuty, N.P., 1990. The study of coastal dunes. In Nordstrom K.F., Psuty N. and Carter B. (eds), *Coastal Dunes: Form and Process*. Wiley, Hoboken, NJ, pp.1–14.
- Castelle, B., Marieu, V., Bujan, S., Splinter, K.D., Robinet, A., Sénéchal, N. and Ferreira, S., 2015. Impact of the winter 2013–2014 series of severe Western Europe storms on a double-barred sandy coast: beach and dune erosion and megacusp embayments. *Geomorphology* 238: 135–148.
- Charlton, R. and Moore, S., 2003. *The Impact of Climate Change on Water Resources in Ireland. Climate Change: Scenarios and Impacts for Ireland*. ERTDI Report Series No.15. Environmental Protection Agency, Johnstown Castle, Ireland.
- Church, M. and Ryder, J.M., 1972. Paraglacial sedimentation: a consideration of fluvial processes conditioned by glaciation. *Bulletin of the Geological Society of America* 83: 3059–3071.
- Church, J.A., Clark, P.U., Cazenave, A., et al., 2013. Sea level change. In Stocker, T.F., Qin, D., Plattner, G.-K., Tignor, M., Allen, S.K., Boschung, J., Nauels, A., Xia, Y., Bex, V. and Midgley, P.M. (eds), *Climate Change 2013: The Physical Science Basis*. Contribution of Working Group I to the Fifth Assessment Report of the Intergovernmental Panel on Climate Change. Cambridge University Press, Cambridge, UK.
- Cingolani, A.M., Noy-Meir, I. and Díaz, S., 2005. Grazing effects on rangeland diversity: a synthesis of contemporary models. *Ecological Applications* 15: 757–773.
- Coco, G., Senechal, N., Rejas, A., Bryan, K.R., Capo, S., Parisot, J.P., Brown, J.A. and MacMahan, J.H.M., 2014. Beach response to a sequence of extreme storms. *Geomorphology* 204: 493–501.
- Coll, J., Bourke, D., Sheehy Skeffington, M., Gormally, M. and Sweeney, J., 2014. Projected loss of active blanket bogs in Ireland. *Climate Research* 59: 103–115. <https://doi.org/10.3354/cr01202>
- Collier, M.J. and Bourke, M., 2020. The case for mainstreaming nature-based solutions into integrated catchment management in Ireland. *Biology and Environment: Proceedings of the Royal Irish Academy* 120(2): 107–113.
- Cooper, J.A.G., 2006. Geomorphology of Irish estuaries: inherited and dynamic controls. *Journal of Coastal Research* 81: 176–180.
- Cooper, J.A.G. and McKenna, J., 2008. Working with natural processes: the challenge for coastal protection strategies. *Geographical Journal* 174: 315–331.
- Cooper, J.A.G. and Pile, J., 2014. The adaptation-resistance spectrum: a classification of contemporary adaptation approaches to climate-related coastal change. *Ocean & Coastal Management* 94: 90–98.
- Cooper, J.A.G., Jackson, D.W.T., Navas, F., McKenna, J. and Malvarez, G., 2004. Identifying storm impacts on an embayed, high-energy coastline: examples from western Ireland. *Marine Geology* 210: 261–280.
- Cooper, A., McCann, T. and Ballard, E., 2005. The effects of livestock grazing and recreation on Irish machair grassland vegetation. *Plant Ecology* 181(2): 255–267.
- Cooper, J.A.G., Jackson, D. and Kelley, J., 2009a. Late Holocene beach evolution: sediment starvation under a falling sea level. *Journal of Coastal Research* 1: 594–598.
- Cooper, J.A.G., Anfuso, G. and Del Rio, L., 2009b. Bad beach management: European perspectives: America's most vulnerable coastal communities. *Geological Society of America* 460: 167–179.
- Cooper, J., Green, A. and Loureiro, C., 2018. Geological constraints on mesoscale coastal barrier behaviour. *Global and Planetary Change* 168: 15–34.
- Cooper, J.A.G., Masselink, G., Coco, G., Short, A.D., Castelle, B., Rogers, K., Anthony, E., Green, A.N., Kelley, J.T., Pilkey, O.H. and Jackson, D.W.T., 2020. Sandy beaches can survive sea-level rise. *Nature Climate Change* 10: 993–995.

- Cowell, P.J. and Thom, B.G., 1994. *Morphodynamics of Coastal Evolution*. Cambridge University Press, Cambridge, UK.
- Crapoulet, A., Hequette, A., Levoy, F. and Bretel, P., 2015. Assessment of shoreline change and coastal sediment budget in the Bay of Wissant northern France using airborne LiDAR. *Géomorphologie: Relief, Processes, Environment* 21: 313–330.
- Crawford, I., Bleasedale, A., Conaghan, J., 1998. Biomar survey of Irish machair sites. *Irish Wildlife Manuals* 3: 127.
- Cronin, K., Devoy, R. and Gault, J., 2007. Modelling estuarine morphodynamics on the south coast of Ireland. *Journal of Coastal Research* 50: 474–479.
- Curtis, T., 1991a. The flora and vegetation of sand dunes in Ireland. In Quigley, M. (ed.), *A Guide to the Sand Dunes of Ireland*. European Union for Dune Conservation and Coastal Management, Dublin.
- Curtis, T., 1991b. A site inventory of the sandy coasts of Ireland. In Quigley, M. (ed.), *A Guide to the Sand Dunes of Ireland*. European Union for Dune Conservation and Coastal Management, Dublin.
- Davies-Colley, R.J. and Smith, D.G., 2007. Turbidity, suspended sediment, and water clarity: a review. *Journal of the American Water Resources Association* 37: 1085–1101.
- Dawson, J.J.C., Billett, M.F. and Hope, D., 2001. Diurnal variations in the carbon chemistry of two acidic peatland streams in north-east Scotland. *Freshwater Biology* 46: 1309–1322.
- DCCAE (Department of Communications, Climate Action and Environment), 2019. *Climate Action Plan 2019 to Tackle Climate Breakdown*. DCCAE, Dublin.
- de Santiago, I., Morichon, D., Abadie, S., Reniers, A., and Liria, P., 2017. A comparative study of models to predict storm impact on beaches. *Natural Hazards* 87: 843–865.
- De Winter, R.C. and Ruessink, B.G., 2017. Sensitivity analysis of climate change impacts on dune erosion: case study for the Dutch Holland coast. *Climatic Change* 141: 685–701.
- Deely, J. and Hynes, S., 2020. Blue-green or grey, how much is the public willing to pay? *Landscape and Urban Planning* 203: 103909.
- Defeo, O., McLachlan, A., Schoeman, D., Schlacher, T., Dugan, J., Jones, A., Lastra, M. and Scapini, F., 2009. Threats to sandy beach ecosystems: a review. *Estuarine Coastal and Shelf Science* 81: 1–12.
- Delaney, C. and Devoy, R., 1995. Evidence from sites in western Ireland of Late Holocene changes in coastal environments. *Marine Geology* 124: 273–287.
- Delaney, A., Devaney, F.M., Martin, J.M. and Barron, S.J., 2013. *Monitoring Survey of Annex I Sand Dune Habitats in Ireland*. Irish Wildlife Manuals No. 75. National Parks and Wildlife Service, Dublin.
- Delgado-Fernandez, I., Jackson, D.W.T., Cooper, J.A.G., Baas, A.C.W., Beyers, J.H.M. and Lynch, K., 2013. Field characterization of three-dimensional lee-side airflow patterns under offshore winds at a beach-dune system. *Journal of Geophysical Research: Earth Surface* 118: 706–721.
- Devoy, R.J.N., 2008. Coastal vulnerability and the implications of sea-level rise for Ireland. *Journal of Coastal Research* 24: 325–341.
- Devoy, R.J.N., 2015a. Sea-level rise: causes, impacts and scenarios for change. In Sherman, D. and Ellis, J. (eds), *Coastal and Marine Hazards, Risks and Disasters*. Elsevier, Amsterdam, pp. 197–242.
- Devoy, R.J.N., 2015b. The development and management of the Dingle Bay spit-barriers of southwest Ireland. In Cooper, J.A.G. and Jackson, D.W. (eds), *Coastal Spits*. Springer: Dordrecht, the Netherlands.
- Devoy, R., Delaney, C., Carter, R. and Jennings, S., 1996. Coastal stratigraphies as indicators of environmental changes upon European Atlantic coasts in the Late Holocene. *Journal of Coastal Research* 12: 564–588.
- Devoy, R., Nichol, S. and Sinnott, A., 2006. Holocene sea-level and sedimentary changes on the south coast of Ireland. *Journal of Coastal Research* 39: 146–150.
- Devoy, R.J.N., Wheeler, A.J., Brunt, B. and Hickey, K., 2021. The coastal environment: physical systems, processes and patterns. In Devoy, R.J.N., Cummins, V., Bartlett, D., Brunt, B. and Kandrot, S. (eds), *Shorelines: The Coastal Atlas of Ireland*. Cork University Press, Cork, Ireland, pp. 12–44.
- Diaz, S. and Cabido, M., 2001. Vive la différence: plant functional diversity matters to ecosystem processes. *Trends in Ecology and Evolution* 1611: 646–655.
- Dick, J.J., Soulsby, C., Birkel, C., Malcolm, I. and Tetzlaff, D., 2016. Continuous dissolved oxygen measurements and modelling metabolism in peatland streams. *PLOS ONE* 11: e0161363.
- Dietrich, W.E., 1982. Settling velocity of natural particles. *Water Resources Research* 18: 1615–1626.
- Dissanayake, P., Brown, J. and Karunarathna, H., 2014. Modelling storm-induced beach/dune evolution: Sefton coast, Liverpool Bay, UK. *Marine Geology* 357: 225–242.
- Dissanayake, P., Brown, J., Wisse, P. and Karunarathna, H., 2015a. Effects of storm clustering on beach/dune evolution. *Marine Geology* 370: 63–75.

- Dissanayake, P.M.P.K., Brown, J. and Karunaratna, H., 2015b. Impacts of storm chronology on the morphological changes of the Formby beach and dune system, UK. *Natural Hazards and Earth System Science* 15: 1533–1543.
- Dolan, R. and Davis, R., 1992. An intensity scale for Atlantic coast northeast storms. *Journal of Coastal Research* 8: 840–853.
- Domenico, P.A. and Schwartz, F.W., 1990. *Physical and Chemical Hydrogeology*. John Wiley & Sons, New York, p. 824.
- Donohue, I., McGarrigle, M.L. and Mills, P., 2006. Linking catchment characteristics and water chemistry with the ecological status of Irish rivers. *Water Research* 40: 91–98.
- Duffy, M. and Devoy, R., 1999. Contemporary process controls on the evolution of sedimentary coasts under low to high energy regimes: western Ireland. *Geologie en Mijnbouw* 77: 333–349.
- Dunne, S., Hannifin, J., Lynch, P., McGrath, R., Nishimura, E., Nolan, P., Ratnam, V., Semmler, T., Sweeney, C., Varghese, S. and Wang, S., 2008. *Ireland in a Warmer World*. Community Climate Change Consortium for Ireland C4I, Dublin.
- EPA (Environmental Protection Agency), 2001. *Parameters of Water Quality. Interpretation and Standards*. EPA, Johnstown Castle, Ireland. Available online: [https://www.epa.ie/pubs/advice/water/quality/Water\\_Quality.pdf](https://www.epa.ie/pubs/advice/water/quality/Water_Quality.pdf) (accessed 20 November 2016).
- EPA (Environmental Protection Agency), 2017. *A Summary of the State of Knowledge on Climate Change Impacts for Ireland*. EPA, Johnstown Castle, Ireland.
- Everard, M., Jones, L. and Watts, B., 2010. Have we neglected the societal importance of sand dunes? An ecosystem services perspective. *Aquatic Conservation: Marine and Freshwater Ecosystems* 20: 476–487.
- Farcy, P., Durand, D., Charria, G., Painting, S.J., Tamminen, T., Collingridge, K., Grémare, A.J., Delauney, L. and Puillat, I., 2019. Toward a European coastal observing network to provide better answers to science and to societal challenges; the JERICO research infrastructure. *Frontiers in Marine Science* 6: 529.
- Farrell, E.J., 2018. “We’re at a critical juncture for coastal management in Ireland”. RTE, 14 August 2018. Available online: <http://www.rte.ie/eile/brainstorm/2018/0810/984223-were-at-a-critical-juncture-for-coastal-management-in-ireland> (accessed 19 August 2020).
- Farrell, E. and Bourke, M., 2018. The future geomorphic landscape in Ireland. *Irish Geography* 51(2): 141–154. <https://doi.org/10.2014/igj.v51i2.1368>
- Farrell, E.J. and Connolly, N., 2019. Historic and contemporary dune inventories to assess dune vulnerability to climate change impacts. *Irish Geography* 52(1): 22–48.
- Farrell, E.J., Carr, L., Ó Fátharta, E., and Bourke, M., 2020. How healthy Kerry sand dunes are worth €9 million a year. Available online: <https://www.rte.ie/brainstorm/2020/0320/1124306-sand-dunes-maharees-kerry-economics-wild-atlantic-way/> (accessed 19 August 2020).
- Flannery, W., Lynch, K. and Cinnéide, M., 2015. Consideration of coastal risk in the Irish spatial planning process. *Land Use Policy* 3: 161–169.
- Flynn, D., Gogol-Prokurat, M., Nogueira, T., Molinari, N. and Richers, B.T., 2009. Loss of functional diversity under land use intensification across multiple taxa. *Ecological Letters* 12: 22–33.
- Fossit, J., 2000. *A Guide to Habitats in Ireland*. The Heritage Council, Dublin.
- Gardner, R. and McLaren, S., 1999. Infiltration and moisture movement in coastal sand dunes, Studland, Dorset, U.K.: preliminary results. *Journal of Coastal Research* 15: 936–949.
- Gardner, E.A., Burningham, H. and Thompson, J.R., 2019. Impacts of climate change and hydrological management on a coastal lake and wetland system. *Irish Geography* 52(1): 1–21.
- Garner, G., Hannah, D.M. and Watts, G., 2017. Climate change and water in the UK: recent scientific evidence for past and future change. *Progress in Physical Geography* 412: 154–170.
- Gault, J., O’Hagan, A.M., Cummins, V., Murphy, J., Vial, T., 2011. Erosion management in Inch beach, south west Ireland. *Ocean and Coastal Management* 54: 930–942.
- Gaynor, K., 2006. The vegetation of Irish machair. *Biology and Environment: Proceedings of the Royal Irish Academy* 106B(3): 311–321.
- Gitay, H. and Noble, I.R., 1997. What are functional types and how should we seek them? In Smith, T.M., Shugart, H.H. and Woodward, F.I. (eds), *Plant Functional Types: Their Relevance to Ecosystem Properties and Global Change*. Cambridge University Press, Cambridge, UK, pp. 3–19.
- Grime, J.P., 1998. Benefits of plant diversity to ecosystems: immediate, filter and founder effects. *Journal of Ecology* 86: 902–910.

- GSI (Geological Survey Ireland), 2020. Groundwater bodies. Available online: <https://www.gsi.ie/en-ie/programmes-and-projects/groundwater/activities/understanding-ireland-groundwater/Pages/Groundwater-bodies.aspx> (accessed 24 June 2020).
- Guilcher, A., 1961. Spits, tombolas and tidal marshes in Connemara and West Kerry, Ireland. *Proceedings of the Royal Irish Academy B: Biological, Geological, and Chemical Science* 61: 283–338.
- Guisado-Pintado, E. and Jackson, D., 2018. Multi-scale variability of storm Ophelia 2017: the importance of synchronised environmental variables in coastal impact. *Science of the Total Environment* 630: 287–301.
- Guisado-Pintado, E. and Jackson, D.W., 2019. Coastal impact from high-energy events and the importance of concurrent forcing parameters: the cases of Storm Ophelia (2017) and Storm Hector (2018) in NW Ireland. *Frontiers in Earth Science* 7: 190. <https://doi.org/10.3389/feart.2019.00190>
- Guisado-Pintado, E., Malvarez, G., Navas, F. and Carrero, R., 2014. Spatial distribution of storm wave energy dissipation for the assessment of beach morphodynamics. *Journal of Coastal Research* 70: 259–265.
- Hall, J. and Murphy, C., 2011. Robust adaptation assessment—climate change and water supply. *International Journal of Climate Change Strategies and Management* 33: 302–319.
- Harrington, S.T. and Harrington, J.R., 2013. An assessment of the suspended sediment rating curve approach for load estimation on the Rivers Bandon and Owenabue, Ireland. *Geomorphology* 185: 27–38.
- Harris, C., 1974. *The Evolution of North Bull Island, Dublin Bay*. Trinity College, Dublin.
- Hauke, J. and Kossowski, T., 2011. Comparison of values of Pearson's and Spearman's correlation coefficients on the same datasets. *Quaestiones Geographicae* 302: 87–93.
- Hem, J.D., 1985. *Study and Interpretation of the Chemical Characteristics of Natural Water*. Department of the Interior, US Geological Survey, Alexandria, USA.
- Hesp, P., 2002. Foredunes and blowouts: initiation, geomorphology and dynamics. *Geomorphology* 48: 245–268.
- Hill, M., Mountford, J., Roy, D. and Bunce, R., 1999. *Ellenberg's Indicator Values for British Plants. ECOFACT Volume 2 Technical Annex*. Institute of Terrestrial Ecology, Huntingdon, UK.
- Hirst, C., Andersson, P.S., Shaw, S., Burke, I.T., Kutscher, L., Murphy, M.J., Maximov, T., Pokrovsky, O.S., Mörrth, C-M., and Porcelli, D., 2017. Characterisation of Fe-bearing particles and colloids in the Lena River basin, NE Russia. *Geochimica et Cosmochimica Acta* 213: 553–573.
- Houser, C., 2009. Synchronization of transport and supply in beach–dune interaction. *Progress in Physical Geography* 33: 733–746.
- Houser, C., Wernette, P., Rentschlar, E., Jones, H., Hammond, B. and Trimble, S., 2015. Post-storm beach and dune recovery: implications for barrier island resilience. *Geomorphology* 234: 54–63.
- Houston, J., Rooney, P.J., Edmondson, S.E. and Rooney, P.J. (eds), 2001. *Coastal Dune Management: Shared Experience of European Conservation Practice*. Liverpool University Press, Liverpool, UK.
- Huang, J., Jackson, D. and Cooper, J., 2002. Morphological monitoring of a high energy beach system using GPS and total station techniques, Runkerry, Co. Antrim, Northern Ireland. *Journal of Coastal Research* 36: 390–398.
- IPCC (Intergovernmental Panel on Climate Change), 2018. *Global Warming of 1.5°C. An IPCC Special Report on the Impacts of Global Warming of 1.5°C above Pre-industrial Levels and Related Global Greenhouse Gas Emission Pathways, in the Context of Strengthening the Global Response to the Threat of Climate Change, Sustainable Development, and Efforts to Eradicate Poverty*. Masson-Delmotte, V., Zhai, P., Pörtner, H.-O., Roberts, D., Skea, J., Shukla, P.R., et al. (eds). World Meteorological Organization, Geneva.
- Jackson, D. and Cooper, J., 1999. Beach fetch distance and aeolian sediment transport. *Sedimentology* 46: 517–522.
- Jackson, D.W.T., Cooper, J.A.G. and del Rio, L., 2005. Geological control of beach morphodynamic state. *Marine Geology* 216: 297–314.
- Jackson, D.W.T., Anfuso, G. and Lynch, K., 2007. Swash bar dynamics on a high-energy mesotidal beach. *Journal of Coastal Research* 738–745.
- Jackson, D.W.T. and Cooper, J.A.G., 2011. Coastal dune fields in Ireland: rapid regional response to climatic change. *Journal of Coastal Research* SI64: 293–297.
- Jackson, D.W.T., Costas, S. and Guisado-Pintado, E., 2019. Large-scale transgressive coastal dune behaviour in Europe during the Little Ice Age. *Global and Planetary Change* 175: 82–91.



- Jastrom, J.D., Zipper, C.E., Zelazny, L.W. and Hyer, K.E., 2010. Increasing precision of turbidity-based suspended sediment concentration and load estimates. *Journal of Environmental Quality* 394: 1306–1316.
- Jennings, S., Orford, J.D., Canti, M., Devoy, R.J.N. and Straker, V., 1998. The role of relative sea-level rise and changing sediment supply on Holocene gravel barrier development: the example of Porlock, Somerset, UK. *The Holocene* 8: 165–181.
- Jilbert, T., Asmala, E., Schröder, C., Tiihonen, R., Myllykangas, J.-P., Virtasalo, J.J., Kotilainen, A., Peltola, P., Ekholm, P. and Hietanen, S., 2018. Impacts of flocculation on the distribution and diagenesis of iron in boreal estuarine sediments. *Biogeosciences* 15: 1243–1271.
- Jungerius, P.D. and Dekker, L.W., 1990. Water erosion in the dunes. In Bakker, T.W., Jungerius, P.D. and Klijn, J.A. (eds), *Dunes of the European Coasts*. Catena, Stuttgart, Germany, pp.185–193.
- Kandrot, S., Farrell, E. and Devoy, R., 2016. The morphological response of foredunes at a breached barrier system to winter 2013/2014 storms on the southwest coast of Ireland. *Earth Surface Processes and Landforms* 41: 2123–2136.
- Karunaratna, H., Pender, D., Ranasinghe, R., Short, A. and Reeve, D., 2014. The effects of storm clustering on beach profile variability. *Marine Geology* 348: 103–112.
- Keijsers, J.G., Giardino, A., Poortinga, A., Mulder, J.P., Riksen, M.J. and Santinelli, G., 2015. Adaptation strategies to maintain dunes as flexible coastal flood defense in The Netherlands. *Mitigation and Adaptation Strategies for Global Change* 20: 913–928.
- Kent, M., Dargie, T. and Reid, C., 2003. The management and conservation of machair vegetation. *Botanical Journal of Scotland* 55: 161–176.
- Khamis K., Bradley, C., Stevens, R., and Hannah, D.M., 2016. Continuous field estimation of dissolved organic carbon concentration and biochemical oxygen demand using dual-wavelength fluorescence, turbidity and temperature. *Hydrological Processes* 31: 540–555.
- Khamis, K., Sorensen, J.P.R., Bradley, C., Hannah, D.M., Lapworth, D.J. and Stevens, R., 2015. In situ tryptophan-like fluorometers: assessing turbidity and temperature effects for freshwater applications. *Environmental Science: Processes & Impacts* 17: 740–752.
- Kindermann, G. and Gormally, M., 2010. Vehicle damage caused by recreational use of coastal dune systems in a Special Area of Conservation (SAC) on the west coast of Ireland. *Journal of Coastal Conservation* 143: 173–188.
- Kindermann, G. and Gormally, M.J., 2013. Stakeholder perceptions of recreational and management impacts on protected coastal dune systems: a comparison of three European countries. *Land Use Policy* 31: 472–485.
- Kleyer, M., Bekker, R., Knevel, I., et al., 2008. The LEDA Traitbase: a database of life-history traits of the Northwest European flora. *Journal of Ecology* 966: 1266–1274.
- Knight, J. and Harrison, S., 2018. Paraglacial evolution of the Irish landscape. *Irish Geography* 51(2): 171–186.
- Komac, B., Pladevall, C., Domenech, M. and Fanlo, R., 2015. Functional diversity and grazing intensity in sub-alpine and alpine grasslands in Andorra. *Applied Vegetation Science* 181: 75–85.
- Krachler, R., Krachler, R.F., Wallner, G., Steier, P., El Abiead, Y., Wiesinger, H., Jirsa, F. and Keppler, B.K., 2016. *Sphagnum*-dominated bog systems are highly effective yet variable sources of bio-available iron to marine waters. *Science of the Total Environment* 556: 53–62.
- Kuusisto, E., 1996. Hydrological measurements. In Bartram, J. and Ballance, R. (eds), *Water Quality Monitoring: A Practical Guide to the Design and Implementation of Freshwater Quality Studies and Monitoring Programmes*. Chapman & Hall, London, UK.
- Laliberté, E., Wells, J.A., DeClerck, F., Metcalfe, D.J. and Catterall, C.P., 2010. Land use intensification reduces functional redundancy and response diversity in plant communities. *Ecological Letters* 13: 76–86.
- Lamhna, E., 1982. The vegetation of saltmarshes and sand-dunes at Malahide Island, County Dublin. *Journal of Life Sciences Royal Dublin Society* 3: 111–129.
- Lawler, D.M., 2016. Turbidity, turbidimetry and nephelometry. In Reedijk, J. (ed.), *Chemistry, I*. Elsevier, Waltham, MA.
- Lawler, D., Rymaszewicz, A., Conroy, L., O'Sullivan, J., Bruen, M., Turner, J. and Kelly-Quinn, M., 2017. *SILTFLUX Literature Review*. Environmental Protection Agency, Johnstown Castle, Ireland.

- Lawlor, A., Torres, J., O'Flynn, B., Wallace, J. and Regan, F., 2012. DEPLOY: a long-term deployment of a water quality sensor monitoring system. *Sensor Review* 321: 29–38.
- Leps, J., De Bello, F., Lavorel, S. and Berman, S., 2006. Quantifying and interpreting functional diversity of natural communities: practical considerations matter. *Preslia* 784: 481–501.
- Lewis, R., Pakeman, R., Angus, S. and Marrs, R., 2014a. Using compositional and functional indicators for biodiversity conservation monitoring of semi-natural grasslands in Scotland. *Biological Conservation* 175: 82–93.
- Lewis, R., Marrs, R. and Pakeman, R., 2014b. Inferring temporal shifts in landuse intensity from functional response traits and functional diversity patterns: a study of Scotland's machair grassland. *Oikos* 123: 334–344.
- Little, M.J. and Grieg-Smith, P., 1975. A survey of tracks and paths in a sand dune ecosystem. II. Vegetation. *Journal of Applied Ecology* 12: 909–930.
- Long, C.B., MacDermot, C.V., Morris, J.H., Sleeman, A.G., Tietzsch-Tyler, D., Aldwell, C.R., Daly, D., Flegg, A.M., McArdle, P.M. and Warren, W.P., 1992. *Geology of North Mayo: A Geological Description to Accompany the Bedrock Geology 1:100 000 Map Series: Sheet 6, North Mayo*. Geological Survey of Ireland, Dublin.
- Loureiro, C. and Cooper, J.A.G., 2018. Temporal variability in winter wave conditions and storminess in the northwest of Ireland. *Irish Geography* 51(2): 155–170. <https://doi.org/10.2014/igj.v51i2.1369>
- Loureiro, C., Ferreira, O. and Cooper, J., 2012. Geologically constrained morphological variability and boundary effects on embayed beaches. *Marine Geology* 329: 1–15.
- Loureiro, C., Ferreira, O. and Cooper, J.A.G., 2014. Non-uniformity of storm impacts on three high-energy embayed beaches. *Journal of Coastal Research* SI(70): 326–331.
- Loureiro, C., Marianne, O.C., Guisado-Pintado, E., Jackson, D. and Cooper, A., 2016. Extreme coastal storms along the north coast of Ireland: hydrodynamic forcing and beach response during the winter seasons of 2013/14 and 2014/15. European Geosciences Union General Assembly, EPSC2016-15290.
- Lynch, K., Jackson, D. and Cooper, J., 2008. Aeolian fetch distance and secondary airflow effects: the influence of micro-scale variables on meso-scale foredune development. *Earth Surface Processes and Landforms* 33: 991–1005.
- Lynch, K., Jackson, D. and Cooper, J., 2009. Fore-dune accretion under offshore winds. *Geomorphology* 105: 139–146.
- Marine Institute, 2020. The Irish Marine Data Buoy Observation Network. Available online: <http://www.marine.ie/Home/site-area/data-services/real-time-observations/irish-marine-data-buoy-observation-network> (accessed 8 March 2021).
- McGourty, J., Wilson, P., Noon, D., Stickley, G. and Longstaff, D., 2000. Investigating the internal structure of Holocene coastal sand dunes using ground-penetrating radar: example from the north coast of Northern Ireland. *Gpr 2000: Proceedings of the Eighth International Conference on Ground Penetrating Radar* 4084: 14–19.
- McKenna, J., O'Hagan, A.M., Power, J., MacLeod, M. and Cooper, A., 2007. Coastal dune conservation on an Irish commonage: community-based management or tragedy of the commons? *Geographical Journal* 173: 157–169.
- McKenna, J., Cooper, J.A.G. and O'Hagan, A.M., 2009. Coastal erosion management and the European principles of ICZM: local versus strategic perspectives. *Journal of Coastal Conservation* 13: 165–173.
- McKenzie, G. and Cooper, J.A.G., 2001. Post emplacement dune evolution of Atlantic coastal dunes, Northwest Ireland. *Journal of Coastal Research* SI34: 602–610.
- Malone, S. and O'Connell, C., 2009. *Ireland's Peatland Conservation Action Plan 2020 – Halting the Loss of Peatland Biodiversity*. Irish Peatland Conservation Council, Kildare, Ireland.
- Maloney, B.K., 1985. A palaeoecological investigation of the Holocene back-beach barrier environment near Carnsore Point, Co. Wexford. *Proceedings of the Royal Irish Academy. Section B: Biological, Geological, and Chemical Science* 85B: 73–89.
- Malvarez, G. and Cooper, J., 2000. A whole surf zone modelling approach as an aid to investigation of nearshore and coastal morphodynamics. *Journal of Coastal Research* 16: 800–815.
- Martins, S.V., Burningham, H. and Pinto-Cruz, C., 2018. Climate variability impacts on coastal dune slack ecohydrology. *Irish Geography* 51(2): 261–284. <https://doi.org/10.2014/igj.v51i2.1374>
- Mason, N., Mouillot, D., Lee, W. and Wilson, J., 2005. Functional richness, functional evenness and functional divergence: the primary components of functional diversity. *Oikos* 1111: 112–118.
- Masselink, G. and van Heteren, S., 2014. Response of wave-dominated and mixed-energy barriers to storms. *Marine Geology* 352: 321–347.

- Masselink, G., Scott, T., Poate, T., Russell, P., Davidson, M. and Conley, D., 2016a. The extreme 2013/2014 winter storms: hydrodynamic forcing and coastal response along the southwest coast of England. *Earth Surface Processes and Landforms* 41(3): 378–391.
- Masselink, G., Castelle, B., Scott, T., Dodet, G., Suanez, S., Jackson, D. and Floc'h, F., 2016b. Extreme wave activity during 2013/2014 winter and morphological impacts along the Atlantic coast of Europe. *Geophysical Research Letters* 43(5): 2135–2143.
- May, L., Place, C., O'Hea, B., Lee, M., Dillane, M. and McGinnity, P., 2005. Modelling soil erosion and transport in the Burrishoole catchment, Newport, Co. Mayo, Ireland. *Freshwater Forum* 231: 139–154.
- Micallef, A. and Williams, A., 2009. *Beach Management*. Routledge, London.
- Miller, R.L., Bradford, W.L. and Peters, N.E., 1988. *Specific Conductance: Theoretical Considerations and Application to Analytical Quality Control*. United States Government Printing Office, Denver, USA.
- Morton, R.A., Paine, J.G. and Gibeau, J.C., 1994. Stages and durations of post-storm beach recovery, southeastern Texas Coast, USA. *Journal of Coastal Research* 10: 884–908.
- Murphy, C. and Charlton, R.A., 2008. Climate change and water resources. In Sweeney, J., Albanito, F., Brereton, A., Caffarra, A., Charlton, R., Donnelly, A., Fealy, R., Fitzgerald, J., Holden, N., Jones, M. and Murphy, C. (eds), *Climate Change – Refining the Impacts for Ireland: STRIVE Report*. Environmental Protection Agency, Johnstown Castle, Ireland. Available online: <http://eprints.maynoothuniversity.ie/2682/1/sweeney-report-strive-12-for-web-low-res.pdf> (accessed 14 July 2017).
- Murray, A., 2017. *Natural Flood Management: Adopting Ecosystem Approaches to Managing Flood Risk*. Friends of the Earth, Dublin, Ireland.
- Nolan, P., 2015. *Ensemble of Regional Climate Model Projections for Ireland*. Environmental Protection Agency, Johnstown Castle, Ireland.
- NPWS (National Parks and Wildlife Services), 2013a. *Site Synopsis: Doogort Machair/Lough Doo SAC*. Available online: <https://www.npws.ie/sites/default/files/protected-sites/synopsis/SY001497.pdf> (accessed 19 August 2019).
- NPWS (National Parks and Wildlife Services), 2013b. *The Status of EU Protected Habitats and Species in Ireland. Habitat Assessments Volumes 1–3. Version 1.1*. NPWS and Department of Arts, Heritage and the Gaeltacht, Dublin.
- NPWS (National Parks and Wildlife Services), 2017. *Doogort Machair/Lough Doo SAC (Site Code: 001497). Conservation Objectives Supporting Document – Coastal Habitats. Version 1*. Available online: [https://www.npws.ie/sites/default/files/publications/pdf/Doogort%20Machair,%20Lough%20Doo%20SAC%20\(001497\)%20Conservation%20objectives%20supporting%20document%20-%20Coastal%20habitats%20\[Version%201\].pdf](https://www.npws.ie/sites/default/files/publications/pdf/Doogort%20Machair,%20Lough%20Doo%20SAC%20(001497)%20Conservation%20objectives%20supporting%20document%20-%20Coastal%20habitats%20[Version%201].pdf) (accessed 26 April 2021).
- O'Connor, M., Cooper, J. and Jackson, D., 2007. Morphological behaviour of headland-embayment and inlet-associated beaches, Northwest Ireland. *Journal of Coastal Research* 50: 626–630.
- O'Connor, M.C., Cooper, J.A.G. and Jackson, D.W.T., 2011. Decadal behavior of tidal inlet-associated beach systems, northwest Ireland, in relation to climate forcing. *Journal of Sedimentary Research* 81: 38–51.
- O'Driscoll, C., de Eyto, E., O'Connor, M., Rodgers, M. and Xiao, L., 2013. Biotic response to forest harvesting in acidic blanket peat fed streams: a case study from Ireland. *Forest Ecology and Management* 310: 729–739.
- O'Keeffe, C., 2008. *The Status of EU Protected Habitats and Species in Ireland: Conservation Status in Ireland of Habitats and Species Listed in the European Council Directive on the Conservation of Habitats, Flora and Fauna 92/43/EEC*. National Parks and Wildlife Service, Dublin.
- O'Neill, F., Martin, J.R., Devaney, F.M., Perrin, P.M., 2010. *Irish Semi-natural Grasslands Survey – Annual Report No. 3: Co. Donegal, Dublin, Kildare & Sligo*. BEC Consultants, Dublin. Available online: [http://www.botanicalenvironmental.com/wp-content/uploads/2011/10/2010\\_ISGS\\_Report\\_and\\_Appendices.pdf](http://www.botanicalenvironmental.com/wp-content/uploads/2011/10/2010_ISGS_Report_and_Appendices.pdf) (accessed 19 August 2019).
- O'Shea, M., Murphy, J. and Sala, P., 2011. Monitoring the morphodynamic behaviour of a breached barrier beach system and its impacts on an estuarine system. *OCEANS 2011 IEEE*, Santander, Spain, pp. 1–8.
- Orford, J., 1988. Alternative interpretations on man-induced shoreline changes in Rosslare Bay, SE Ireland. *Transactions of the Institute of British Geographers* 13: 65–78.
- Orford, J.D., Carter, R.W.G. and Jennings, S.C., 1996. Control domains and morphological phases in gravel-dominated coastal barriers of Nova Scotia. *Journal of Coastal Research* 12(3): 589–604.
- Orford, J.D., Cooper, J.A.G. and McKenna, J., 1999. Mesoscale temporal changes to foredunes at Inch Spit, south-west Ireland. *Zeitschrift für Geomorphologie* 43: 439–461.

- Orford, J., Psuty, N., Sherman, D. and Meyer-Arendt, K., 2005. The controls on late-Holocene coastal dune formation on leeside coasts of the British Isles. *Coasts under Stress II* 141: 135–152.
- Pakeman, R.J., 2011. Functional diversity indices reveal the impacts of land use intensification on plant community assembly. *Journal of Ecology* 99: 1143–1151.
- Perlman, H., 2016. *pH Water Properties*. Available online: <http://water.usgs.gov/edu/ph.html> (accessed 3 July 2018).
- Perriquet, M., Léonardi, V., Henry, T. and Jourde, H., 2014. Saltwater wedge variation in a non-anthropogenic coastal karst aquifer influenced by a strong tidal range (Burren, Ireland). *Journal of Hydrology* 519: 2340–2365. <https://doi.org/10.1016/j.jhydrol.2014.10.006>
- Pilkey, O.H. and Cooper, J.A.G., 2014. *The Last Beach*. Duke University Press, Durham, NC.
- Poole, G.C. and Berman, C.H., 2001. An ecological perspective on in-stream temperature: natural heat dynamics and mechanisms of human-caused thermal degradation. *Environmental Management* 27: 787–802.
- Power, J., McKenna, J., MacLeod, M.J., Cooper, A.J.G. and Convie, G., 2000. Developing integrated participatory management strategies for Atlantic dune systems in county Donegal, Northwest Ireland. *Ambio* 29: 143–149.
- Prabu, P.C., Wondimu, L. and Tesso, M., 2011. Assessment of water quality of Huluka and Alaltu Rivers of Ambo, Ethiopia. *Journal of Agricultural Science and Technology* 131: 131–138.
- Purcell, P., Bruen, M., O'Sullivan, J., Cocchiglia, L. and Kelly-Quinn, M., 2012. Water quality monitoring during the construction of the M3 motorway in Ireland. *Water and Environment Journal* 262: 175–183.
- Quigley, M., 1991. *A Guide to the Sand Dunes of Ireland*. Compiled for the 3rd Congress of the European Union for Dune Conservation and Coastal Management, Galway, Ireland.
- Regan, F., Lawlor, A., O'Flynn, B. and Wallace, J., 2011, *DEPLOY: Smart Demonstration of Online Water Quality Monitoring on the River Lee, Cork, Ireland*. Environmental Protection Agency, Johnstown Castle, Ireland. Available online: [http://oar.marine.ie/bitstream/10793/716/1/STRIVE\\_Report\\_82\\_DEPLOY.pdf](http://oar.marine.ie/bitstream/10793/716/1/STRIVE_Report_82_DEPLOY.pdf) (accessed 30 June 2017).
- Ricotta, C. and Moretti, M., 2011. CWM and Rao's quadratic diversity: a unified framework for functional ecology. *Oecologia* 167: 181–188.
- Ritchie, W., 1974. Spatial variation of shell content between and within “machair” systems. In Ranwell, D.S. (ed.), *Sand Dune Machair*. Institute of Terrestrial Ecology, Cambridge, UK, pp. 9–12.
- Roberts, T.M., Wang, P. and Puleo, J.A., 2013. Storm-driven cyclic beach morphodynamics of a mixed sand and gravel beach along the Mid-Atlantic Coast, USA. *Marine Geology* 346: 403–421.
- Ryle, T., Murray, A., Connolly, K. and Swann, M., 2009. *Coastal Monitoring Project 2004–2006. A Report to the National Parks and Wildlife Service*. Available online: [www.npws.ie/sites/default/files/publications/pdf/Ryle\\_et\\_al\\_2009\\_Coastal\\_Monitoring\\_Project.pdf](http://www.npws.ie/sites/default/files/publications/pdf/Ryle_et_al_2009_Coastal_Monitoring_Project.pdf) (accessed 19 August 2019).
- Rymaszewicz, A., O'Sullivan, J.J., Bruen, M., Turner, J.N., Lawler, D.M., Conroy, E. and Kelly-Quinn, M., 2017. Measurement differences between turbidity instruments, and their implications for suspended sediment concentration and load calculations: a sensor inter-comparison study. *Journal of Environmental Management* 199: 99–108.
- Sallenger, A.H., 2000. Storm impact scale for barrier islands. *Journal of Coastal Research* 16: 890–895.
- Scarelli, F.M., Sistilli, F., Fabbri, S., Cantelli, L., Barboza, E.G. and Gabbianelli, G., 2017. Seasonal dune and beach monitoring using photogrammetry from UAV surveys to apply in the ICZM on the Ravenna coast (Emilia-Romagna, Italy). *Remote Sensing Applications: Society and Environment* 7: 27–39.
- Schleppi, P., Waldner, P.A. and Fritschi, B., 2006. Accuracy and precision of different sampling strategies and flux integration methods for runoff water: comparisons based on measurements of the electrical conductivity. *Hydrological Processes* 202: 395–410.
- Scott, T., Masselink, G. and Russell, P., 2011. Morphodynamic characteristics and classification of beaches in England and Wales. *Marine Geology* 286(1–4): 1–20.
- Scott, T., Masselink, G., O'Hare, T., Saulter, A., Poate, T., Russell, P., Davidson, M. and Conley, D., 2016. The extreme 2013/2014 winter storms: beach recovery along the southwest coast of England. *Marine Geology* 382: 224–241.
- Sholkovitz, E.R., Boyle, E.A., Price, N.B., 1978. The removal of dissolved humic acids and iron during estuarine mixing. *Earth Planetary Science Letters* 40: 130–136.
- Silva, R., Martinez, M., Oderiz, I., Mendoza, E. and Feagin, R., 2016. Response of vegetated dune–beach systems to storm conditions. *Coastal Engineering* 109: 53–62.

- SmartBay, 2020. SmartBay: test, validate, innovate.  
Available online: <https://www.smartbay.ie/> (accessed 8 March 2021).
- Smith, G.F., O'Donoghue, P., O'Hora, K. and Delaney, E., 2011. *Best Practice Guidance for Habitat Survey and Mapping*. The Heritage Council, Kilkenny, Ireland.
- Smith, D.E., Hunt, N., Firth, C.R., Jordan, J.T., Fretwell, P.T., Harman, M., Murdy, J., Orford, J.D. and Burnside, N.G., 2012. Patterns of Holocene relative sea level change in the North of Britain and Ireland. *Quaternary Science Reviews* 54: 58–76.
- Sorensen, J.P.R., Lapworth, D.J., Marchant, B.P., Nkhuwa, D.C.W., Pedley, S., Stuart, M.E., Bell, R.A., Chirwa, M., Kabika, J., Liemisa, M. and Chibesa, M., 2015. In-situ tryptophan-like fluorescence: a real-time indicator of faecal contamination in drinking water supplies. *Water Research* 81: 38–46.
- Sottocornola, M., Laine, A., Kiely, G., Byrne, K.A. and Tuittila, E.S., 2009. Vegetation and environmental variation in an Atlantic blanket bog in South-western Ireland. *Plant Ecology* 203(1): 69.
- Spencer, T., Brooks, S.M., Evans, B.R., Tempest, J.A. and Möller, I., 2015. Southern North Sea storm surge event of 5 December 2013: water levels, waves and coastal impacts. *Earth-Science Reviews* 146: 120–145.
- Splinter, K.D., Carley, J.T., Golshani, A. and Tomlinson, R., 2014. A relationship to describe the cumulative impact of storm clusters on beach erosion. *Coastal Engineering* 83: 49–55.
- St-Hilaire, A., Brun, G., Courtenay, S.C., Ouarda, T., Boghen, A.D. and Bobee, B., 2004. Multivariate analysis of water quality in the Richibucto drainage basin New Brunswick, Canada. *Journal of the American Water Resources Association* 403: 691–703.
- Stéphan, P., Suanez, S. and Fichaut, B., 2015. Long-, mid- and short-term evolution of coastal gravel spits of Brittany, France. In Randazzo, G., Jackson, D.W.T, Cooper, A.G. (eds), *Sand and Gravel Spits*. Springer, Cham, Switzerland, pp. 275–288.
- Story, A., Moore, R.D. and Macdonald, J.S., 2003. Stream temperatures in two shaded reaches below cutblocks and logging roads: downstream cooling linked to subsurface hydrology. *Canadian Journal of Forest Research* 338: 1383–1396.
- Suanez, S., Cariolet, J.M., Cancouët, R., Arduin, F. and Delacourt, C., 2012. Dune recovery after storm erosion on a high-energy beach: Vougot beach, Brittany France. *Geomorphology* 139–140: 16–33.
- SWRCB (State Water Resources Control Board), 2002. Electrical Conductivity/Salinity Fact Sheet. In The Clean Water Team Guidance Compendium for Watershed Monitoring and Assessment, California State Water Resources Control Board. Available online: [http://www.swrcb.ca.gov/water\\_issues/programs/swamp/docs/cwt/guidance/3130en.pdf](http://www.swrcb.ca.gov/water_issues/programs/swamp/docs/cwt/guidance/3130en.pdf) (accessed August 2020).
- Sweeney, J., Wilson, J., Mayes, E., Minchin, D., Embrow, C., Wilson, J., Donnelly, A., Jones, M.B., Byrne, C., Farrell, E.P. and Byrne, K.A., 2003. *Climate Change: Scenarios and Impacts for Ireland: Final Report*. Environmental Protection Agency, Johnstown Castle, Ireland. Available online: [http://mural.maynoothuniversity.ie/2684/1/epa\\_climate\\_change\\_scenarios\\_ertdi15.pdf](http://mural.maynoothuniversity.ie/2684/1/epa_climate_change_scenarios_ertdi15.pdf) (accessed 20 July 2017).
- Swift, L., Devoy, R., Wheeler, A., Sutton, G. and Gault, J., 2006. Sedimentary dynamics and coastal changes on the south coast of Ireland. *Journal of Coastal Research* SI39: 227–232.
- Tedd, K., Coxon, C., Misstear, B., Daly, D., Mannix, A. and Hunter Williams, T., 2017. Assessing and developing natural background levels for chemical parameters in Irish groundwater. Environmental Protection Agency, Johnstown Castle, Ireland.
- Thompson, J., Cassidy, R., Doody, D.G. and Flynn, R., 2014. Assessing suspended sediment dynamics in relation to ecological thresholds and sampling strategies in two Irish headwater catchments. *Science of the Total Environment* 468: 345–357.
- Tsoar, H., 2005. Sand dunes mobility and stability in relation to climate. *Physica A: Statistical Mechanics and its Applications* 3571: 50–56.
- Uhrich, M.A. and Bragg, H.M., 2003. *Monitoring Instream Turbidity to Estimate Continuous Suspended-sediment Loads and Yields and Clay-water Volumes in the Upper North Santiam River Basin, Oregon, 1998–2000*. No. 2003–4098. Available online: <https://pubs.er.usgs.gov/publication/wri034098> (accessed 24 June 2017).
- UKHO (UK Hydrographic Office), 2008. VORF Model VORF-UK08. UKHO, Liverpool, UK.
- Wade, A.J., Palmer-Felgate, E.J., Halliday, S.J., Skeffington, R.A., Loewenthal, M., Jarvie, H.P., et al., 2012. Hydrochemical processes in lowland rivers: insights from *in situ*, high-resolution monitoring. *Hydrology and Earth System Sciences* 1611: 4323–4342.
- Walling, D.E., 1983. The sediment delivery problem. *Journal of Hydrology* 65(1–3): 209–237.



- Wang, S., McGrath, R., Hanafin, J., Lynch, P., Semmler, T. and Nolan, P., 2008. The impact of climate change on storm surges over Irish waters. *Ocean Modelling* 251: 83–94.
- Webb, B.W., 1996. Trends in stream and river temperature. *Hydrological Processes* 102: 205–226.
- Webb, B.W., Hannah, D.M., Moore, R.D., Brown, L.E. and Nobilis, F., 2008. Recent advances in stream and river temperature research. *Hydrological Processes* 227: 902–918.
- Wetzel, R.G., 2001. *Limnology: Lake and River Ecosystems*. 3rd ed. Academic Press, San Diego, CA.
- Wilcock, F. and Carter, R., 1977. Environmental approach to restoration of badly eroded sand dunes. *Biological Conservation* 11: 279–291.
- Williams, J., Esteves, L. and Rochford, L., 2015. Modelling storm responses on a high-energy coastline with XBeach. *Modeling Earth Systems and Environment* 1: 3.
- Wilson, P. and McKenna, J., 1996. Holocene evolution of the River Bann estuary and adjacent coast, Northern Ireland. *Proceedings of the Geologists Association* 107: 241–252.
- Wilson, P., Thompson, K. and Hodgson, J., 1999. Specific leaf area and leaf dry matter content as alternative predictors of plant strategies. *New Phytologist* 143: 155–162.
- Wintle, A.G., Clarke, M.L., Musson, F.M., Orford, J.D. and Devoy, R.J.N., 1998. Luminescence dating of recent dunes on Inch Spit, Dingle Bay, southwest Ireland. *Holocene* 8: 331–339.
- Woodroffe, C.D., 2002. *Coasts: Form, Process and Evolution*. Cambridge University Press, Cambridge, UK.
- Wright, L.D. and Short, A.D., 1984. Morphodynamic variability of surf zones and beaches a synthesis. *Marine Geology* 56: 93–118.
- Zheng, S., Ren, H., Lan, Z., Li, W., Wang, W. and Bai, Y., 2010. Effects of grazing on leaf traits and ecosystem functioning in Inner Mongolian grasslands: scaling from species to community. *Biogeosciences* 7: 1117–1132.

# Abbreviations

<b>BH</b>	Borehole
<b>CH</b>	Canopy height
<b>CMP</b>	Coastal Monitoring Project
<b>CORINE</b>	Coordination of Information on the Environment
<b>CTD</b>	Conductivity, temperature and depth
<b>CWM</b>	Community-weighted mean
<b>DEM</b>	Digital elevation model
<b>DO</b>	Dissolved oxygen
<b>DOM</b>	Dissolved organic matter
<b>EC</b>	Electrical conductivity
<b>EPA</b>	Environmental Protection Agency
<b>ER</b>	Effective rainfall
<b>FNU</b>	Formazin nephelometric unit
<b>FTU</b>	Formazin turbidity unit
<b>GIS</b>	Geographic information system
<b>GNSS</b>	Global navigation satellite system
<b>GPS</b>	Global Positioning System
<b>HEC-RAS</b>	Hydrologic Engineering Center – River Analysis System
<b><math>H_s</math></b>	Significant wave height
<b>ICIP</b>	Ireland's Climate Information Platform
<b>JERICO</b>	Joint European Research Infrastructure of Coastal Observatories
<b>L</b>	Light
<b>LDMC</b>	Leaf dry matter content
<b>N</b>	Nitrogen
<b>NBD</b>	Nearshore–beach–dune
<b>NPWS</b>	National Parks and Wildlife Service
<b>NTU</b>	Nephelometric turbidity unit
<b>PE</b>	Potential evapotranspiration
<b>RFU</b>	Relative fluorescence unit
<b>SAC</b>	Special Area of Conservation
<b>SC</b>	Specific conductance
<b>SLA</b>	Specific leaf area
<b>SM</b>	Seed mass
<b>SPA</b>	Special Protection Area
<b>SSC</b>	Suspended sediment concentration
<b>TDS</b>	Total dissolved solids
<b>TLF</b>	Tryptophan-like fluorescence
<b>TV</b>	Terminal velocity
<b>VIC</b>	Volumetric ion content
<b>WFD</b>	Water Framework Directive
<b>WP</b>	Work package

# Appendix 1 Exploration of the Statistical Relationships Between the Water Parameters

**Table A1.1. Spearman's rank correlation matrix for all data (WP6)**

Sensor	Temperature	EC	Turbidity	pH	DO	WL	Tf	Tide
Temperature	1.000	-0.265 <sup>a</sup>	0.359 <sup>a</sup>	0.190 <sup>a</sup>	-0.825 <sup>a</sup>	-0.235 <sup>a</sup>	-0.497 <sup>a</sup>	0.009
EC	-0.265 <sup>a</sup>	1.000	0.384 <sup>a</sup>	0.671 <sup>a</sup>	0.079 <sup>a</sup>	-0.233 <sup>a</sup>	0.478 <sup>a</sup>	-0.024 <sup>a</sup>
Turbidity	0.359 <sup>a</sup>	0.384 <sup>a</sup>	1.000	0.575 <sup>a</sup>	-0.418 <sup>a</sup>	-0.078 <sup>a</sup>	-0.013	0.010
pH	0.190 <sup>a</sup>	0.671 <sup>a</sup>	0.575 <sup>a</sup>	1.000	-0.365 <sup>a</sup>	-0.319 <sup>a</sup>	0.071 <sup>a</sup>	-0.020 <sup>a</sup>
DO	-0.825 <sup>a</sup>	0.079 <sup>a</sup>	-0.418 <sup>a</sup>	-0.365 <sup>a</sup>	1.000	0.426 <sup>a</sup>	0.521 <sup>a</sup>	0.006
WL	-0.235 <sup>a</sup>	-0.233 <sup>a</sup>	-0.078 <sup>a</sup>	-0.319 <sup>a</sup>	0.426 <sup>a</sup>	1.000	0.082 <sup>a</sup>	-0.045 <sup>a</sup>
Tryptophan fluorescence	-0.497 <sup>a</sup>	0.478 <sup>a</sup>	-0.013	0.071 <sup>a</sup>	0.521 <sup>a</sup>	0.082 <sup>a</sup>	1.000	-0.013
Tide	0.009	-0.024 <sup>a</sup>	0.010	-0.02 <sup>a</sup>	0.006	-0.045 <sup>a</sup>	-0.013	1.000

<sup>a</sup>Correlation is significant at the  $p=0.01$  level (two-tailed), with the highest positive and negative correlations highlighted in blue and red, respectively.

<sup>b</sup>Tryptophan fluorescence

WL, water level.

**Table A1.2. Spearman's rank correlation matrix for summer 2016 (June to August)**

Sensor	Temperature	EC	Turbidity	pH	DO	WL	Tide
Temperature	1.000	0.172 <sup>a</sup>	0.360 <sup>a</sup>	0.318 <sup>a</sup>	-0.410 <sup>a</sup>	-0.336 <sup>a</sup>	0.068 <sup>a</sup>
EC	0.172 <sup>a</sup>	1.000	0.727 <sup>a</sup>	0.913 <sup>a</sup>	-0.456 <sup>a</sup>	-0.429 <sup>a</sup>	0.012
Turbidity	0.360 <sup>a</sup>	0.727 <sup>a</sup>	1.000	0.720 <sup>a</sup>	-0.453 <sup>a</sup>	-0.225 <sup>a</sup>	0.015
pH	0.318 <sup>a</sup>	0.913 <sup>a</sup>	0.720 <sup>a</sup>	1.000	-0.501 <sup>a</sup>	-0.433 <sup>a</sup>	0.012
DO	-0.410 <sup>a</sup>	-0.456 <sup>a</sup>	-0.453 <sup>a</sup>	-0.501 <sup>a</sup>	1.000	0.354 <sup>a</sup>	0.024
WL	-0.336 <sup>a</sup>	-0.429 <sup>a</sup>	-0.225 <sup>a</sup>	-0.433 <sup>a</sup>	0.354 <sup>a</sup>	1.000	-0.049 <sup>a</sup>
Tide	0.068 <sup>a</sup>	0.012	0.015	0.012	0.024	-0.049 <sup>a</sup>	1.000

<sup>a</sup>Correlation is significant at the  $p=0.01$  level (two-tailed), with the highest positive and negative correlations highlighted in blue and red, respectively.

WL, water level.

**Table A1.3. Spearman's rank correlation matrix for autumn 2016 (September to November)**

Sensor	Temperature	EC	Turbidity	pH	DO	WL	Tide
Temperature	1.000	-0.610 <sup>a</sup>	0.023	-0.148 <sup>a</sup>	-0.446 <sup>a</sup>	0.437 <sup>a</sup>	0.044 <sup>a</sup>
EC	-0.610 <sup>a</sup>	1.000	0.603 <sup>a</sup>	0.681 <sup>a</sup>	-0.185 <sup>a</sup>	-0.568 <sup>a</sup>	-0.034 <sup>b</sup>
Turbidity	0.023	0.603 <sup>a</sup>	1.000	0.688 <sup>a</sup>	-0.601 <sup>a</sup>	-0.248 <sup>a</sup>	0.015
pH	-0.148 <sup>a</sup>	0.681 <sup>a</sup>	0.688 <sup>a</sup>	1.000	-0.471 <sup>a</sup>	-0.377 <sup>a</sup>	-0.005
DO	-0.446 <sup>a</sup>	-0.185 <sup>a</sup>	-0.601 <sup>a</sup>	-0.471 <sup>a</sup>	1.000	0.117 <sup>a</sup>	-0.004
WL	0.437 <sup>a</sup>	-0.568 <sup>a</sup>	-0.248 <sup>a</sup>	-0.377 <sup>a</sup>	0.117 <sup>a</sup>	1.000	-0.021
Tide	0.044 <sup>a</sup>	-0.034 <sup>b</sup>	0.015	-0.005	-0.004	-0.021	1.000

<sup>a</sup>Correlation is significant at the  $p=0.01$  level (two-tailed), with the highest positive and negative correlations highlighted in blue and red, respectively.

<sup>b</sup>Correlation is significant at the  $p=0.05$  level (two-tailed).

WL, water level.

**Table A1.4. Spearman's rank correlation matrix for winter 2016/2017 (December to February)**

Sensor	Temperature	EC	Turbidity	pH	DO	WL	RFU	Tide
Temperature	1.000	-0.103 <sup>a</sup>	0.040 <sup>b</sup>	0.010	-0.275 <sup>a</sup>	-0.177 <sup>a</sup>	-0.851 <sup>a</sup>	0.026
EC	-0.103 <sup>a</sup>	1.000	0.234 <sup>a</sup>	0.750 <sup>a</sup>	-0.381 <sup>a</sup>	-0.323 <sup>a</sup>	0.548 <sup>a</sup>	-0.034 <sup>b</sup>
Turbidity	0.040 <sup>a</sup>	0.234 <sup>a</sup>	1.000	0.536 <sup>a</sup>	-0.433 <sup>a</sup>	0.004	0.048	0.041 <sup>a</sup>
pH	0.010	0.750 <sup>a</sup>	0.536 <sup>a</sup>	1.000	-0.533 <sup>a</sup>	-0.265 <sup>a</sup>	0.415 <sup>a</sup>	-0.013
DO	-0.275 <sup>a</sup>	-0.381 <sup>a</sup>	-0.433 <sup>a</sup>	-0.533 <sup>a</sup>	1.000	0.410 <sup>a</sup>	0.259 <sup>a</sup>	0.007
WL	-0.177 <sup>a</sup>	-0.323 <sup>a</sup>	0.004	-0.265 <sup>a</sup>	0.410 <sup>a</sup>	1.000	-0.089 <sup>a</sup>	-0.066 <sup>a</sup>
RFU	-0.851 <sup>a</sup>	0.548 <sup>a</sup>	0.048 <sup>a</sup>	0.415 <sup>a</sup>	0.259 <sup>a</sup>	-0.089 <sup>a</sup>	1.000	-0.006
Tide	0.026	-0.034 <sup>b</sup>	0.041 <sup>a</sup>	-0.013	0.007	-0.066 <sup>a</sup>	-0.006	1.000

<sup>a</sup>Correlation is significant at the  $p=0.01$  level (two-tailed), with the highest positive and negative correlations highlighted in blue and red, respectively.

<sup>b</sup>Correlation is significant at the  $p=0.05$  level (two-tailed).

WL, water level.

**Table A1.5. Spearman's rank correlation matrix for spring 2017 (March to May)**

Sensor	Temperature	EC	Turbidity	pH	DO	WL	RFU	Tide
Temperature	1.000	0.620 <sup>a</sup>	0.694 <sup>a</sup>	0.619 <sup>a</sup>	-0.718 <sup>a</sup>	-0.317 <sup>a</sup>	0.140 <sup>a</sup>	0.041 <sup>a</sup>
EC	0.620 <sup>a</sup>	1.000	0.914 <sup>a</sup>	0.949 <sup>a</sup>	-0.396 <sup>a</sup>	-0.305 <sup>a</sup>	-0.018	0.019
Turbidity	0.694 <sup>a</sup>	0.914 <sup>a</sup>	1.000	0.916 <sup>a</sup>	-0.547 <sup>a</sup>	-0.225 <sup>a</sup>	0.005	0.015
pH	0.619 <sup>a</sup>	0.949 <sup>a</sup>	0.916 <sup>a</sup>	1.000	-0.351 <sup>a</sup>	-0.277 <sup>a</sup>	-0.063 <sup>a</sup>	0.013
DO	-0.718 <sup>a</sup>	-0.396 <sup>a</sup>	-0.547 <sup>a</sup>	-0.351 <sup>a</sup>	1.000	0.156 <sup>a</sup>	-0.013	-0.003
WL	-0.317 <sup>a</sup>	-0.305 <sup>a</sup>	-0.225 <sup>a</sup>	-0.277 <sup>a</sup>	0.156 <sup>a</sup>	1.000	-0.198 <sup>a</sup>	-0.104 <sup>a</sup>
RFU	0.140 <sup>a</sup>	-0.018	0.005	-0.063 <sup>a</sup>	-0.013	-0.198 <sup>a</sup>	1.000	0.035 <sup>b</sup>
Tide	0.041 <sup>a</sup>	0.019	0.015	0.013	-0.003	-0.104 <sup>a</sup>	0.035 <sup>b</sup>	1.000

<sup>a</sup>Correlation is significant at the  $p=0.01$  level (two-tailed), with the highest positive and negative correlations highlighted in blue and red, respectively.

<sup>b</sup>Correlation is significant at the  $p=0.05$  level (two-tailed).

WL, water level.

**Table A1.6. Spearman's rank correlation matrix for summer 2017 (June to August)**

Sensor	Temperature	EC	Turbidity	pH	DO	WL	RFU	Tide
Temperature	1.000	0.143 <sup>a</sup>	0.034 <sup>b</sup>	0.161 <sup>a</sup>	-0.140 <sup>a</sup>	-0.054 <sup>a</sup>	0.491 <sup>a</sup>	0.049 <sup>a</sup>
EC	0.143 <sup>a</sup>	1.000	-0.034 <sup>b</sup>	0.786 <sup>a</sup>	-0.356 <sup>a</sup>	-0.513 <sup>a</sup>	0.100	-0.030 <sup>b</sup>
Turbidity	0.034 <sup>b</sup>	-0.034 <sup>b</sup>	1.000	-0.104 <sup>a</sup>	-0.051 <sup>a</sup>	0.093 <sup>a</sup>	0.135 <sup>a</sup>	-0.004
pH	0.161 <sup>a</sup>	0.786 <sup>a</sup>	-0.104 <sup>a</sup>	1.000	-0.484 <sup>a</sup>	-0.395 <sup>a</sup>	-0.047 <sup>a</sup>	-0.035 <sup>b</sup>
DO	-0.140 <sup>a</sup>	-0.356 <sup>a</sup>	-0.051 <sup>a</sup>	-0.484 <sup>a</sup>	1.000	0.322 <sup>a</sup>	0.009	0.029
WL	-0.054 <sup>a</sup>	-0.513 <sup>a</sup>	0.093 <sup>a</sup>	-0.395 <sup>a</sup>	0.322 <sup>a</sup>	1.000	-0.064 <sup>a</sup>	-0.058 <sup>a</sup>
RFU	0.491 <sup>a</sup>	0.100	0.135 <sup>a</sup>	-0.047 <sup>a</sup>	0.009	-0.064 <sup>a</sup>	1.000	0.051 <sup>a</sup>
Tide	0.049 <sup>a</sup>	-0.030 <sup>b</sup>	-0.004	-0.035 <sup>b</sup>	0.029	-0.058 <sup>a</sup>	0.051 <sup>a</sup>	1.000

<sup>a</sup>Correlation is significant at the  $p=0.01$  level (two-tailed), with the highest positive and negative correlations highlighted in blue and red, respectively.

<sup>b</sup>Correlation is significant at the  $p=0.05$  level (two-tailed).

WL, water level.

**Table A1.7. Spearman's rank correlation matrix for autumn 2017 (September to November) ( $n=4363$ )**

Sensor	Temperature	EC	Turbidity	pH	DO	WL	RFU	Tide
Temperature	1.000	-0.001	0.228 <sup>a</sup>	0.053 <sup>a</sup>	-0.707 <sup>a</sup>	-0.405 <sup>a</sup>	-0.068 <sup>a</sup>	0.047 <sup>a</sup>
EC	-0.001	1.000	0.341 <sup>a</sup>	0.758 <sup>a</sup>	-0.390 <sup>a</sup>	-0.029	-0.175 <sup>a</sup>	-0.035 <sup>b</sup>
Turbidity	0.228 <sup>a</sup>	0.341 <sup>a</sup>	1.000	0.261 <sup>a</sup>	-0.338 <sup>a</sup>	-0.061 <sup>a</sup>	-0.050 <sup>a</sup>	0.034 <sup>b</sup>
pH	0.053 <sup>a</sup>	0.758 <sup>a</sup>	0.261 <sup>a</sup>	1.000	-0.475 <sup>a</sup>	-0.250 <sup>a</sup>	-0.199 <sup>a</sup>	-0.011
DO	-0.707 <sup>a</sup>	-0.390 <sup>a</sup>	-0.338 <sup>a</sup>	-0.475 <sup>a</sup>	1.000	0.373 <sup>a</sup>	0.274 <sup>a</sup>	-0.011
WL	-0.405	-0.029	-0.061 <sup>a</sup>	-0.250 <sup>a</sup>	0.373 <sup>a</sup>	1.000	0.231 <sup>a</sup>	-0.074 <sup>a</sup>
RFU	-0.068 <sup>a</sup>	-0.175 <sup>a</sup>	-0.050 <sup>a</sup>	-0.199 <sup>a</sup>	0.274 <sup>a</sup>	0.231 <sup>a</sup>	1.000	-0.018
Tide	0.047 <sup>a</sup>	-0.035 <sup>b</sup>	0.034 <sup>b</sup>	-0.011	-0.011	-0.074 <sup>a</sup>	-0.018	1.000

<sup>a</sup>Correlation is significant at the  $p=0.01$  level (two-tailed), with the highest positive and negative correlations highlighted in blue and red, respectively.

<sup>b</sup>Correlation is significant at the  $p=0.05$  level (two-tailed).

WL, water level.

**Table A1.8. Spearman's rank correlation matrix for winter 2017/2018 (December to February) ( $n=4282$ )**

Sensor	Temperature	EC	Turbidity	pH	DO	WL	RFU	Tide
Temperature	1.000	-0.397 <sup>a</sup>	0.446 <sup>a</sup>	0.066 <sup>a</sup>	-0.696 <sup>a</sup>	0.129 <sup>a</sup>	-0.762 <sup>a</sup>	-0.009
EC	-0.397 <sup>a</sup>	1.000	-0.383 <sup>a</sup>	0.244 <sup>a</sup>	0.176 <sup>a</sup>	0.325 <sup>a</sup>	0.351 <sup>a</sup>	-0.052 <sup>a</sup>
Turbidity	0.446 <sup>a</sup>	-0.383 <sup>a</sup>	1.000	0.269 <sup>a</sup>	-0.415 <sup>a</sup>	-0.060 <sup>a</sup>	-0.304 <sup>a</sup>	0.036 <sup>b</sup>
pH	0.066 <sup>a</sup>	0.244 <sup>a</sup>	0.269 <sup>a</sup>	1.000	-0.521 <sup>a</sup>	0.011	-0.061 <sup>a</sup>	-0.038 <sup>b</sup>
DO	-0.696 <sup>a</sup>	0.176 <sup>a</sup>	-0.415 <sup>a</sup>	-0.521 <sup>a</sup>	1.000	-0.111	0.610 <sup>a</sup>	0.037 <sup>b</sup>
WL	0.129 <sup>a</sup>	0.325 <sup>a</sup>	-0.060 <sup>a</sup>	0.011	-0.111 <sup>a</sup>	1.000	-0.109 <sup>a</sup>	-0.092 <sup>a</sup>
RFU	-0.762 <sup>a</sup>	0.351 <sup>a</sup>	-0.304 <sup>a</sup>	-0.061 <sup>a</sup>	0.610 <sup>a</sup>	-0.109 <sup>a</sup>	1.000	0.011
Tide	-0.009	-0.052 <sup>a</sup>	0.036 <sup>b</sup>	-0.038 <sup>b</sup>	0.037 <sup>b</sup>	-0.092 <sup>a</sup>	0.011	1.000

<sup>a</sup>Correlation is significant at the  $p=0.01$  level (two-tailed), with the highest positive and negative correlations highlighted in blue and red, respectively.

<sup>b</sup>Correlation is significant at the  $p=0.05$  level (two-tailed).

WL, water level.

**Table A1.9. Spearman's rank correlation matrix for spring 2018 (March to May) ( $n=1694$ )**

Sensor	Temperature	EC	Turbidity	pH	DO	WL	RFU	Tide
Temperature	1.000	-0.572 <sup>a</sup>	-0.517 <sup>a</sup>	-0.431 <sup>a</sup>	-0.083 <sup>a</sup>	0.206 <sup>a</sup>	-0.948 <sup>a</sup>	0.000
EC	-0.572 <sup>a</sup>	1.000	0.761 <sup>a</sup>	0.868 <sup>a</sup>	-0.252 <sup>a</sup>	-0.273 <sup>a</sup>	0.615 <sup>a</sup>	0.018
Turbidity	-0.517 <sup>a</sup>	0.761 <sup>a</sup>	1.000	0.720 <sup>a</sup>	-0.100 <sup>a</sup>	-0.282 <sup>a</sup>	0.548 <sup>a</sup>	-0.005
pH	-0.431 <sup>a</sup>	0.868 <sup>a</sup>	0.720 <sup>a</sup>	1.000	-0.289 <sup>a</sup>	-0.132 <sup>a</sup>	0.442 <sup>a</sup>	-0.019
DO	-0.083 <sup>a</sup>	-0.252 <sup>a</sup>	-0.100 <sup>a</sup>	-0.289 <sup>a</sup>	1.000	0.020	0.094 <sup>a</sup>	0.019
WL	0.206 <sup>a</sup>	-0.273 <sup>a</sup>	-0.282 <sup>a</sup>	-0.132 <sup>a</sup>	0.020	1.000	-0.261 <sup>a</sup>	-0.130
RFU	-0.948 <sup>a</sup>	0.615 <sup>a</sup>	0.548 <sup>a</sup>	0.442 <sup>a</sup>	0.094 <sup>a</sup>	-0.261 <sup>a</sup>	1.000	0.000
Tide	0.000	.018	-.005	-.019	.019	-.130 <sup>a</sup>	.000	1.000

<sup>a</sup>Correlation is significant at the  $p=0.01$  level (two-tailed), with the highest positive and negative correlations highlighted in blue and red, respectively.

<sup>b</sup>Correlation is significant at the  $p=0.05$  level (two-tailed).

WL, water level.



**AN GHNÍOMHAIREACHT UM CHAOMHNÚ COMHSHAOIL**  
Tá an Gníomhaireacht um Chaomhnú Comhshaoil (GCC) freagrach as an gcomhshaoil a chaomhnú agus a fheabhsú mar shócmhainn luachmhar do mhuintir na hÉireann. Táimid tiomanta do dhaoine agus don chomhshaoil a chosaint ó éifeachtaí díobhálacha na radaíochta agus an truaillithe.

**Is féidir obair na Gníomhaireachta a roinnt ina trí phríomhréimse:**

**Rialú:** Déanaimid córais éifeachtacha rialaithe agus comhlionta comhshaoil a chur i bhfeidhm chun torthaí maithe comhshaoil a sholáthar agus chun díriú orthu siúd nach gcloíonn leis na córais sin.

**Eolas:** Soláthraimid sonraí, faisnéis agus measúnú comhshaoil atá ar ardchaighdeán, spriocdhírthe agus tráthúil chun bonn eolais a chur faoin gcinnteoireacht ar gach leibhéal.

**Tacaíocht:** Bimid ag saothrú i gcomhar le grúpaí eile chun tacú le comhshaoil atá glan, táirgiúil agus cosanta go maith, agus le hiompar a chuirfidh le comhshaoil inbhuanaithe.

**Ár bhFreagrachtaí**

**Ceadúnú**

Déanaimid na gníomhaíochtaí seo a leanas a rialú ionas nach ndéanann siad dochar do shláinte an phobail ná don chomhshaoil:

- saoráidí dramhaíola (*m.sh. láithreáin líonta talún, loisceoirí, stáisiúin aistrithe dramhaíola*);
- gníomhaíochtaí tionsclaíocha ar scála mór (*m.sh. déantúsaíocht cógaisíochta, déantúsaíocht stroighne, stáisiúin chumhachta*);
- an diantalmhaíocht (*m.sh. muca, éanlaith*);
- úsáid shrianta agus scaoileadh rialaithe Orgánach Géinmhodhnaithe (*OGM*);
- foinsí radaíochta ianúcháin (*m.sh. trealamh x-gha agus radaiteiripe, foinsí tionsclaíocha*);
- áiseanna móra stórála peitril;
- scardadh dramhuisce;
- gníomhaíochtaí dumpála ar farraige.

**Forfheidhmiú Náisiúnta i leith Cúrsaí Comhshaoil**

- Clár náisiúnta iniúchtaí agus cigireachtaí a dhéanamh gach bliain ar shaoráidí a bhfuil ceadúnas ón nGníomhaireacht acu.
- Maoirseacht a dhéanamh ar fhreagrachtaí cosanta comhshaoil na n-údarás áitiúil.
- Caighdeán an uisce óil, arna sholáthar ag soláthraithe uisce phoiblí, a mhaoirsiú.
- Obair le húdaráis áitiúla agus le gníomhaireachtaí eile chun dul i ngleic le coireanna comhshaoil trí chomhordú a dhéanamh ar líonra forfheidhmiúcháin náisiúnta, trí dhíriú ar chiontóirí, agus trí mhaoirsiú a dhéanamh ar leasúchán.
- Cur i bhfeidhm rialachán ar nós na Rialachán um Dhramhthrealamh Leictreach agus Leictreonach (DTLL), um Shrian ar Shubstaintí Guaiseacha agus na Rialachán um rialú ar shubstaintí a ídionn an ciseal ózóin.
- An dlí a chur orthu siúd a bhriseann dlí an chomhshaoil agus a dhéanann dochar don chomhshaoil.

**Bainistíocht Uisce**

- Monatóireacht agus tuairisciú a dhéanamh ar cháilíocht aibhneacha, lochanna, uisce idirchriosacha agus cósta na hÉireann, agus screamhuisc; leibhéil uisce agus sruthanna aibhneacha a thomhas.
- Comhordú náisiúnta agus maoirsiú a dhéanamh ar an gCreat-Treoir Uisce.
- Monatóireacht agus tuairisciú a dhéanamh ar Cháilíocht an Uisce Snámha.

**Monatóireacht, Anailís agus Tuairisciú ar an gComhshaoil**

- Monatóireacht a dhéanamh ar cháilíocht an aeir agus Treoir an AE maidir le hAer Glan don Eoraip (CAFÉ) a chur chun feidhme.
- Tuairisciú neamhspleách le cabhrú le cinnteoireacht an rialtais náisiúnta agus na n-údarás áitiúil (*m.sh. tuairisciú tréimhsiúil ar staid Chomhshaoil na hÉireann agus Tuarascálacha ar Tháscairí*).

**Rialú Astaíochtaí na nGás Ceaptha Teasa in Éirinn**

- Fardail agus réamh-mheastacháin na hÉireann maidir le gáis cheaptha teasa a ullmhú.
- An Treoir maidir le Trádáil Astaíochtaí a chur chun feidhme i gcomhair breis agus 100 de na táirgeoirí dé-ocsaíde carbóin is mó in Éirinn.

**Taighde agus Forbairt Comhshaoil**

- Taighde comhshaoil a chistiú chun brúnna a shainathint, bonn eolais a chur faoi bheartais, agus réitigh a sholáthar i réimsí na haeráide, an uisce agus na hinbhuanaitheachta.

**Measúnacht Straitéiseach Timpeallachta**

- Measúnacht a dhéanamh ar thionchar pleananna agus clár beartaithe ar an gcomhshaoil in Éirinn (*m.sh. mórfhleananna forbartha*).

**Cosaint Raideolaíoch**

- Monatóireacht a dhéanamh ar leibhéil radaíochta, measúnacht a dhéanamh ar nochtadh mhuintir na hÉireann don radaíocht ianúcháin.
- Cabhrú le pleananna náisiúnta a fhorbairt le haghaidh éigeandálaí ag eascairt as taismí núicléacha.
- Monatóireacht a dhéanamh ar fhorbairtí thar lear a bhaineann le saoráidí núicléacha agus leis an tsábháilteacht raideolaíochta.
- Sainseirbhísí cosanta ar an radaíocht a sholáthar, nó maoirsiú a dhéanamh ar sholáthar na seirbhísí sin.

**Treoir, Faisnéis Inrochtana agus Oideachas**

- Comhairle agus treoir a chur ar fáil d’earnáil na tionsclaíochta agus don phobal maidir le hábhair a bhaineann le caomhnú an chomhshaoil agus leis an gcosaint raideolaíoch.
- Faisnéis thráthúil ar an gcomhshaoil ar a bhfuil fáil éasca a chur ar fáil chun rannpháirtíocht an phobail a spreagadh sa chinnnteoireacht i ndáil leis an gcomhshaoil (*m.sh. Timpeall an Tí, léarscáileanna radóin*).
- Comhairle a chur ar fáil don Rialtas maidir le hábhair a bhaineann leis an tsábháilteacht raideolaíoch agus le cúrsaí práinnfhreagartha.
- Plean Náisiúnta Bainistíochta Dramhaíola Guaisí a fhorbairt chun dramhaíl ghuaiseach a chosaint agus a bhainistiú.

**Múscailt Feasachta agus Athrú Iompraíochta**

- Feasacht chomhshaoil níos fearr a ghiniúint agus dul i bhfeidhm ar athrú iompraíochta dearfach trí thacú le gnóthais, le pobail agus le teaghlaigh a bheith níos éifeachtúla ar acmhainní.
- Tástáil le haghaidh radóin a chur chun cinn i dtithe agus in ionaid oibre, agus gníomhartha leasúcháin a spreagadh nuair is gá.

**Bainistíocht agus struchtúr na Gníomhaireachta um Chaomhnú Comhshaoil**

Tá an ghníomhaíocht á bainistiú ag Bord lánaimseartha, ar a bhfuil Ard-Stiúrthóir agus cúigear Stiúrthóirí. Déantar an obair ar fud cúig cinn d’Oifigí:

- An Oifig um Inmharthanacht Comhshaoil
- An Oifig Forfheidhmithe i leith cúrsaí Comhshaoil
- An Oifig um Fianaise is Measúnú
- Oifig um Chosaint Radaíochta agus Monatóireachta Comhshaoil
- An Oifig Cumarsáide agus Seirbhísí Corparáideacha

Tá Coiste Comhairleach ag an nGníomhaireacht le cabhrú léi. Tá dáréag comhaltaí air agus tagann siad le chéile go rialta le plé a dhéanamh ar ábhair inní agus le comhairle a chur ar an mBord.

## From Source to Sink: Responses of a Coastal Catchment to Large-scale Changes (Golden Strand Catchment, Achill Island, County Mayo)



Authors: Eugene Farrell, Mary Bourke, Tiernan Henry, Gesche Kindermann, Kevin Lynch, Terry Morley, Barry O'Dwyer, John O'Sullivan and Jonathan Turner

### Identifying Pressures

One of the key challenges facing Ireland in the coming decades is the need to increase our resilience to extreme weather events that are impacting, in many cases in devastating ways, our natural and built environments. Concurrently, human-induced pressures such as grazing, poor farming practices, recreation, urbanisation, sand and gravel mining, pollution, invasive species and erosion are impacting critical ecosystem services (e.g. regulation of flooding and erosion). A fundamental scientific requirement to build landscape resilience is having extensive regional monitoring programmes that measure the forcing and system response (via states, triggers, thresholds and feedback mechanisms). Field studies tracing the movement of sediment between sources (catchment) and sinks (offshore) are important to identify transport pathways and predict regional and localised seabed mobility to changing ocean climates. This research project fills a knowledge gap by implementing a set of integrated, cross-disciplinary field experiments to measure patterns in the sediment and water pathways in Golden Strand catchment, Achill Island, County Mayo. The results highlight (1) the variability in behaviour of different earth systems within catchments and (2) the urgent need to conduct long-term field-based monitoring programmes.

### Informing Policy

Climate action to “build capacity” and “increase climate resilience” is now implemented in Irish policy via the Climate Action Plan 2019 and the National Adaptation Framework. The challenge for coastal communities, scientists and managers is to design adaptation measures that are attainable and sustainable so that they can work together to protect and conserve ecosystems and the goods and services they provide (erosion and flood control, habitat, water, amenities, etc.). The results from this study illustrate that (1) many parts of our coastline are attuned to high-energy wave conditions and require extreme storms to cause significant change; (2) existing agricultural practices along coasts are unsustainable and adversely impacting ecosystems; and (3) peatland-dominated catchments have unique hydrological characteristics that require monitoring programmes (of at least 10 years) to effectively capture inherent environmental variability. These results are critical to direct local authority sectors to apply climate policy objectives in different types of catchments and mobilise communities to identify solutions for the pressure points so that future opportunities are not lost.

### Developing Solutions

The increase in frequency of extreme weather events and sea level rise is now locked in for Ireland on account of human-induced climate changes over the past century. There is an urgent need to build better regional-scale landscape models and forecasting and alert systems. Building large-scale, reduced-complexity models of the evolution of Irish landscapes to changing climates requires accurate and confirmable predictions of local-scale changes in very specific environments. The results from this project highlight the need for substantial investment to support longitudinal (years to decades) and multi-disciplinary (geomorphology, ecology, hydrology, climatology, oceanography) monitoring programmes to build an inventory of case studies. The most efficient way to do this is to install a dense nationwide network of low-cost field sensors to continuously collect data that can provide the necessary input for environmental management and planning decisions. In Ireland the loss and/or degradation of ecosystems needs to be framed within new climate policy and planning guidelines as a loss of an integral element of local and regional natural heritage that is of considerable scientific, conservation and recreational value.